

9-2011

Wachusett Reservoir Contaminant Spill Modeling Using CE-QUAL W2

Cory S. Devonis

Follow this and additional works at: https://scholarworks.umass.edu/cee_ewre



Part of the [Environmental Engineering Commons](#)

Devonis, Cory S., "Wachusett Reservoir Contaminant Spill Modeling Using CE-QUAL W2" (2011). *Environmental & Water Resources Engineering Masters Projects*. 41.

<https://doi.org/10.7275/ZBKQ-A791>

This Article is brought to you for free and open access by the Civil and Environmental Engineering at ScholarWorks@UMass Amherst. It has been accepted for inclusion in Environmental & Water Resources Engineering Masters Projects by an authorized administrator of ScholarWorks@UMass Amherst. For more information, please contact scholarworks@library.umass.edu.

**WACHUSETT RESERVOIR CONTAMINANT SPILL MODELING USING
CE-QUAL W2**

A Master's Project Presented By

Cory S. Devonis

Submitted to the Department of Civil and Environmental Engineering of the
University of Massachusetts in partial fulfillment of the requirements for the degree of

MASTERS OF SCIENCE

in

Environmental Engineering

September 2011

Department of Civil and Environmental Engineering

University of Massachusetts

Amherst, MA 01003

WACHUSETT RESERVOIR CONTAMINANT SPILL MODELING USING CE-QUAL W2

A Masters Project Presented

By

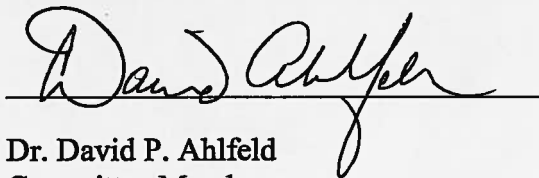
Cory S. Devonis

Environmental Engineering Program
Department of Civil and Environmental Engineering
University of Massachusetts, Amherst

Approved as to style and content by:



Dr. John E. Tobiason
Committee Chairperson



Dr. David P. Ahlfeld
Committee Member



Dr. David P. Ahlfeld, Graduate Program Director

M.S. in Environmental Engineering

Acknowledgements

I would like to personally thank the Massachusetts Department of Conservation and Recreation (DCR), who funded this research; for without them I may never of had this unique experience.

Data was supplied by DCR, the Massachusetts Water Resources Authority (MWRA), the National Oceanic and Atmospheric Administration (NOAA), and the United States Geological Survey (USGS). Thank you to everyone at MWRA and DCR who have been invaluable to gathering the required data possible to develop the CE-QUAL W2 models and the quick responses when data was required.

My time at UMass would not have been possible without the guidance of my advisor Dr. John Tobiason, who provided me with this opportunity at a time in my life when I was unsure as to what I was going to do. Your vast knowledge in all fields of environmental engineering is overwhelming and I hope one day I can be as knowledgeable as you. Thank you for your patience, guidance, and support throughout my graduate career.

I would also like to thank Dr. David Ahlfeld who was like a second advisor to me. Your guidance and support throughout this project has helped my understanding of the fundamentals of modeling and the Wachusett Reservoir system. Thank you for your comments and support.

Thank you to Bryan Sojkowski for showing me everything that I now know about this project, if it weren't for you I would not have been able to learn the model so quickly and effectively. I would also like to thank Mikaela Laverty, my desk mate, for being patient with me and answering all the questions I had whether for our project or for a class you took years ago. I would also like to thank Kyung Hwa, whose help has been invaluable and his knowledge of MATLAB amazes me.

I would also like to make a special thank you to my fiancé, Molly O'Malley. You moved to a strange new town without knowing anyone in order to be with me. Thank you for sticking with me, especially when there were times I could not spend any time with you because of classes and research. Without you my graduate experience would not have been the same. Thank you for your love and support throughout the process.

Finally I would like to thank my parents, Jessica and Robert Rego, and my grandparents, Robert and Anita Robideau, who supported me throughout the years and believed that I can do anything. Thank you for believing in me and helping me through the rough times. Without all of you behind me, none of this would be possible.

Executive Summary

This research studies contaminant spills in the Wachusett Reservoir by two dimensional modeling utilizing CE-QUAL W2. The Wachusett Reservoir, located in central Massachusetts, has a capacity of 65 billion gallons and is the primary water source for the metropolitan Boston area. There are numerous inflows and outflows to and from the Wachusett Reservoir, with the Quabbin Aqueduct supplying approximately half of the total water entering the Wachusett. The Quabbin Aqueduct connects the Quabbin Reservoir (412 billion gallons) to the Wachusett Reservoir and supplies water to maintain desired water surface elevations in the Wachusett during time of high demand and low flows, typically during the summer months.

The CE-QUAL W2 V3.6 model was utilized to simulate spill contaminants for years 2003 to 2008. Sojkowski (2011) updated Matthews (2007) 2003 and 2004 models from V3.5 to V3.6, and also created models for calendar years 2005 and 2006. Models were successfully created for calendar year 2007 and 2008 and were calibrated to temperature and specific conductance data for the North Basin of the Wachusett Reservoir. Calibration was obtained by changing a variety of CE-QUAL W2 parameters to minimize the error between simulated results in Segment 42 and the measured North Basin data.

The modeled spill scenarios included density of the contaminant, seasonal trends, Quabbin transfer, daily variation, high inflow events, and wind influence. It was determined that the density of the contaminant had an effect in the Spring and Summer seasons, with no effect in the Fall season with respect to arrival time and behavior at the Cosgrove Intake. A spill that transports on the top of the water column (low density/high temperature spill) typically arrives earlier in the Spring and Summer seasons due to exposure to meteorological conditions (wind), while a contaminant spill that travels in the middle and bottom of the water column (medium

and high density/medium and low temperature spills) typically have arrival times later than a warm spill with similar behavior due to the hydrological conditions within the reservoir.

Seasonal patterns are established with a Spring arrival of two to five days, a Summer arrival of five to fourteen days, and a Fall arrival of four to ten days. The seasonal patterns were assessed by selecting one spill day for each season and year to represent the entire season for the selected year. To assess variability within a season, daily variations were evaluated in order to identify differences in behavior if spills occurred within a twenty day time period; it was found that for some years there were similar arrival times and behaviors, while some seasons of some years demonstrated completely variable arrival times and behavior due to the meteorological and hydrological conditions during the time period. It was found that the arrival time window for seasons was lengthened by one to two days, however, shorter arrival times did not result.

The Quabbin transfer was found to have a significant impact on the behavior of the contaminant spill during the summer months, where the variability in spill concentration at the Cosgrove Intake was completely dampened when the Quabbin Aqueduct was shut off twelve hours after the spill occurred; however, little to no impact on the arrival time was found.

High inflow events correlate to storm events and were investigated because of the increased risk of a tanker truck accident during a storm. The results indicate that the high inflow events dictate when the spill will arrive and how it will behave with little dependence on the spill date in a five day period around the date of the storm. Wind influence was investigated and found to have a significant role in the arrival time of surficial spills; given the right meteorological conditions, wind can produce arrival times as early as two days after the spill occurs.

Table of Contents

Acknowledgements.....	iii
Executive Summary.....	v
Table of Contents.....	vii
List of Figures.....	ix
List of Tables.....	xiv
1 INTRODUCTION.....	1
1.1 Scope and Objectives.....	1
1.2 Wachusett Reservoir System.....	1
1.2.1 Inflows and Outflows.....	4
1.2.2 Data Collection.....	7
2 BACKGROUND.....	9
2.1 Modeling.....	9
2.2 CE-QUAL W2.....	9
2.3 Literature Review.....	10
2.4 Past UMass Work.....	14
3 CE-QUAL W2 MODEL DEVELOPMENT.....	15
3.1 CE-QUAL W2 Grid and Segments.....	15
3.2 Data Collection.....	17
3.2.1 Meteorological Data.....	17
3.2.2 Water Balance.....	18
3.2.3 Specific Conductance/TDS.....	21
3.3 Calibration.....	21
3.3.1 Water Balance Calibration.....	21
3.3.2 Initial Conditions - Temperature.....	25
3.3.3 Initial Conditions - Specific Conductance.....	28
3.3.4 Wind Sheltering Coefficient.....	37
3.3.5 Bottom Heat Exchange Coefficient.....	39
3.3.6 Sediment Temperature.....	41
3.3.7 Ice On/Off.....	43
3.4 Final Calibration Results.....	44

3.4.1	Temperature and Specific Conductance Profiles	45
3.5	Spill Simulation.....	55
3.5.1	Spill Date Selection.....	56
4	RESULTS	58
4.1	Seasonal Influence.....	58
4.1.1	Spring Season Spills	59
4.1.2	Summer Season Spill	64
4.1.3	Fall Season Spill	68
4.2	Quabbin Transfer Influence	72
4.3	Daily Variability in Spill Behavior	75
4.4	High Inflow Influence	80
4.5	Wind Influence.....	88
4.5.1	Modeled Year 2003 Spring Warm Spill	88
4.5.2	Modeled Year 2007 Spring Warm Spill	91
5	SUMMARY, CONCLUSIONS AND RECOMMENDATIONS	94
5.1	Summary	94
5.2	Conclusions	95
5.3	Recommendations	96
	REFERENCES	97
	APPENDIX A - TIME SERIES OF MAJOR INFLOWS/OUTFLOWS	99
	APPENDIX B - WACHUSETT RESERVOIR CAPACITY AND ELEVATION FROM MWRA	105

List of Figures

Figure 1.1: Wachusett Reservoir (Google Maps)	2
Figure 1.2: Location of Basins, inflows, and outflows	3
Figure 1.3: MWRA water supply system	4
Figure 1.4: Water surface elevation and major inflows into Wachusett Reservoir 2008	6
Figure 1.5: Water surface elevations and major outflows from the Wachusett Reservoir 2008	7
Figure 3.1: CE-QUAL W2 top view of segments.....	16
Figure 3.2: CE-QUAL W2 profile view of layers	17
Figure 3.3: Measured and uncalibrated calculated WSE for 2007	20
Figure 3.4: Measured and uncalibrated calculated WSE for 2008	20
Figure 3.5: 2007 calibrated WSE simulation.....	23
Figure 3.6: 2008 calibrated WSEsimulation.....	24
Figure 3.7: Difference between measured and calibrated WSE	24
Figure 3.8: Varying initial temperature calibration, 4/10/2007	26
Figure 3.9: Varying initial temperature calibration, 6/25/2007	26
Figure 3.10: Varying initial temperature calibration, 4/23/2008	27
Figure 3.11: Varying initial temperature calibration, 6/26/2008	28
Figure 3.12: Varying initial specific conductance calibration, 1/25/2007	30
Figure 3.13: Varying initial specific conductance calibration, 4/10/2007	30
Figure 3.14: Varying initial specific conductance calibration, 6/25/2007	31
Figure 3.15: Flow weighted specific conductance of all major contributing inflows, 2007	32
Figure 3.16: Comparing specific conductance at the Cosgrove Intake measured taken every 15 minutes with CE-QUAL W2 output for varying initial specific conductance concentration for calendar year 2007	33
Figure 3.17: Varying initial specific conductance calibration, 3/6/2008.....	35

Figure 3.18: Varying initial specific conductance calibration, 4/23/2008.....	35
Figure 3.19: Varying initial specific conductance calibration, 6/26/2008.....	36
Figure 3.20: Varying initial specific conductance calibration, 9/8/2008.....	36
Figure 3.21: Comparing specific conductance at the Cosgrove Intake measured taken every 15 minutes with CE-QUAL W2 output for varying initial specific conductance concentration for calendar year 2008	37
Figure 3.22: Impact of varying WSC, 7/2/2007	38
Figure 3.23: Impact of varying WSC, 7/3/2008	39
Figure 3.24: Varying CBHE, 6/25/2007	40
Figure 3.25: Varying CBHE, 10/15/2007	41
Figure 3.26: Varying sediment temperature, 6/25/2007	42
Figure 3.27: Varying sediment temperature, 11/1/2007	42
Figure 3.28: Comparison of on and off ice calculation, 3/6/2008	43
Figure 3.29: Comparison of on and off ice calculation, 6/9/2008	44
Figure 3.30: 2007 temperature calibration profiles, North Basin (Segment 42)	47
Figure 3.31: 2007 specific conductance calibration profiles, North Basin (Segment 42)	49
Figure 3.32: 2008 temperature calibration profiles, North Basin (Segment 42)	51
Figure 3.33: 2008 specific conductance calibration profiles, North Basin (Segment 42)	53
Figure 4.1: Relative contaminant concentration at the Cosgrove Intake for 2007 Spring, Summer, and Fall cold spills for the entire year	59
Figure 4.2: Relative contaminant concentration behavior at Cosgrove Intake for 2007 Spring, spill temperature variations for spill at Rt. 140 Bridge on Julian Day 119	60
Figure 4.3: Relative contaminant concentration behavior at Cosgrove Intake for 2008 Spring, spill temperature variations for spill at Rt. 140 Bridge on Julian Day 122	61
Figure 4.4: Relative contaminant concentration behavior at Cosgrove Intake for Spring model years 2003-2008 with warm spill at the Rt. 140 Bridge	62

Figure 4.5: Relative contaminant concentration behavior at Cosgrove Intake for Spring model years 2003-2007 with medium spill at the Rt. 140 Bridge	63
Figure 4.6: Relative contaminant concentration behavior at Cosgrove Intake for Spring model years 2003-2008 with cold spill at the Rt. 140 Bridge	63
Figure 4.7: Relative contaminant concentration behavior at Cosgrove Intake for 2007 Summer, spill temperature variations for spill at Rt. 140 Bridge on Julian Day 222	65
Figure 4.8: Relative contaminant concentration behavior at Cosgrove Intake for 2008 Summer, spill temperature variations for spill at Rt. 140 Bridge on Julian Day 227	65
Figure 4.9: Relative contaminant concentration behavior at Cosgrove Intake for Summer model years 2003-2008 with warm spill at the Rt. 140 Bridge	66
Figure 4.10: Relative contaminant concentration behavior at Cosgrove Intake for Summer model years 2003-2008 with medium spill at the Rt. 140 Bridge	67
Figure 4.11: Relative contaminant concentration behavior at Cosgrove Intake for Summer model years 2003-2008 with cold spill at the Rt. 140 Bridge	67
Figure 4.12: Relative contaminant concentration behavior at Cosgrove Intake for 2007 Fall, spill temperature variations for spill at Rt. 140 Bridge on Julian Day 318	69
Figure 4.13: Relative contaminant concentration behavior at Cosgrove Intake for 2007 Fall, spill temperature variations for spill at Rt. 140 Bridge on Julian Day 318	69
Figure 4.14: Relative contaminant concentration behavior at Cosgrove Intake for Fall model years 2004-2008 with warm spill at the Rt. 140 Bridge	70
Figure 4.15: Relative contaminant concentration behavior at Cosgrove Intake for Fall model years 2004-2008 with medium spill at the Rt. 140 Bridge	71
Figure 4.16: Relative contaminant concentration behavior at Cosgrove Intake for Fall model years 2004-2008 with cold spill at the Rt. 140 Bridge	71
Figure 4.17: Relative contaminant concentration behavior at Cosgrove Intake for Summer model year 2007 warm spill by varying the state of the Quabbin Transfer.....	73

Figure 4.18: Relative contaminant concentration behavior at Cosgrove Intake for Summer model year 2007 cold spill by varying the state of the Quabbin Transfer 74

Figure 4.19: Relative contaminant concentration behavior at Cosgrove Intake for Summer model year 2008 warm spill by varying the state of the Quabbin Transfer..... 74

Figure 4.20: Relative contaminant concentration behavior at Cosgrove Intake for Summer model year 2008 cold spill by varying the state of the Quabbin Transfer 75

Figure 4.21: Relative contaminant concentration behavior at Cosgrove Intake for Spring model year 2005 warm spill; varied spill date ten days before and after original date in five day intervals..... 76

Figure 4.22: Relative contaminant concentration behavior at Cosgrove Intake for Summer model year 2008 warm spill; varied spill dates, ten days before and after original date in five day intervals..... 77

Figure 4.23: Relative contaminant concentration behavior at Cosgrove Intake for Fall model year 2006 warm spill; varied spill dates, ten days before and after original date in five day intervals 78

Figure 4.24 Relative contaminant concentration behavior at Cosgrove Intake for Spring model year 2003 warm spill; varied spill date, ten days before and after original date in five day intervals..... 79

Figure 4.25: Relative contaminant concentration behavior at Cosgrove Intake for Summer model year 2007 warm spill; varied spill date ten days before and after original date in five day intervals..... 80

Figure 4.26: Relative contaminant concentration behavior at Cosgrove Intake for Summer model year 2003 warm spill; varied spill date, two days before and after original date in one day intervals to evaluate high inflow events with “Days After Spill” time..... 81

Figure 4.27: Relative contaminant concentration behavior at Cosgrove Intake for Summer model year 2003 warm spill; varied spill date, two days before and after original date in one day intervals to evaluate high inflow events with “Julian Day” time..... 82

Figure 4.28: Relative contaminant concentration behavior at Cosgrove Intake for Summer model year 2003 cold spill; varied spill date, two days before and after original date in one day intervals to evaluate high inflow events in “Days After Spill” time	83
Figure 4.29: Relative contaminant concentration behavior at Cosgrove Intake for Summer model year 2003 cold spill; varied spill date, two days before and after original date in one day intervals to evaluate high inflow events in “Julian Day” time	84
Figure 4.30: Relative contaminant concentration behavior at Cosgrove Intake for Spring model year 2005 warm spill; varied spill date before, during, and after original date in one day intervals to evaluate high inflow events with “Days After Spill” time (high inflows Julian day 88-93)....	85
Figure 4.31: Relative contaminant concentration behavior at Cosgrove Intake for Spring model year 2005 warm spill; varied spill date before, during, and after original date in one day intervals to evaluate high inflow events with “Julian Day” time (high inflows Julian day 88-93).....	86
Figure 4.32: Relative contaminant concentration behavior at Cosgrove Intake for model year 2008 warm spill; varied spill date before, during, and after original date in one day intervals to evaluate high inflow events with “Days After Spill” time (high inflows Julian day 65-69).....	87
Figure 4.33: Relative contaminant concentration behavior at Cosgrove Intake for model year 2008 warm spill; varied spill date before, during, and after original date in one day intervals to evaluate high inflow events with “Julian Day” time (high inflows Julian day 65-69).....	87
Figure 4.34: 2003 Spring comparison of contaminant concentration behavior at Cosgrove by varying wind speed with spill on Julian Day 117	90
Figure 4.35: Wind Rose (m/s) for Julian Day 117.5 to 118.9.....	91
Figure 4.36: 2007 Spring comparison of contaminant concentration behavior at Cosgrove by varying wind speed with spill on Julian day 119	92
Figure 4.37: Wind Rose (m/s) for Julian Day 119.5 to 121.9.....	93

List of Tables

Table 1.1: Percentage Distribution of Total Inflow and Outflows (By Volume)	5
Table 3.1: Cloud Cover Data Conversion.....	18
Table 3.2: Comparison of Range of Historical Average Calibration Factors to New Factors	23
Table 3.3: Parameter Results of Final Calibration.....	45
Table 3.4: Average Daily Wind Comparison for all Six Years	57

1 INTRODUCTION

This report presents the results of two dimensional modeling of the Wachusett Reservoir, done at the University of Massachusetts Amherst (UMass), using the software CE-QUAL W2 V3.6 (CE-QUAL) during the period of January 2010 to May 2011. This work is the product of a collaborative effort with the Massachusetts Department of Conservation and Recreation (DCR) and the Massachusetts Water and Resources Authority (MWRA). The focus of the research is to better understand the hydrodynamics of the Wachusett Reservoir and the behavior of a potential contaminant spill at the Route 140 bridge under a variety of conditions.

1.1 Scope and Objectives

The purpose of this research is to model the hydrodynamics and water quality of the Wachusett Reservoir using CE-QUAL W2 to simulate a contaminant spill. For this project we have focused on six years, 2003 to 2008, of modeled spill scenarios in the Thomas Basin where two high traffic volume highway bridges cross the reservoir. Certain parameters are analyzed to examine impacts on the resulting Cosgrove outflow contaminant concentration. These include seasonal influence, spill temperature variation, Quabbin transfer influence, high inflow events and daily variation. The objectives include development of two dimensional models for calendar years, 2007 and 2008, and simulations of spill scenarios for calendar years 2003 to 2008.

1.2 Wachusett Reservoir System

The Wachusett Reservoir is critical to the water supply system for the metropolitan Boston area. Construction of the Wachusett Dam finished in 1908 and was able to provide water for 29

municipalities, becoming the largest public water supply reservoir in the world at the time (MWRA, 2006). The Reservoir is located in central Massachusetts, managed by DCR and MWRA, and supplies water to the Boston Metropolitan area (Figure 1.1). Wachusett Reservoir has a capacity of approximately 65 billion gallons (0.25 km^3) with a length of 8.4 miles (13.5 km), a surface area of 6.3 square miles (16.3 km^2), and a maximum depth of 120 feet (36.6 meters). The Wachusett Reservoir can be divided into three separate basins, and has inflow from nine tributaries and the Quabbin Aqueduct. Water travels from the northwestern basin (Thomas Basin), through the South Basin, to the North Basin, where it is typically exits through the Cosgrove Intake or the Nashua River. All inflow and outflow locations are shown in Figure 1.2.



Figure 1.1: Wachusett Reservoir (Google Maps)

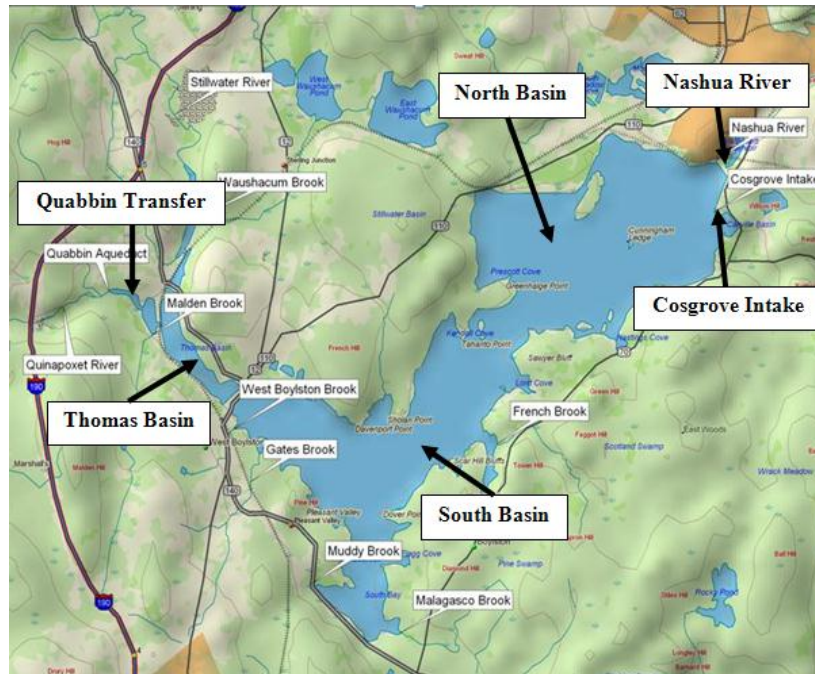


Figure 1.2: Location of Basins, inflows, and outflows

One of the largest sources for inflow is water transferred from the Quabbin reservoir, accounting for approximately 34% to 59% of total inflows for calendar years 2003 to 2008. The Quabbin Reservoir completed construction in 1946 becoming the largest man-made reservoir in the world dedicated to water supply, with a capacity of 412 billion gallons (MWRA, 2006). The Quabbin Aqueduct was constructed in order to connect the Quabbin Reservoir to the Wachusett Reservoir through a rock tunnel. With the two reservoirs connected, the Wachusett Reservoir is able to receive water from the Quabbin Reservoir; transfers are common in times of lower precipitation and high demand for the Boston area. The MWRA water system supplies 50 communities, 44 of which are in the Boston and MetroWest region (MWRA, 2009), as shown in Figure 1.3. Drinking water exits the Wachusett Reservoir through the Cosgrove Intake, where it is sent to the Carroll Water Treatment Plant for treatment and distribution. It should be noted that the quality of water from the Wachusett and Quabbin Reservoirs is near drinking water standards without

treatment, in large part due to the fact that 85% of the total watershed area is protected naturally by forests and wetlands, thanks to the conservation efforts of DCR and MWRA. As a result, MWRA has a waiver of filtration so treatment consists of disinfection and corrosion control.

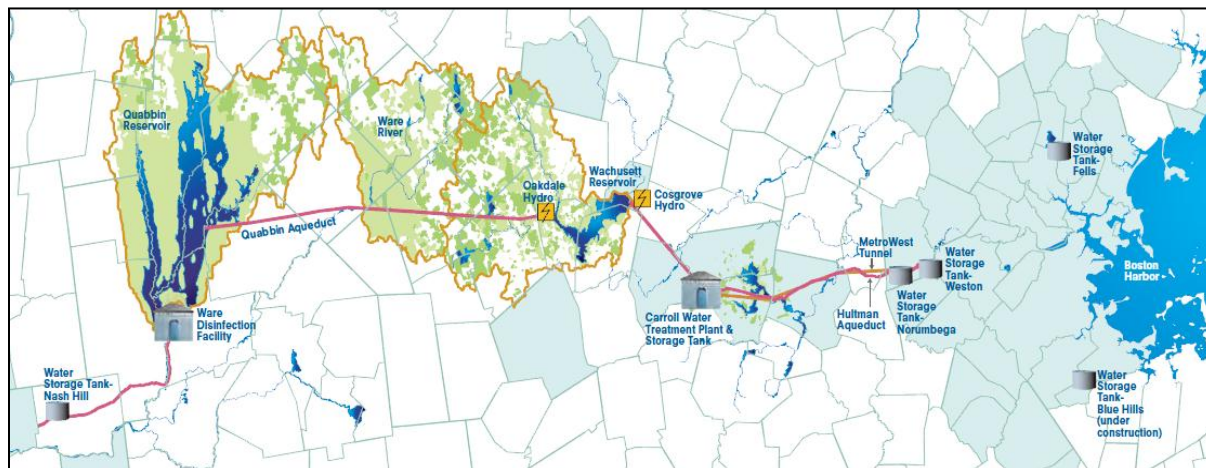


Figure 1.3: MWRA water supply system

1.2.1 Inflows and Outflows

The purpose of this section is to describe the inflows and outflows for the Wachusett Reservoir.

Table 1.1 shows the relative distribution among the inflows and outflows for calendar years 2003 to 2008. Inflows into the Wachusett Reservoir consist of nine tributaries, the Quabbin Aqueduct, direct precipitation, and direct runoff into the reservoir. However, the majority of the tributary inflow is from two tributaries, Stillwater River and Quinapoxet River. Overall, the most significant inflows are the Quabbin Aqueduct, precipitation, direct runoff, Stillwater River, and Quinapoxet River. These sources make up 92% to 96% of the total inflows for 2003 to 2008.

Table 1.1: Percentage Distribution of Total Inflow and Outflows (By Volume)

		2003	2004	2005	2006	2007	2008
Inflows:	Quabbin Aqueduct	43.5	59.1	34.5	37.5	52.8	38.1
	Direct Precipitation	5.23	4.74	6.04	4.91	4.62	6.10
	Direct Runoff	9.20	5.29	11.4	9.95	8.09	11.1
	Stillwater River	14.0	8.3	17.7	15.8	12.4	17.0
	Quinapoxet River	21.4	18.7	22.1	24.7	16.3	19.8
	Washacum Brook	2.86	1.65	3.55	3.09	2.52	3.44
	Malden Brook	0.57	0.33	0.71	0.62	0.50	0.69
	Boylston Brook	0.19	0.11	0.24	0.21	0.17	0.23
	Gates Brook	1.42	0.82	1.76	1.53	1.25	1.70
	Muddy Brook	0.31	0.18	0.39	0.34	0.27	0.37
	Malagasco Brook	0.40	0.23	0.49	0.43	0.35	0.48
	French Brook	0.90	0.52	1.11	0.97	0.79	1.08
Outflows:	Cosgrove Intake	66.0	60.2	84.0	76.7	72.3	69.2
	Nashua River Release	14.1	15.3	7.1	12.7	9.7	15.2
	Town Withdrawals	0.74	0.71	0.65	0.58	0.53	0.61
	Nashua Spillway	*	1.83	2.99	5.53	5.78	0.80
	Wachusett Aqueduct	13.8	16.6	0.00	0.00	7.37	10.2
	Evaporation	3.71	3.75	4.01	4.52	4.32	3.96
	Other	1.72	1.64	1.31	0.00	0.00	0.00

Figure 1.4 shows the major inflows versus date for calendar year 2008, which is a typical representation for all years as can be seen in Appendix A. A second y-axis is used in Figure 1.4 to show the reservoir water surface elevation, which indicates how the reservoir responds to inflows and outflows. It can be seen that when a high inflow event happens, usually because of rain, the elevation of the reservoir increases as well.

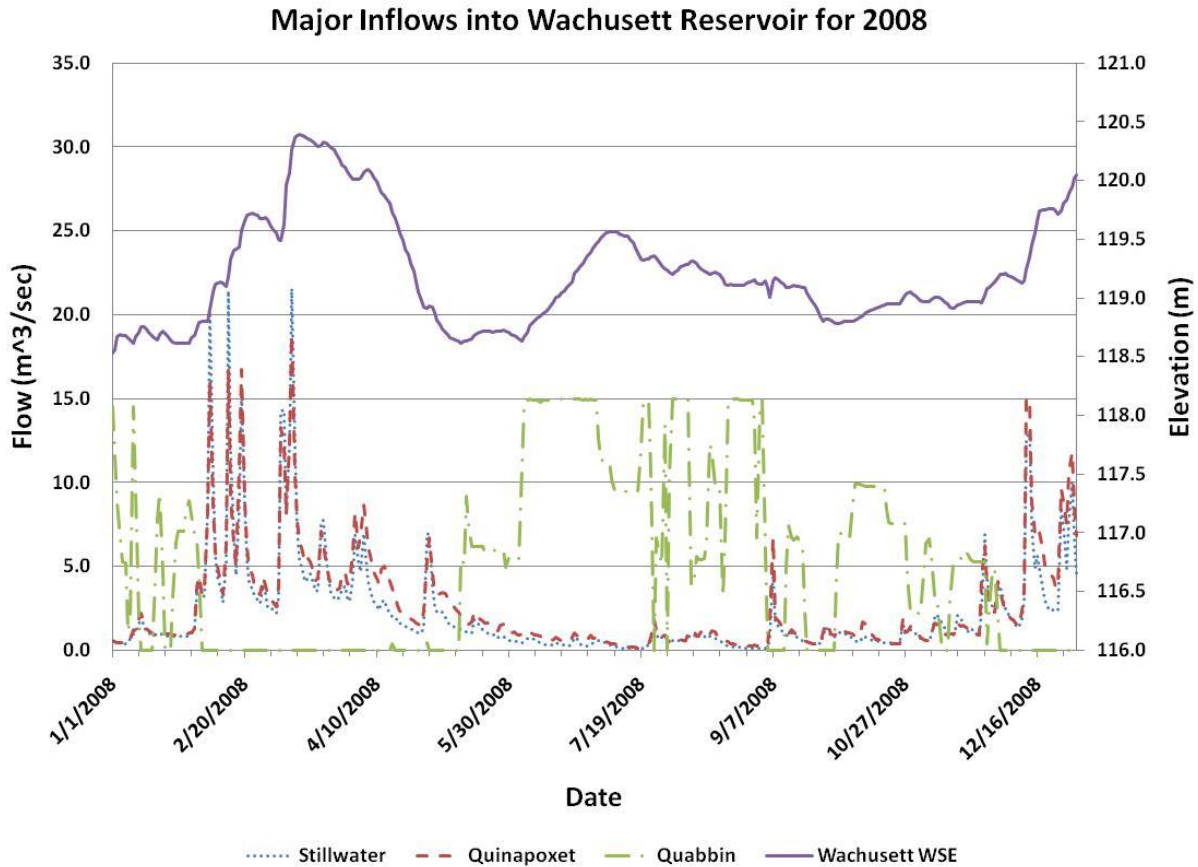


Figure 1.4: Water surface elevation and major inflows into Wachusett Reservoir 2008

Outflows from the Wachusett Reservoir consist of the Cosgrove Intake, the Nashua River release, withdrawals from surrounding towns, the Nashua Spillway, the Wachusett Aqueduct, and evaporation. The Cosgrove intake is the main outflow from the reservoir, accounting for 60% to as much as 80% of the total outflows. Water withdrawn via the Cosgrove flows to the Carroll WTP for use in metropolitan Boston. The Wachusett Reservoir also supplies water for the headwaters of the Nashua River which begins on the downstream side of the Wachusett Dam. The Nashua Spillway is used to maintain the elevation of the Wachusett reservoir; if the elevation becomes too high, water flows over the spillway and discharges into the Nashua River. The most significant outflows consist of the Cosgrove Intake, the Nashua River release, and the

Nashua Spillway, which account for 77% to as much as 95% of the total outflows. Figure 1.5 shows the major outflows from the Wachusett Reservoir, with daily flows on the y-axis over the entire year by date on the x-axis. A secondary y-axis is used to show the daily water surface elevation of the reservoir. A full account of all outflow graphs for all years are presented in Appendix A.

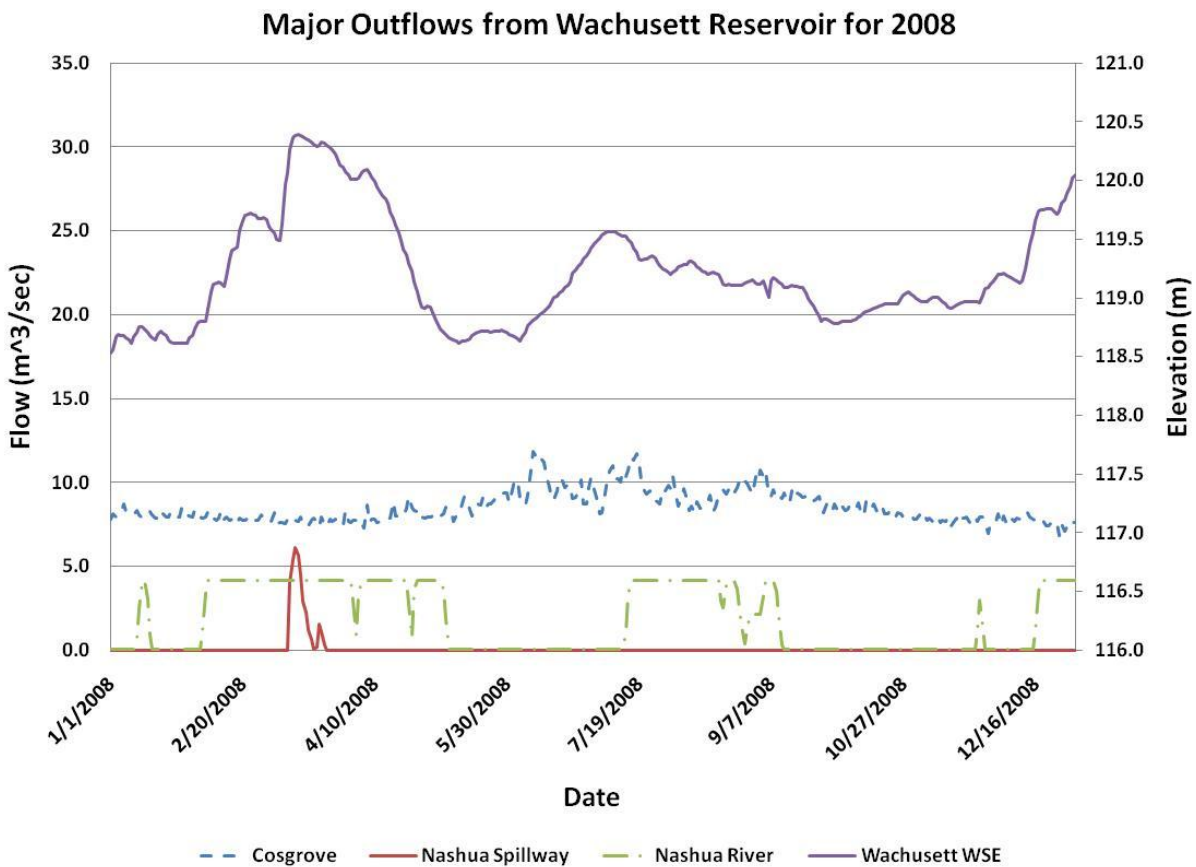


Figure 1.5: Water surface elevations and major outflows from the Wachusett Reservoir 2008

1.2.2 Data Collection

Hydrodynamic and water quality data are required in order to develop the hydrodynamic and water quality models. Flow through the Quabbin Aqueduct is measured by the MWRA because

they control the flow to meet the demand. Flows in the two major tributaries (Stillwater and Quinapoxet Rivers) are measured by the United States Geological Survey (USGS) through gages located on the rivers. The gage readings are recorded every fifteen minutes, supplying a good temporal resolution of the flow data. The other tributary flows are calculated, as described further in the CE-QUAL W2 Model Development section. Precipitation is measured at a weather station located at the Worcester Airport. Note that there is a weather station located on the Wachusett Reservoir, however it has been found that it is not consistently functional and has not always captured precipitation for the entire year. Reservoir outflows are measured or estimated by MWRA, who supply UMass with the data.

Water quality measurements are taken within the reservoir periodically throughout the year by the DCR team going out on a boat to collect water samples in the North Basin and at other locations. Measurements are taken more often, about once per week, from May to August due to warmer weather and the desire for frequent assessment of algal activity. Other measurements are taken in the spring and fall months, but less frequently, about every 2 weeks, while no measurements are taken in the winter months when there is ice cover. The water quality parameters that are measured include temperature, specific conductance, dissolved oxygen, and pH. These measurements are taken at one meter intervals with depth, providing a profile of water quality. Profiles during the year show transitions between destratified and stratified conditions with respect to temperature.

Tributary water quality data are also collected by the DCR team. Measurements are taken about once per week and include measurements of *Escherichia coli*, fecal coliform, specific conductance, temperature, and turbidity.

2 BACKGROUND

2.1 Modeling

Computer modeling is used throughout all disciplines involving science and engineering in order to help understand a variety of problems. For this report, hydrodynamic and water quality modeling are of interest. Hydrodynamic computer models use numerical methods to simulate water flow and temperature using equations from physics and thermodynamics. Models may be used to assess how many people may be able to be served by a given body of water, simulate how a river or reservoir may respond to a one hundred year storm, identify the transport of a water molecule to determine hydraulic residence time, and many other purposes. Water quality models simulate concentrations of constituents such as contaminants, nutrients, and microbes within a body of water, based on equations from biology, water chemistry and physics. Models can be developed for water quality purposes to predict contaminant degradation, identify the source of contamination, help identify an effective procedure to clean up a contaminant using chemical methods, and many other scenarios. As helpful as models can be, it is important that the person or persons developing such a model have experience within the field that they are trying to model and have knowledge of all the model parameters in order to appropriately understand and interpret model results. If model parameters are not estimated properly, model results may not be applicable.

2.2 CE-QUAL W2

CE-QUAL W2 is a two-dimensional, laterally averaged, hydrodynamic and water quality model using finite difference approximations. This model is most applicable for long narrow water

bodies because the model is laterally averaged; however, it has been applied to many different applications for rivers, lakes, reservoirs, and estuaries.

CE-QUAL W2 Version 1.0 was initially developed in 1975 by Edinger and Buchack, however, the name of the model at the time was LARM (Laterally Averaged Reservoir Model) (Coles and Wells, 2008). With the help of the Water Quality Modeling Group at the US Army Corps of Engineers Waterways Experiment Station, new water quality algorithms were applied to LARM which resulted in CE-QUAL W2 Version 1.0. Additional versions were created in order to improve calculation accuracy and decrease computation time relative to the prior version. The current model available is CE-QUAL W2 Version 3.6.

CE-QUAL W2 was chosen for this project due to the long narrow geometry of the Wachusett Reservoir, and because of the short model run time. The latest model is used because of greater accuracy, shorter computational times, and the fact that Version 3.5 files (model version used in most recent UMass work) are compatible with Version 3.6. For a full account of model updates, see the CE-QUAL W2 user manual by Cole et. al. (2008) available at www.cee.pdx.edu/w2/.

2.3 Literature Review

The purpose of this section is to present past work involving CE-QUAL W2 in order to present the potential range of applications of the two dimensional model. The UMass/DCR project uses CE-QUAL W2 to model the hydrodynamics and water quality of the Wachusett Reservoir in order to determine worst case scenarios of a spill using a conservative tracer, however, in many cases, this model is applied to simulate water quality issues to help identify water quality management strategies.

Water quality problems are found throughout the world in lakes, reservoirs, rivers, and the ocean. The Neuse River Estuary (Neuse) in North Carolina has been plagued with high chlorophyll-a and low dissolved oxygen concentrations for almost 30 years (Bowen and Hieronymus, 2003). The Neuse is the second largest watershed in North Carolina, approximately 16,000 km² in area. Bowen and Hieronymus were charged with developing a model in order to evaluate a total maximum daily load (TMDL) for the watershed, which will be used to determine actions required to eliminate the water quality problems. Many models were considered, both two and three dimensional, but in the end CE-QUAL W2 Version 2.0 was selected mainly because of the relative simplicity and short run times. Bowen and Hieronymus (2003) modified the code to calculate parameters that CE-QUAL W2 did not include, such as: allowing the simulations of three separate algal groups; adding a predictive model of light attenuation; and modifying a predictive sediment model to include two additional state variables and a sediment denitrification feature. The river was simulated from June 1, 1997 to December 31, 2000, using June 1997 to December 1999 for calibration of parameters, while January 2000 to December 2000 was used for a model verification exercise. The results of the TMDL analysis found that a 5% reduction in nutrient loading would eliminate water quality impairment for chlorophyll-a by lowering water quality exceedances below 10%; however, even a 30% reduction in nutrient loading would not eliminate the other water quality exceedances, with exceedances of approximately 5% (Bowen and Hieronymus, 2003). In order to apply this method for other models, the model residual, defined as the logarithmic difference of the predicted and observed chlorophyll a concentrations, is required to be unbiased and normally distributed, however, it was found that the model residuals were neither unbiased nor normally distributed.

A model was developed for the Patuxent estuary (Patuxent) in Maryland in order to address impacts of current and projected land use changes on water quality (Lung and Bai, 2003). There were two previous modeling studies conducted for the Patuxnet; Hydrosience (1981), and a model developed by Lung (1990, 1992) (Lung and Bai, 2003). Both models, however, could only calculate water quality without any hydrodynamic modeling, and the previous models had to be linked with a separate hydrodynamic model. With improved hardware and software, CE-QUAL was later selected for the study because it could simulate both hydrodynamics and water quality simultaneously. The model simulation ran from August 1, 1997 to July 31, 1998. The model was able to estimate hydrodynamic and water quality properties within satisfaction. There were two scenarios that were used in the calibrated model from scenarios based on a paper written by Weller et al. (2003): double developed and point source, and halve crop, developed, and point source (Lung and Bai, 2003). The two scenarios deal with possible changes in water and material discharges for the entire Patuxent watershed under alternate watershed scenarios, where their names describe the changes in alternate watershed scenarios. The double developed and point source scenario resulted in a total nitrogen increase of 135%, a total phosphorus increase of 124%, and a sediment oxygen demand increase of 20%. The halve crop, developed, and point source scenario resulted in a total nitrogen decrease of 52%, a total phosphorus decrease of 55%, and a sediment oxygen demand decrease of 25% (Lung and Bai, 2003). This study was used as a baseline to identify how the Patuxent would respond to certain scenarios under 1997-1998 conditions.

The Feitsui Reservoir (Feitsui) has been declining in water quality in the past decade or so based on the trophic state index (TSI) proposed by Carlson (1977) (Kuo et al., 2003). A CE-QUAL W2 model was developed by Kuo et al. (2003) to determine water quality management strategies

on the Feitsui. The model was run from the beginning of calendar year 1996 to the end of calendar year 1997, where 1996 was used for model calibration and 1997 was used for model validation. The model was able to predict water temperature and water quality parameters within the range of measured data, which were considered satisfactory results. The model verified previous claims of phosphorous being the limiting nutrients in the Feitsui, so water quality management strategies were focused on the reduction of phosphorous within Peishih Creek, which was found to contain the majority of the nutrient reaching the Feitshu. The model found that if the phosphorous load was reduced by 50% then the lake would switch trophic state from eutrophic/mesotrophic to oligotrophic (Kuo et al., 2003). The results of this study were useful in identifying limiting nutrients, the major sources of nutrient loading, while also identifying criteria for nutrient reduction strategies.

The Mingder Reservoir (Mingder) located in Taiwan has water quality that varies between mesotrophic and eutrophic, as determined using the TSI method (Liu, 2008). A water quality model using CE-QUAL W2 Version 3.0 was developed by Wen-Cheng Liu et. al. (2008). Two calendar years were simulated, January 1, 2003 to December 31, 2004. A similar finding was found for the Mingder as for the Feitsui, where phosphorous was identified as the limiting nutrient with the majority of the nutrient loading in the main inflow. Using a similar method as Kuo et al. (2003), it was determined that reducing the phosphorus load by 20% would improve the Mingder trophic state to mesotrophic and a 80% total phosphorus reduction would improve the trophic state to oligotrophic (Lui and Chen, 2008). From these results, watershed water quality management strategies were established to be implemented in the future.

2.4 Past UMass Work

Camp, Dresser & Mckee, Inc., along with FTN Associates, LTD, originally modeled the Wachusett Reservoir using CE-QUAL W2, calibrated for calendar years 1987, 1990, and 1992 (CDM, 1995). The model was later obtained by UMass, where Alejandro Joaquin (2001) developed a water budget on a daily time scale and constructed new models for calendar years 1998 and 1999 to model the effects of the Quabbin transfer on the Wachusett Reservoir composition (Tobiason, 2002). Daniel Butrick (2005) developed models for calendar years 2001 to 2002, where he updated the CE-QUAL W2 source code to include light induced decay of UV_{254} absorbance as part of the modeling of natural organic matter. Thomas Matthews (2007) developed models for calendar years 2003 and 2004 to model the fate and transport of fecal coliform due to a sewage pump station overflow. Matthews also modified the CE-QUAL W2 v.3.5 source code to include light induced coliform decay. Christina Stauber (2009) used the model years 2003 and 2004, developed by Matthews, to examine the behavior of a spill of ammonium nitrate and fuel oil number 1 under different wind conditions, temperatures of the spill, and state of the Quabbin transfer. Stauber modified the CE-QUAL W2 v.3.5 source code to include volatilization to better simulate benzene. Bryan Sojkowski (2011) developed models for calendar years 2005 and 2006 using new CE-QUAL W2 v.3.6, while also converting models for 2003 and 2004 from version 3.5 to version 3.6. Sojkowski used modeled years 2003 to 2006 to simulate a conservative tracer spill and analyze the arrival time and behavior of the spill at the Cosgrove Intake, while identifying similarities between arrival times for all years for the Spring, Summer, and Fall seasons. This report expands on the spill behavior modeling efforts.

3 CE-QUAL W2 MODEL DEVELOPMENT

Model results are very important, however, it is equally as important to understand how models are developed. The purpose of this section is to describe the development of CE-QUAL W2 models for calendar years 2007 and 2008. A large portion of project work consists of developing and calibrating the models, so it is necessary to document the process.

3.1 CE-QUAL W2 Grid and Segments

Camp, Dresser, and McKee (CDM) developed the original modeling grid for the Wachusett Reservoir in 1994 (CDM, 1995), which it was later updated by Joaquin (Joaquin, 2001). The original grid consisted of 26 layers and 62 segments, while the updated grid consists of 47 layers and 64 segments. The Joaquin grid is shown in Figure 3.1 and Figure 3.2. Figure 3.1 presents a top view of the segments, where the main body of the reservoir consists of segments 2 through 46. The South Bay is represented by segments 49 through 51. Segments 54 through 62 represent the wide portion of the reservoir which would not be accurately represented by increasing the width of the main body segments.

The reservoir grid captures key features of the Wachusett Reservoir. Segment 15 is much narrower than the adjacent upstream and downstream segments to simulate the constriction of the reservoir due to the Route 12 Bridge. Segment 39 is not as wide as its surrounding segments to represent the Narrows, which separates the South Basin from the North Basin. Another key feature is Segments 45 and 46, where Segment 45 represents the cofferdam which was built in order to keep water out during the construction of the Cosgrove Intake. When construction was completed, only the top was cut off to allow water to flow into the Cosgrove Intake, leaving most of the cofferdam and a relatively shallow water depth. Segment 46 represents the area adjacent

to the Cosgrove Intake, where CE-QUAL withdraws water that flows to the Carroll Water Treatment Plant.

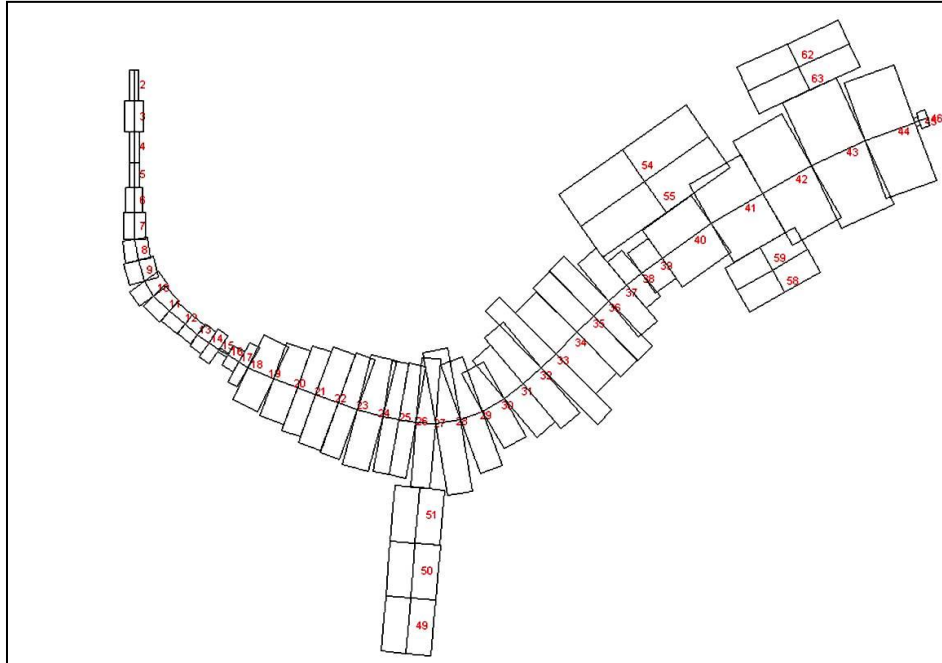


Figure 3.1: CE-QUAL W2 top view of segments.

Figure 3.2 presents a profile view of the model grid, showing the layers and their thickness. The top 31 layers are 0.5 meters thick, layers 32 and 33 are 0.75 meters thick, and layers 34 through 47 are 1.5 meters thick. The layers are labeled from top to bottom, where layer 1 is the top of the reservoir and layer 47 is the bottom. Finer grid layers at the top of the reservoir were created to better simulate the thermocline in higher resolution.

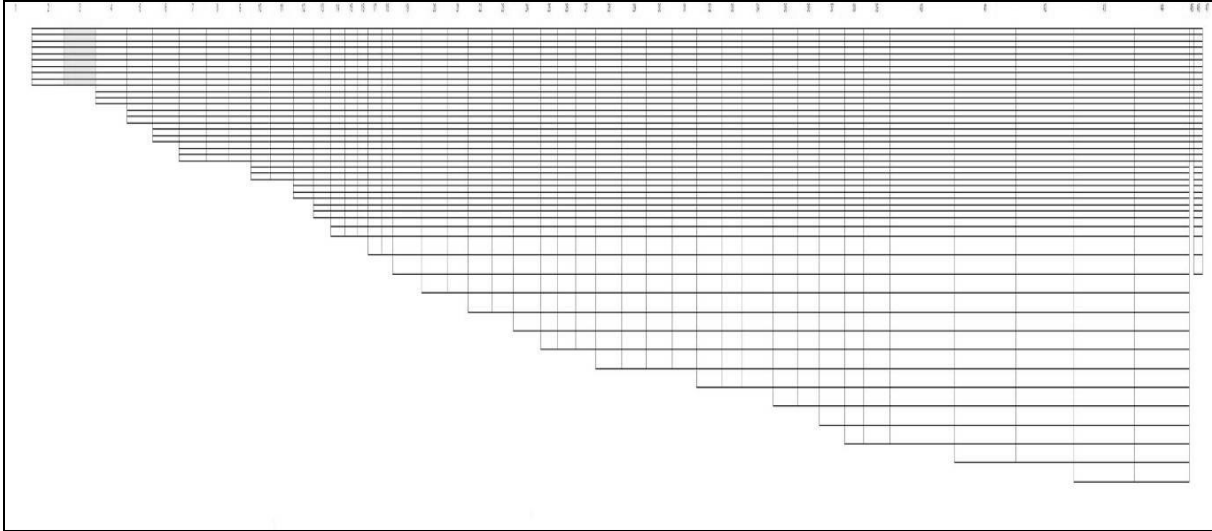


Figure 3.2: CE-QUAL W2 profile view of layers

3.2 Data Collection

The collection of appropriate temporal resolution hydrodynamic and water quality measured data is essential to produce an accurate, calibrated, model. Data needed for this project include reservoir inflows and outflows, meteorological conditions, and water quality, including specific conductance. The raw data are converted into files that can be read by the CE-QUAL W2 algorithm.

3.2.1 Meteorological Data

Meteorological data were acquired from the National Climatic Data Center (NCDC) website, where weather station data from across the world are gathered and available for public use.

Worcester Airport weather station is the closest (about ten miles southwest) available weather station to the Wachusett Reservoir, and is assumed to have similar weather conditions as occur at Wachusett Reservoir. The required meteorological data include air temperature, dew point

temperature, wind speed, wind direction, and cloud cover; measurements are recorded every fifteen minutes.

The only calculation needed to process the NCDC data is for cloud cover. NCDC uses descriptive words for cloud cover: clear, scattered, broken, and overcast. CE-QUAL W2 requires that the input data for cloud cover be in the range from zero to ten, with zero being clear and ten being total cloud cover. Therefore, the descriptive cloud cover words were translated into numerical values, as shown in Table 3.1.

Table 3.1: Cloud Cover Data Conversion

NCDC Cloud Cover Description	Numerical Equivalent (0-10)
Clear	0
Scattered	3.125
Broken	7.5
Overcast	10

3.2.2 Water Balance

A water balance model was developed in the Excel software spreadsheet by Kennedy (2003), in order to calculate water surface elevation based on daily inflows and outflows for the Wachusett Reservoir. As stated previously, four of the major inflows are measured directly: Stillwater and Quinapoxet Rivers are measured using USGS gages, Quabbin Aqueduct is measured by MWRA, and precipitation is measured at the Worcester Airport weather station. There are no recording gages on the other tributaries, therefore, flows for the other six tributaries and direct runoff are calculated using a runoff coefficient multiplied by the tributary area. The runoff coefficient is based on the Stillwater River and is the ratio of its flow to watershed area.

$$Tributary\ Flow = \left(\frac{Stillwater\ Flow}{Stillwater\ Watershed\ Area} \right) * TributaryArea$$

All of the outflows are measured by the MWRA, except for evaporation, which is calculated to develop an accurate water balance. Loss by evaporation is calculated based on surface temperature, dew point temperature, and wind speed, as presented in Equation 1. This equation is based on calculations made in CE-QUAL W2.

$$Q_{evap} \left(\frac{m^3}{s} \right) = \left\{ \beta \left(\frac{mmHg}{^{\circ}C} \right) * [Surface\ Temp(^{\circ}C) - Dew\ Temp(^{\circ}C)] * f(W) \left(\frac{W}{m^2\ mmHG} \right) \right\} * 0.006417 \left(\frac{m^5}{W\ s} \right) \quad Eq.(1)$$

Using the daily inflow and outflows, the water balance spreadsheet calculates the daily changes in reservoir storage volume based on a known initial total volume on January 1st of each year.

The water surface elevation (WSE) is calculated based on a Wachusett capacity versus elevation equation that was determined from capacity and elevation information provided by MWRA and can be seen in Appendix B.

Figure 3.3 and Figure 3.4 show the difference between the uncalibrated calculated WSE from the water balance and the measured WSE (from MWRA) for calendar years 2007 and 2008, respectively. It should be noted that the calculated and measured WSE do not match perfectly due to error or uncertainties in measured and calculated inflows and outflows. To correct this problem, calibration is needed as discussed later in this section of this report.

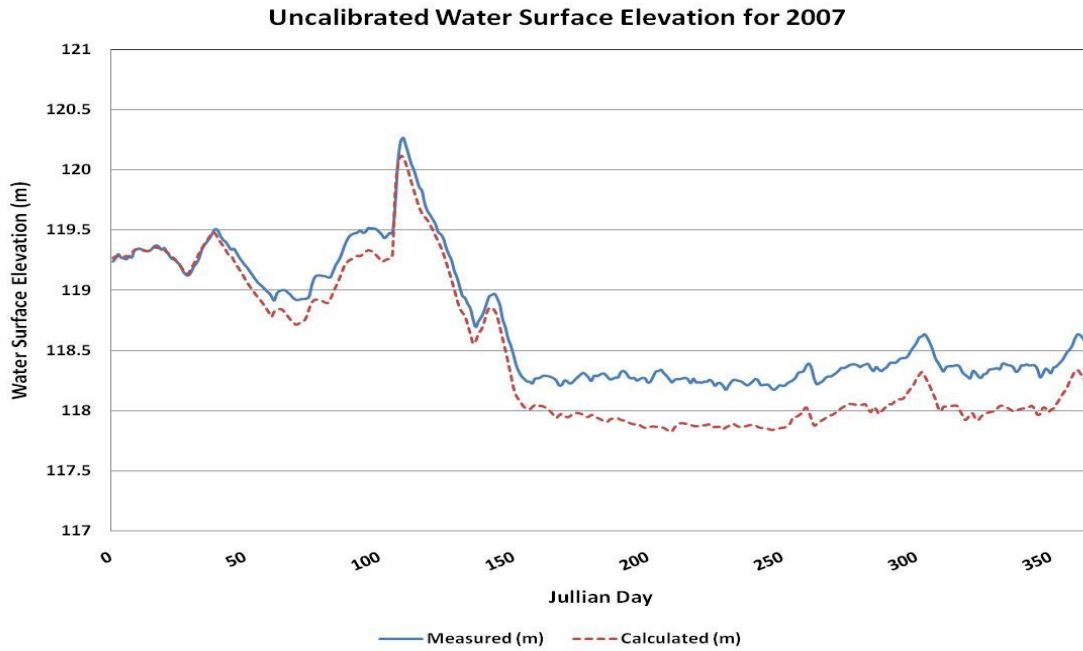


Figure 3.3: Measured and uncalibrated calculated WSE for 2007

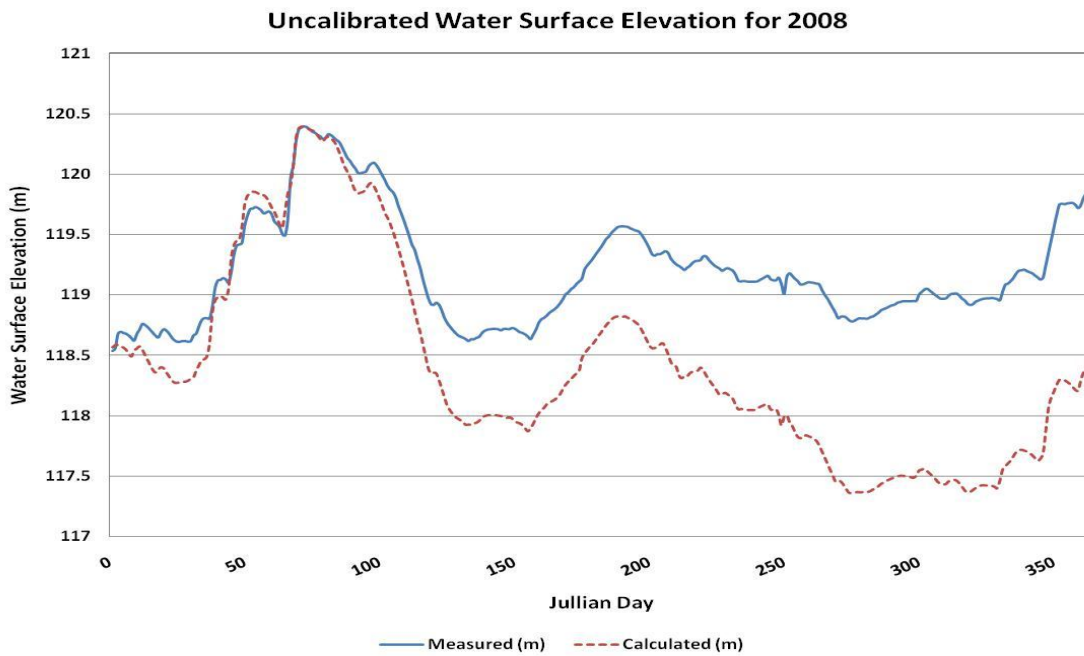


Figure 3.4: Measured and uncalibrated calculated WSE for 2008

3.2.3 Specific Conductance/TDS

Specific conductance is a measurement of the ability of water to conduct electricity. CE-QUAL W2 models the total dissolved solids (TDS) concentration in the water. The relationship between specific conductance and TDS is greatly affected by the types of dissolved solids in the water, however Matthews (2007) established a relationship which is based on a constant relative ionic composition, presented in Equation 2. Equation 2 is used to convert measured specific conductance to TDS for model inputs and calculated TDS to calculated specific conductance for comparison of model output to measured specific conductance.

$$TDS \left(\frac{mg}{L} \right) = 0.6 * Specific\ Conductance \left(\frac{\mu S}{cm} \right) \quad Eq.(2)$$

3.3 Calibration

Models rarely simulate reality well enough to be used without calibration due to possible errors in measured inputs and because many equations have variable parameters to describe the physical description of the environment or other physical/chemical attributes. Calibration is conducted to create a model with realistic simulations and predictions; this requires measured data to compare to the model simulations. During the calibration process, conducting a sensitivity analysis is a good way to identify the influence of certain parameters. A sensitivity analysis involves varying only one parameter over a range of values to identify the impact of that parameter on model outputs.

3.3.1 Water Balance Calibration

The water balance spreadsheet has multiplier calibration factors that can be applied to each inflow to account for error and variability of the data. Calibration factors are applied to inflows

only because the inflow measurements are considered to be less accurate due to stream gage measurements while outflows are measured at the defined outflows. The calibration factors are set to a default value of 1.0; a calibration factor of 1.1 increases the flow by 10%. Using the SOLVER function in Excel, the calibration factors are variable with constraints set to not let them vary beyond a selected specific amount, typically no more than 30%. The Quabbin Aqueduct inflow is only allowed to vary as much as 15% because it is a measured controlled flow. The calibration is used to minimize the sum of square residuals (SSR) for water volume simulation which is calculated as follows:

$$SSR = \sum (Measured\ Volume - Calculated\ Volume)^2$$

Calibration factors have been calculated for calendar years 1994 to 2008 and vary about 10% on average, with exceptions in some years due to unaccountable errors in measured data. Table 3.2 presents average calibration factors for 1994 to 2006, the historical ranges, and the calibration factors used for creating the 2007 and 2008 models. After calibration, the calculated WSE becomes significantly more accurate as shown in Figure 3.5 for 2007 and Figure 3.6 for 2008. Figure 3.7 shows the differences between the calibrated and measured WSE, where a value of zero means that the calibrated WSE equals the measured WSE. The largest difference in calibrated and measured WSE is 0.45 meters, which is within an acceptable range; the goal is for all differences to be less than 0.15 meters (0.5 feet).

Table 3.2: Comparison of Range of Historical Average Calibration Factors to New Factors

Inflow	Annual Averages (1994-2006)	Range (1994-2006)	2007	2008
Quabbin Aqueduct	1.02	0.93-1.16	1.01	1.10
Stillwater River	0.99	0.7-1.28	1.04	1.02
Quinapoxet River	1.08	0.82-1.30	1.04	1.04
Wausacum Brook	1.14	0.78-1.65	1.05	1.03
Nashua River	0.95	0.76-1.04	1.06	0.94
Direct Runoff	1.13	0.76-1.62	1.05	1.03
Malden	1.09	0.78-1.35	1.05	1.03
W. Boylston	1.11	0.78-1.35	1.05	1.03
Gates	1.16	0.78-2.00	1.05	1.03
Muddy	1.09	0.78-1.35	1.05	1.03
Malagasco	1.09	0.78-1.35	1.05	1.03
French	1.09	0.78-1.35	1.05	1.03

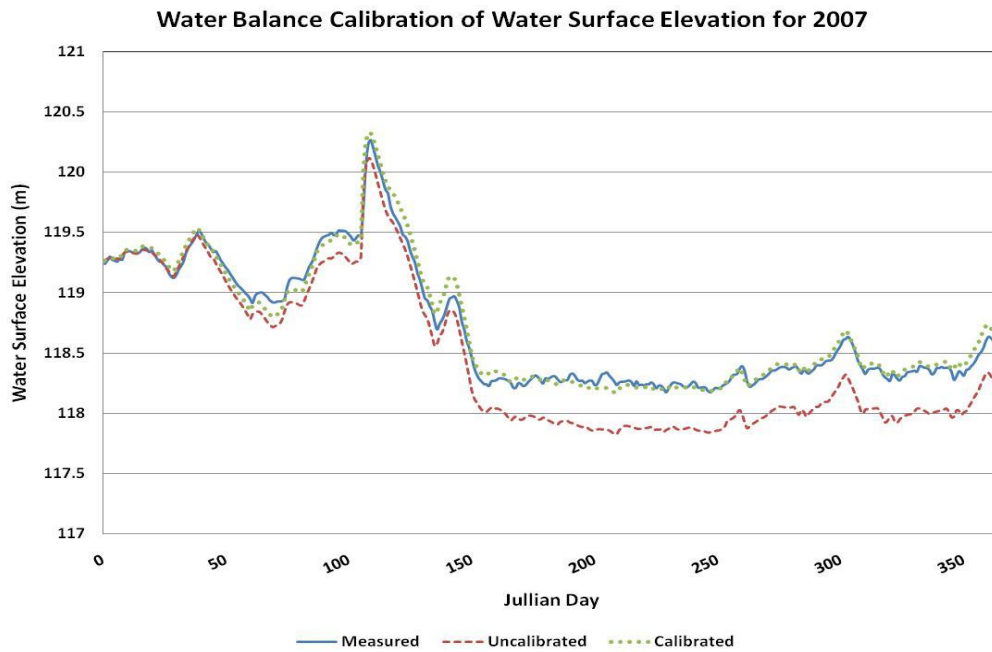


Figure 3.5: 2007 calibrated WSE simulation

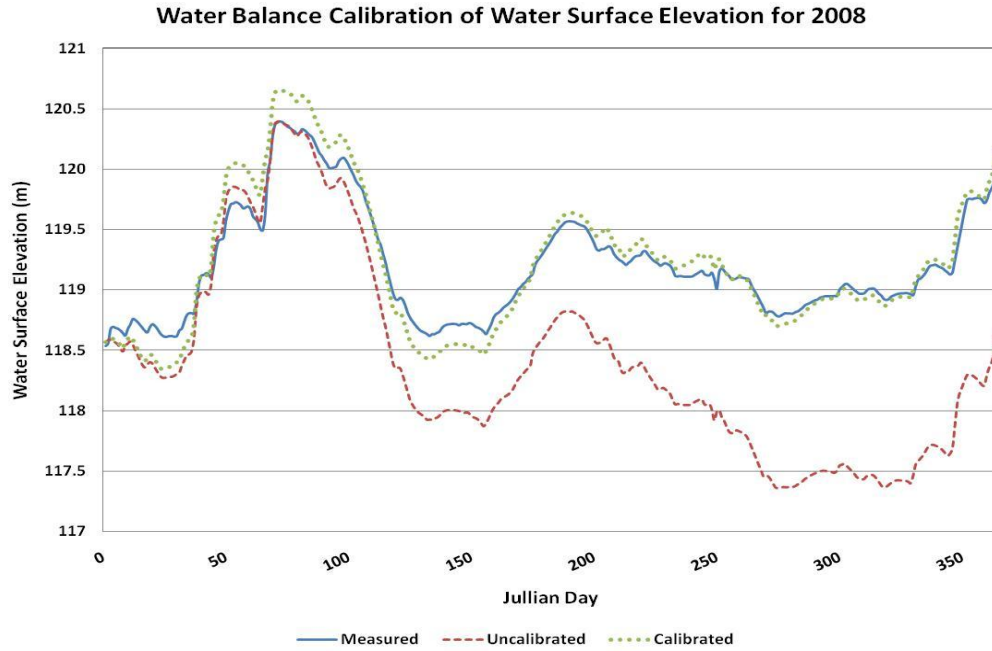


Figure 3.6: 2008 calibrated WSEsimulation

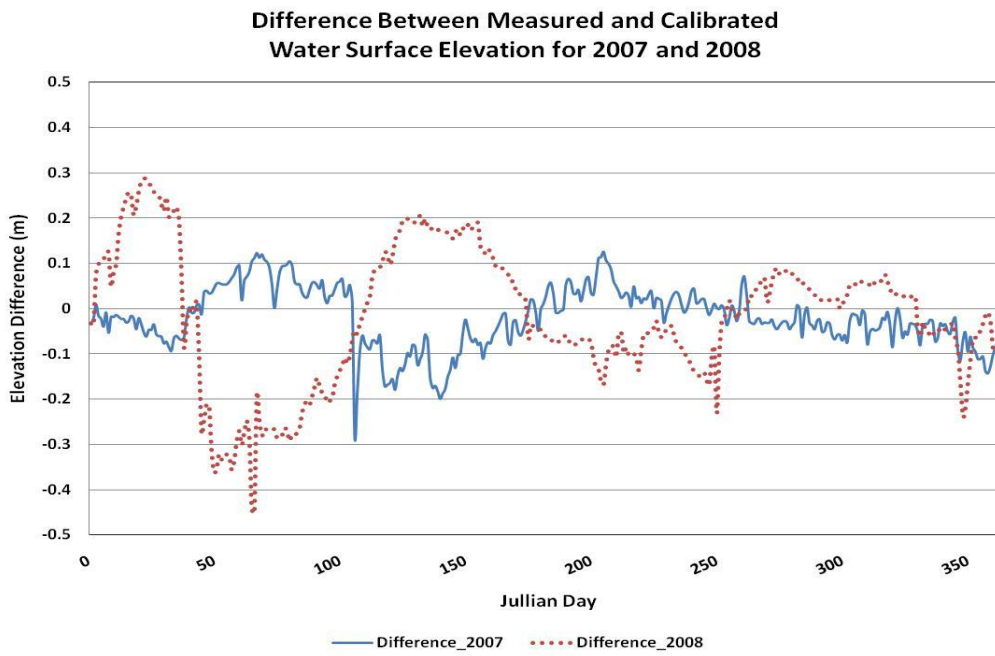


Figure 3.7: Difference between measured and calibrated WSE

3.3.2 Initial Conditions - Temperature

There are two initial condition water quality parameters that are used in calibrating the models: water temperature and TDS. The initial (January 1) temperature and TDS are applied as uniform initial conditions for the entire reservoir, implying a completely mixed condition. Initial conditions hold more significance for simulations for dates early in the year; initial conditions have less impact on simulated conditions later in the year. Estimates of the initial reservoir temperature are obtained online from an MWRA website, where temperature data taken every fifteen minutes at the Cosgrove intake are available. The average temperatures on January 1, 2007 and January 1, 2008 were 5.2°C and 2.5°C respectively.

3.3.2.1 Reservoir Temperature - 2007

A sensitivity analysis of the impact of varying the initial temperature on the simulated temperatures was conducted, as presented in Figure 3.8 and Figure 3.9. Figure 3.8 shows a sensitivity analysis for 4/10/2007, where the results show that there is a difference in the predictions of about 1°C for varying the initial temperatures from 0 to 10°C. The temperature profiles for each case are uniform, implying a completely mixed reservoir. Figure 3.9 shows the same sensitivity analysis for 6/25/2007, where it can be seen that there is little to no difference in the simulated temperature profile for the varying initial temperatures. The temperature profile shows a high temperature gradient implying that the reservoir is stratified, with high temperatures in the epilimnion and low temperatures in the hypolimnion. No difference in profiles for each case shows that the temperature in June is mostly controlled by the cumulative

effects of weather conditions to that date, with little impact of the reservoir water temperature on January 1.

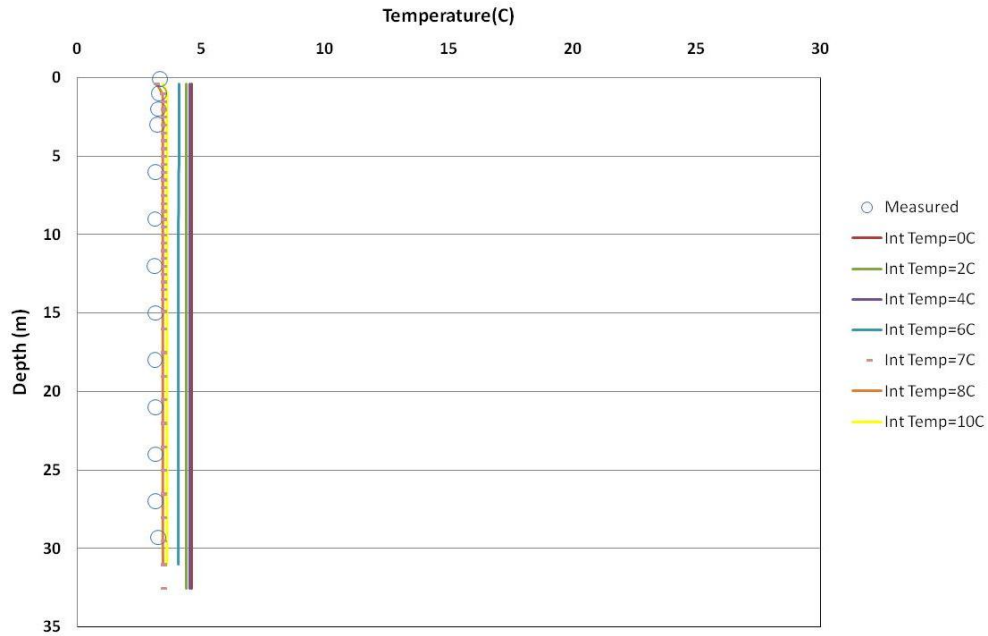


Figure 3.8: Varying initial temperature calibration, 4/10/2007

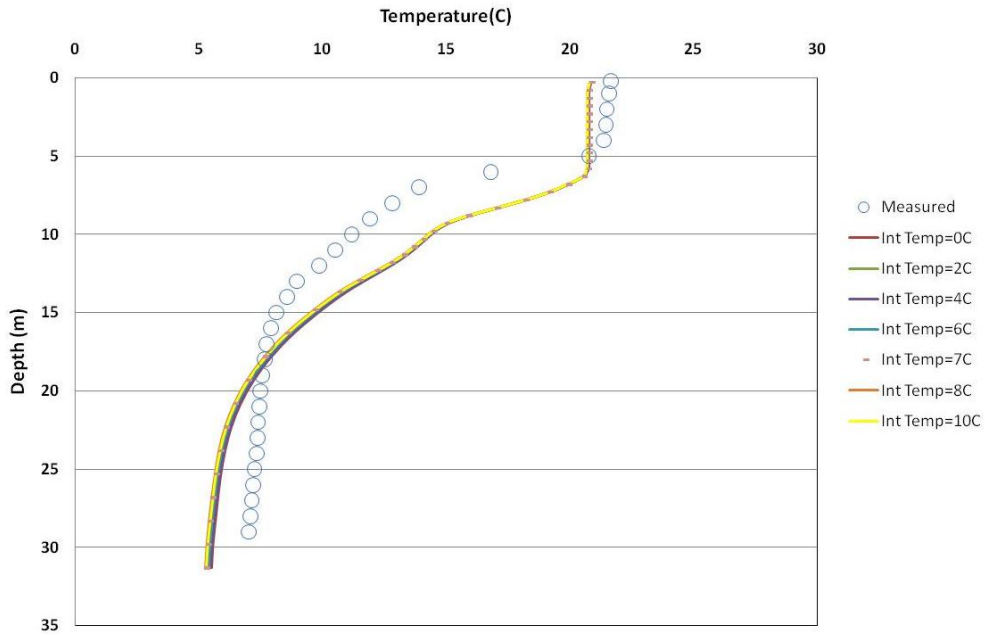


Figure 3.9: Varying initial temperature calibration, 6/25/2007

3.3.2.2 Reservoir Temperature - 2008

A similar sensitivity analysis was performed for calendar year 2008 and the results can be seen in Figure 3.10 and Figure 3.11. Figure 3.10 presents results for April 23, 2008 where it can be seen that the reservoir is beginning stratification. An odd result for early 2008 profile data is that the initial temperatures of 0°C and 2°C result in higher predicted surface reservoir temperatures on April 23 than beginning the model with higher initial temperatures; it is unclear as to why the model is producing these results, however, this effect is damped out later in the year. One possibility may be that initial warmer temperatures may cause the Spring overturn later in the year and cause cooler surface temperatures in April. The model does not capture the measured data very well, however it does capture the time of stratification well. Figure 3.11 presents results for June 26, 2008, where the initial temperature does not have any effect on the simulated profile, which indicates that the temperature of the reservoir in June is controlled by meteorological conditions in prior months. The model accurately simulates the depth of the epilimnion of about six meters.

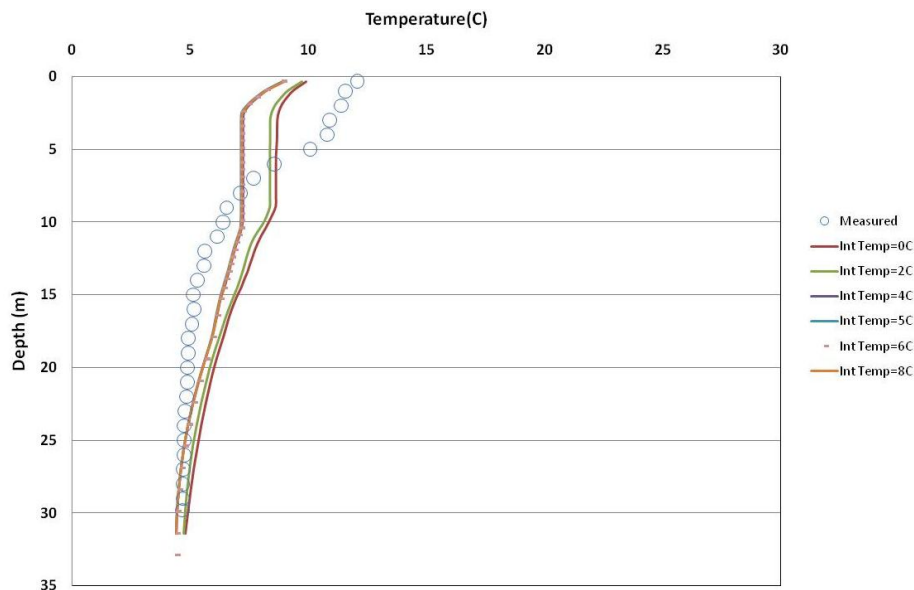


Figure 3.10: Varying initial temperature calibration, 4/23/2008

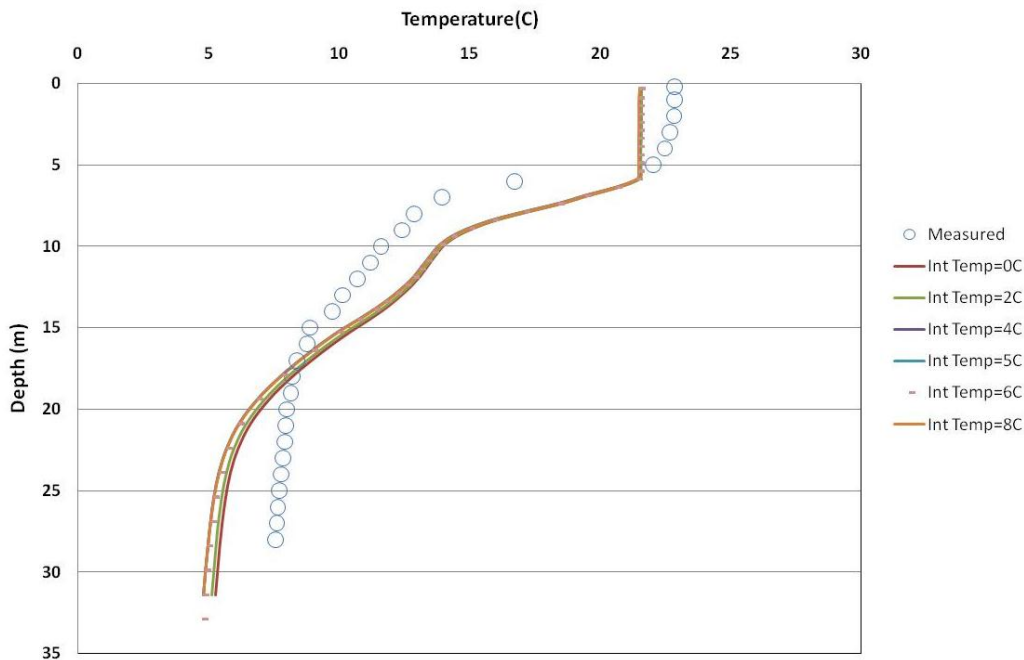


Figure 3.11: Varying initial temperature calibration, 6/26/2008

3.3.3 Initial Conditions - Specific Conductance

Specific conductance is the other water quality parameter used because of available measured data and the overall relatively conservative nature of specific conductance. MWRA also measures specific conductance at the Cosgrove Intake every fifteen minutes. The average Cosgrove Intake specific conductance values on January 1, 2007 and January 1, 2008 were 117 $\mu\text{S}/\text{cm}$ and 100 $\mu\text{S}/\text{cm}$ respectively. An analysis of the sensitivity of simulated specific conductance profiles to initial specific conductance was performed using a range of initial specific conductance from 75.0 to 166.7 $\mu\text{S}/\text{cm}$ for calendar year 2007 and 66.7 to 166.7 $\mu\text{S}/\text{cm}$ for calendar year 2008.

3.3.3.1 Reservoir Specific Conductance - 2007

The year 2007 is a special situation where there is measured data as early as January 25, 2007; Figure 3.12 presents the sensitivity analysis for that day. It would seem that an initial condition of 116.7 $\mu\text{S}/\text{cm}$ is the correct choice. However, this is not the case for later profiles, as shown in Figure 3.13 and Figure 3.14. Figure 3.13 presents the results of a sensitivity analysis of the impact of varying the initial specific conductance on the concentration profile for April 10, 2007, the next available measured data. Figure 3.14 presents the same simulations for June 25, 2007. These results show that the initial specific conductance affects results as the year progresses because specific conductance is not affected by meteorological conditions, only by the inflow and outflow specific conductance levels. It should be noted that, in Figure 3.14, a lower initial specific conductance (75.0 $\mu\text{S}/\text{cm}$) value better represents the measured values within the North Basin than a more realistic initial value of 116.7 $\mu\text{S}/\text{cm}$. It is unclear as to why a lower initial specific conductance results in a better calibration profile later in the year, however, it is believed that there may be some missing or inaccurate inflow specific conductance data. It should be noted that the specific conductance does not affect the hydrodynamics of the reservoir and is used for water quality calibration purposes only.

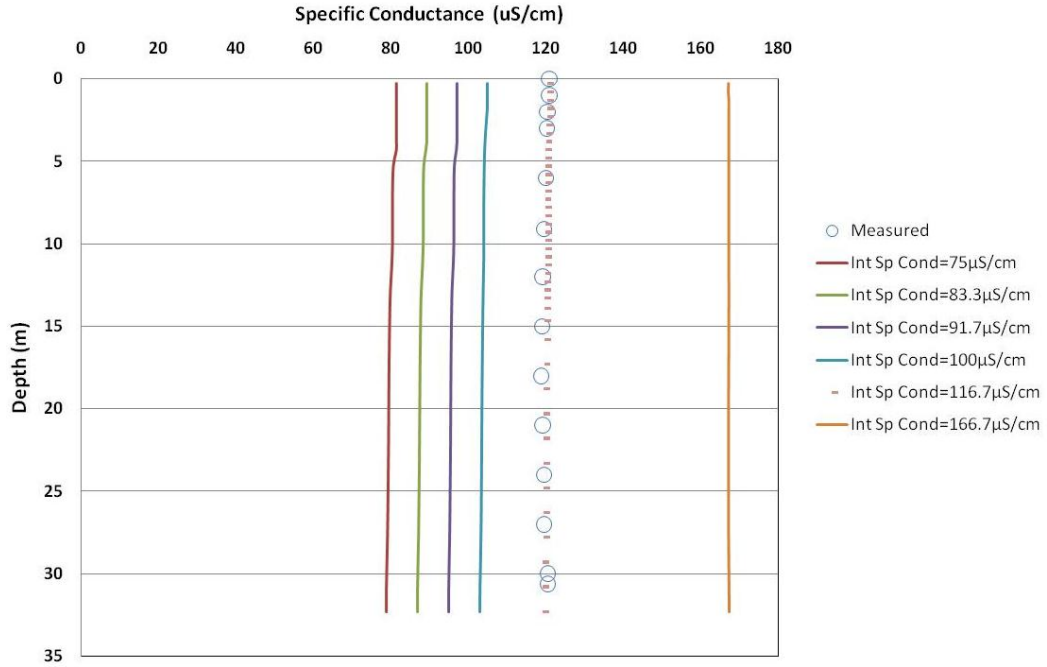


Figure 3.12: Varying initial specific conductance calibration, 1/25/2007

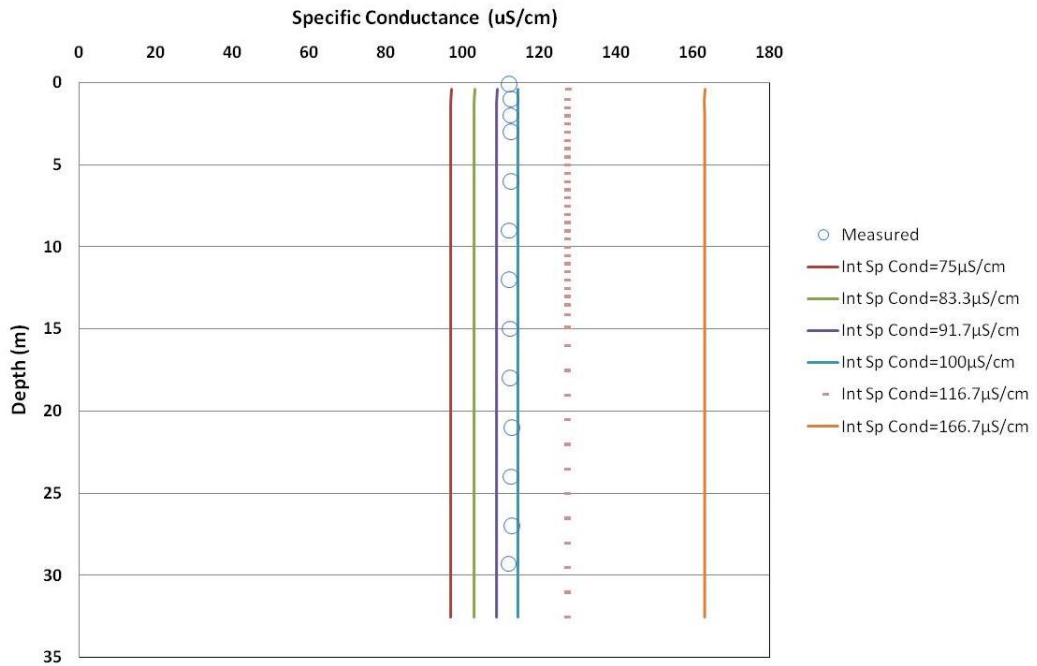


Figure 3.13: Varying initial specific conductance calibration, 4/10/2007

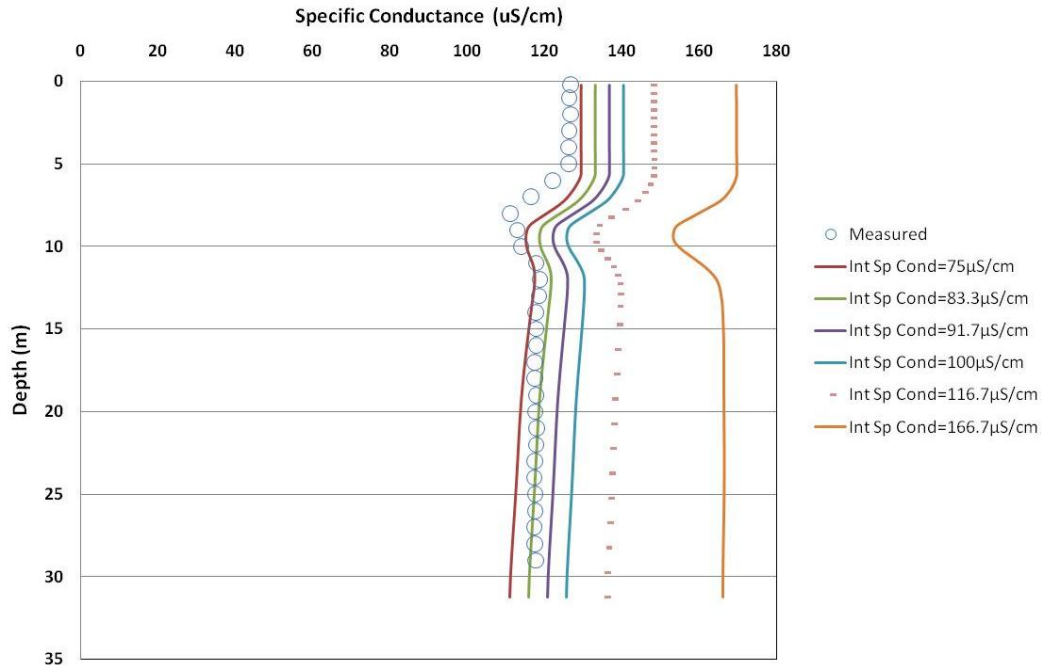


Figure 3.14: Varying initial specific conductance calibration, 6/25/2007

Through an intensive analysis, it was noted that there was an increase in simulated specific conductance between the first measurement data (January 25, 2007) and the second measurement data (April 10, 2007), while the measured value decreased about 9 $\mu\text{S}/\text{cm}$. The simulated increase varies depending on the initial condition selected because of interaction of inflows. The flow weighted specific conductance contribution from the tributaries was examined, as shown in Figure 3.15. It should be noted that the tributaries contributing insignificant amounts were removed from Figure 3.15 for presentation purposes. From this analysis it was discovered that direct runoff was a major contributor to specific conductance input to the reservoir. The direct runoff specific conductance is not a direct measurement, however, as it is calculated as the average of all the other tributaries. It should be noted that the calculated direct runoff specific conductance is not flow weighted, which could be a source of the error because some of the

tributaries have significantly higher specific conductance, such as Gates with an average specific conductance of 700 $\mu\text{S}/\text{cm}$.

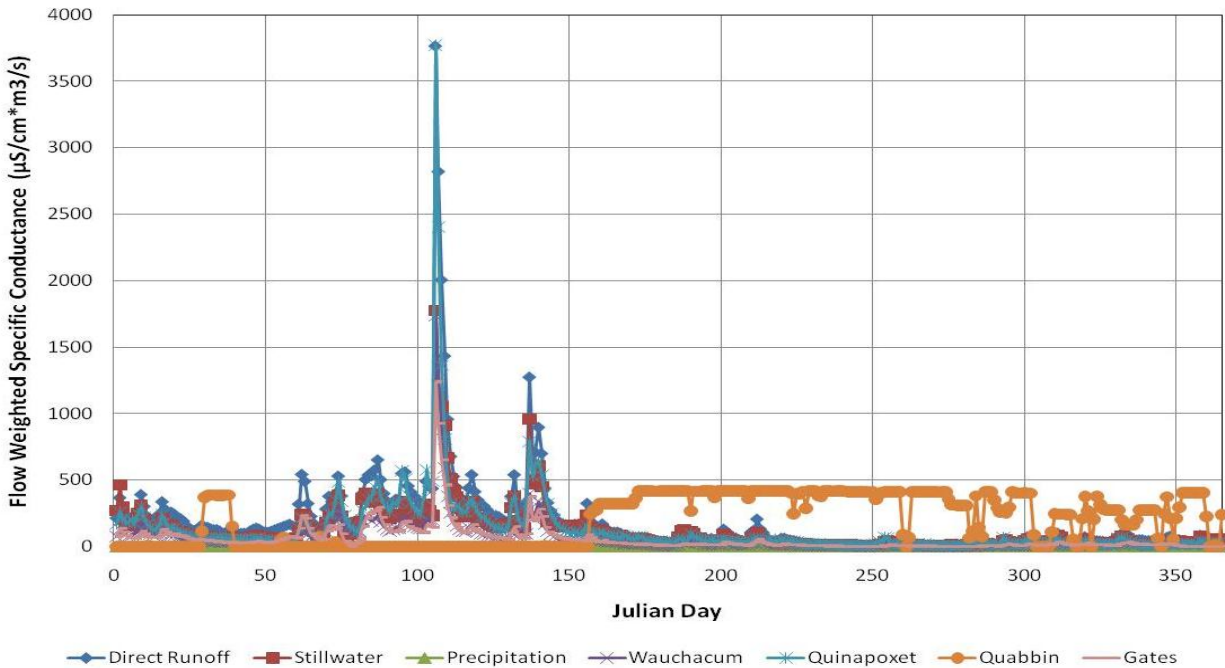


Figure 3.15: Flow weighted specific conductance of all major contributing inflows, 2007

Another possible source of the discrepancy between measured data and model results is that the instrument used to measure specific conductance may not have been calibrated correctly. In order to verify this possibility, the measurements taken automatically every fifteen minutes at the Cosgrove Intake are compared to the CE-QUAL W2 output, presented in Figure 3.16. Results for three different initial conditions (83 $\mu\text{S}/\text{cm}$, 116.7 $\mu\text{S}/\text{cm}$, and 167 $\mu\text{S}/\text{cm}$) are shown along with the measured Cosgrove data. The 83 $\mu\text{S}/\text{cm}$ initial condition best fit the measured North Basin data for the entire year, the 116.7 $\mu\text{S}/\text{cm}$ initial condition was the initial condition based on the Cosgrove Intake measurements, and the 167 $\mu\text{S}/\text{cm}$ initial condition was selected as a high

value to see how the model would respond to an extremely high initial specific conductance. When starting with an initial condition of 116.7 $\mu\text{S}/\text{cm}$, the CE-QUAL output matches the Cosgrove measured data reasonably well, however the model overestimates recorded data during the summer months, with high variability. It should be noted that the measured data spikes up at around Julian day 280, which is believed to be a recalibration of the instrument that is used to calculate the specific conductance. It is very unlikely that the actual specific conductance could spike in that fashion.

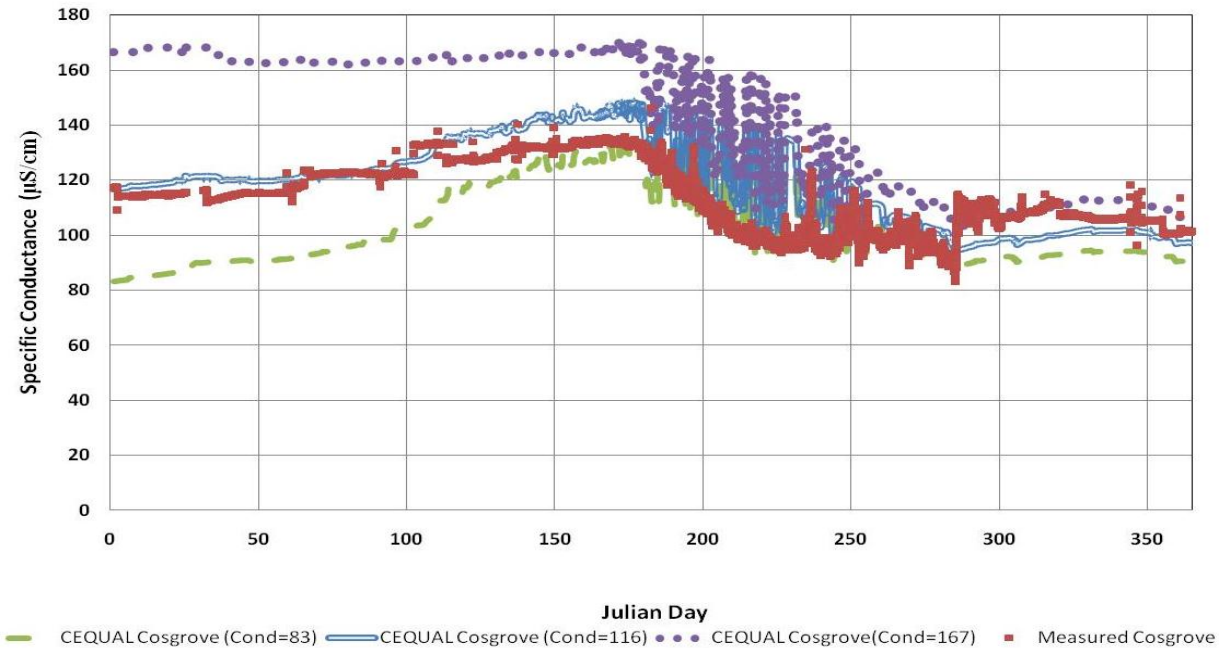


Figure 3.16: Comparing specific conductance at the Cosgrove Intake measured taken every 15 minutes with CE-QUAL W2 output for varying initial specific conductance concentration for calendar year 2007

3.3.3.2 Reservoir Specific Conductance - 2008

A similar sensitivity analysis was performed for calendar year 2008. The first available measurement data are for March 6, 2008, and the results of the sensitivity analysis for that day

are presented in Figure 3.17. The next available measurement data are for April 23, 2008, and the results are presented in Figure 3.18. An initial condition of 83.3 $\mu\text{S}/\text{cm}$ fits the measured data better than the other initial conditions, even though the measured specific conductance at the Cosgrove Intake for January 1, 2008 was 100 $\mu\text{S}/\text{cm}$. The initial condition of 83.3 $\mu\text{S}/\text{cm}$ is the best fit throughout the year, and can be seen in Figure 3.19 and Figure 3.20, where Figure 3.19 shows the results for June 6, 2008 and Figure 3.20 shows the results for September 8, 2008. In each of the figures the initial condition of 83.3 $\mu\text{S}/\text{cm}$ best represents the measured data. A similar check was performed by comparing the online fifteen minute measurements at the Cosgrove Intake to the CE-QUAL output for the entire calendar year 2008, as presented in Figure 3.21. It should be noted that the profile specific conductance measurement device may be calibrated differently than the online device, resulting in discrepancies between measurements on the same dates. The figure presents the measured Cosgrove data and simulations with initial conditions of 83.3 $\mu\text{S}/\text{cm}$ and 100 $\mu\text{S}/\text{cm}$. Interestingly the initial condition of 100 $\mu\text{S}/\text{cm}$ is a better fit than the 83.3 $\mu\text{S}/\text{cm}$ initial condition. It should be noted that the Cosgrove Intake instrument specific conductance response had some problems for this year, with some negative values as measurements and other measurements above 500 $\mu\text{S}/\text{cm}$, which have been removed in Figure 3.21 for presentation purposes.

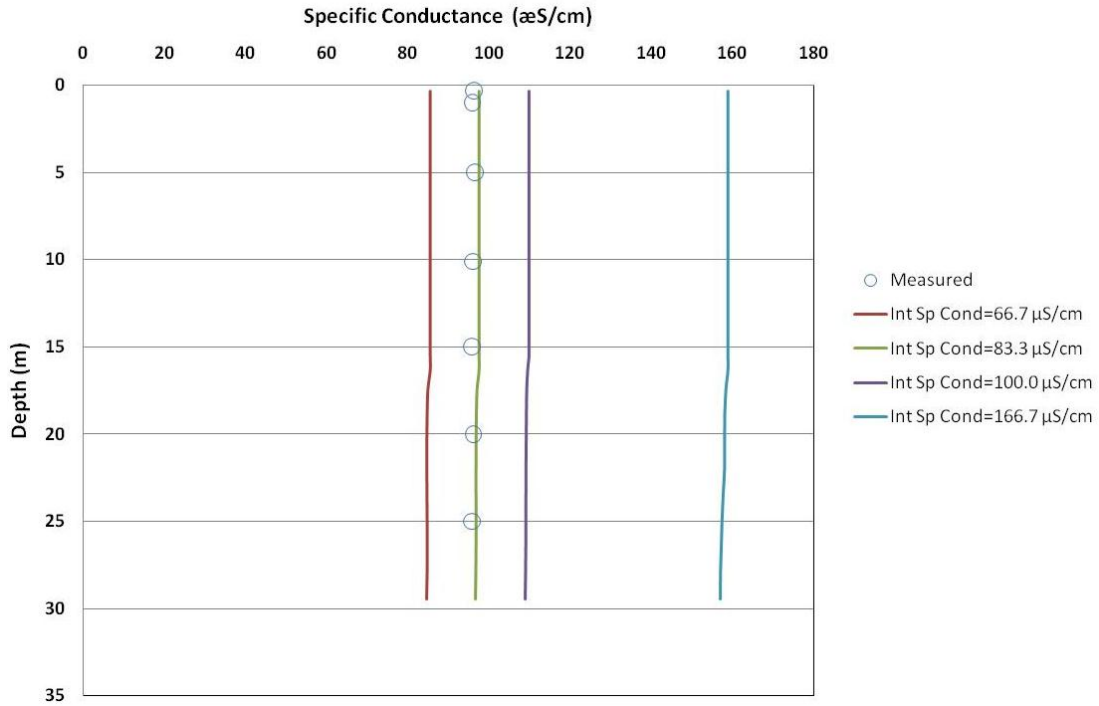


Figure 3.17: Varying initial specific conductance calibration, 3/6/2008

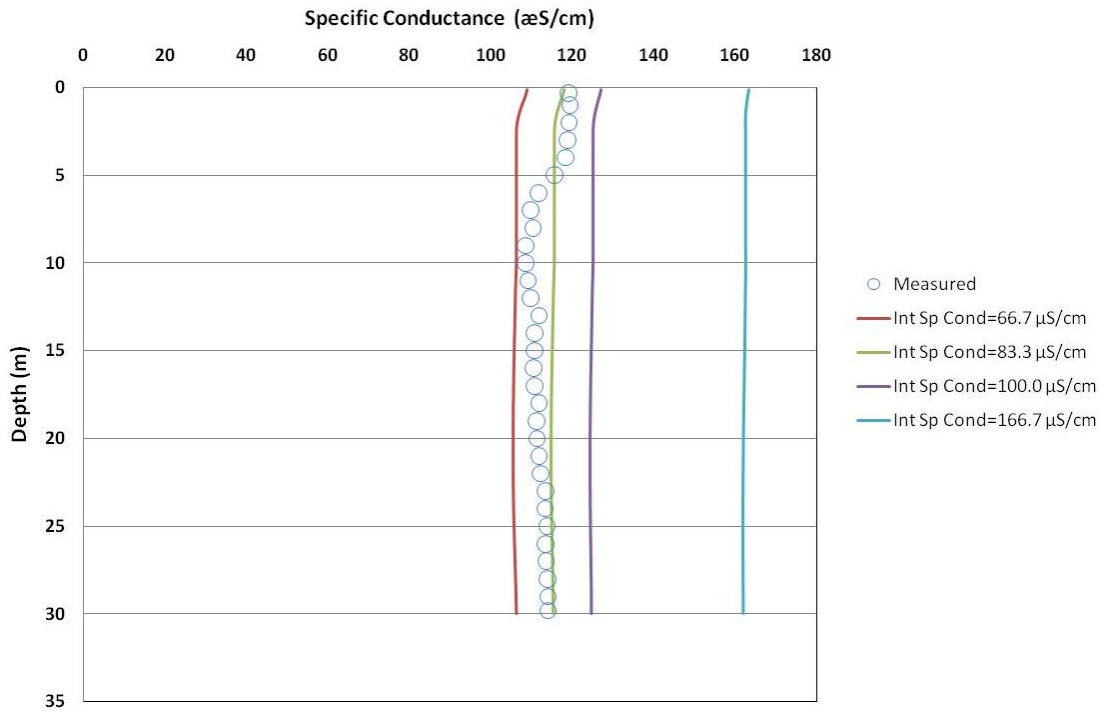


Figure 3.18: Varying initial specific conductance calibration, 4/23/2008

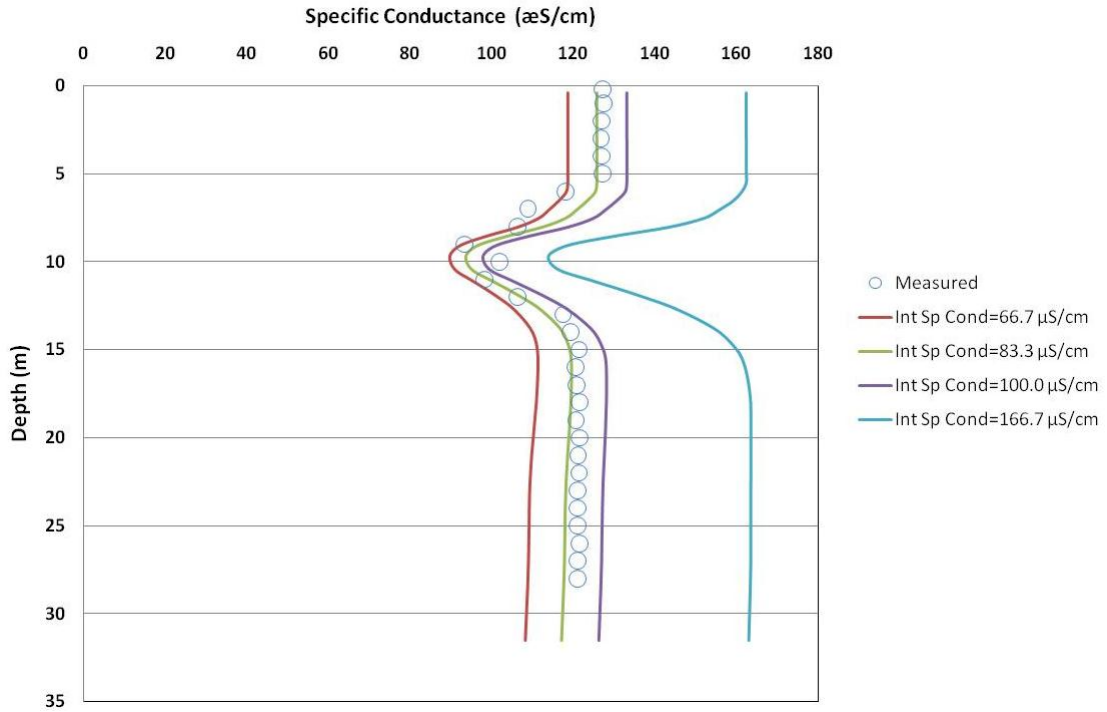


Figure 3.19: Varying initial specific conductance calibration, 6/26/2008

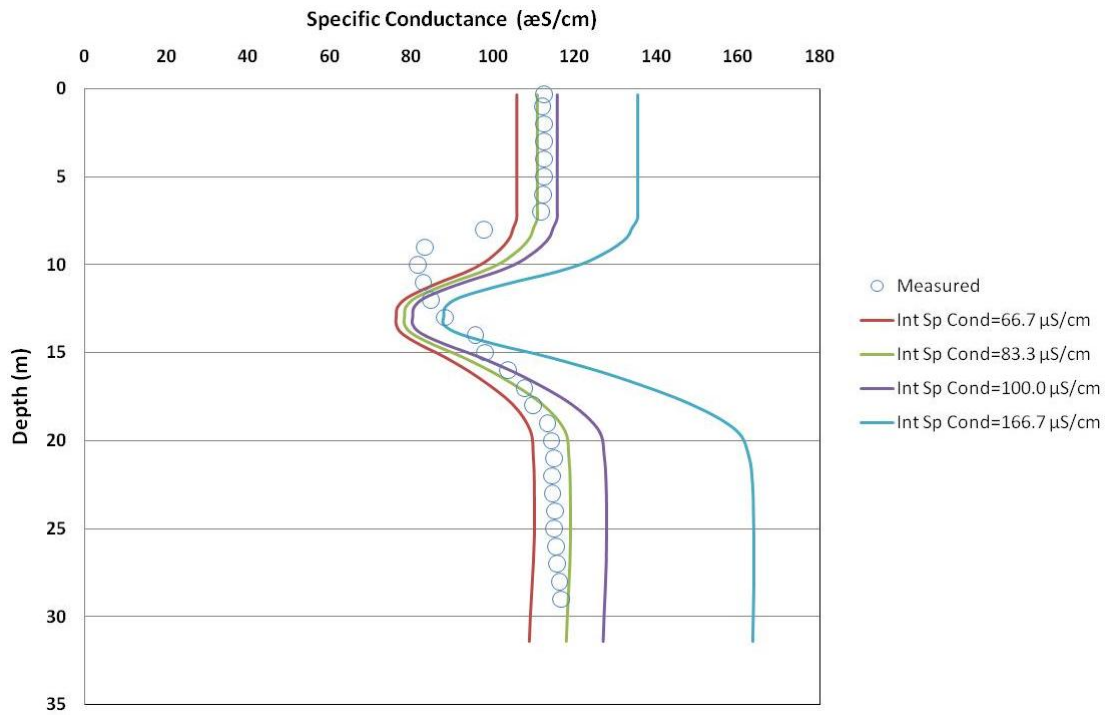


Figure 3.20: Varying initial specific conductance calibration, 9/8/2008

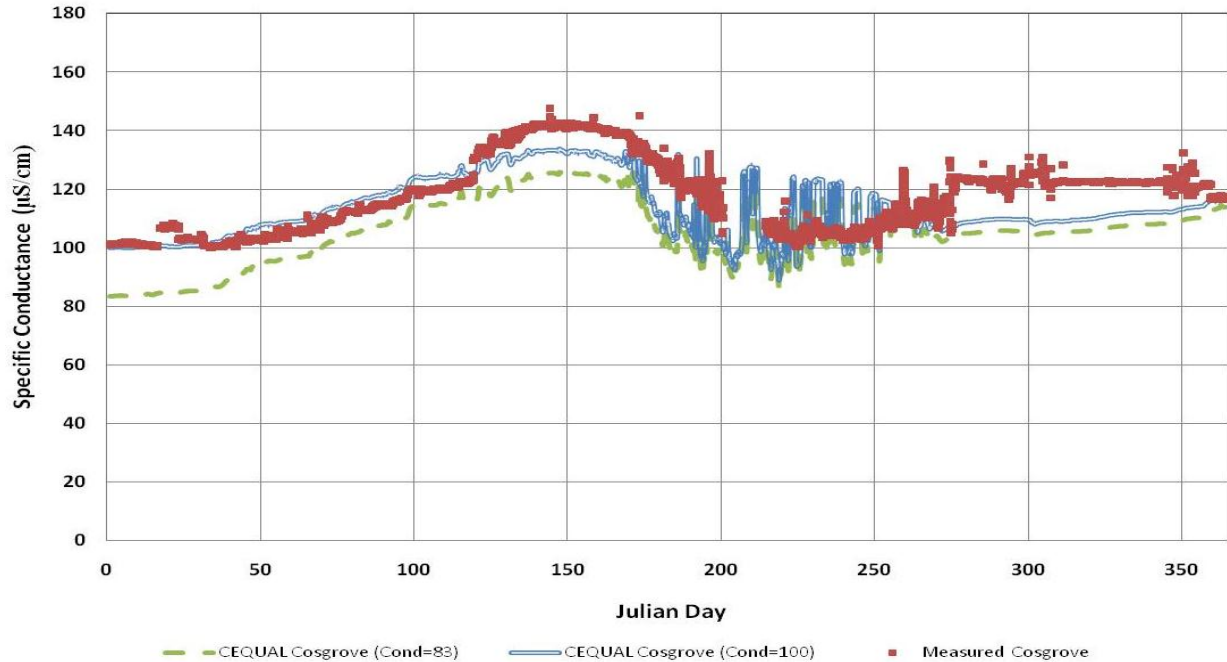


Figure 3.21: Comparing specific conductance at the Cosgrove Intake measured taken every 15 minutes with CE-QUAL W2 output for varying initial specific conductance concentration for calendar year 2008

3.3.4 Wind Sheltering Coefficient

The wind sheltering coefficient (WSC) is used to alter wind velocities at various points on the Wachusett Reservoir by describing the impacts of the surrounding landscape. Values for the WSC range from 0.0 to 1.0, where a value of 1.0 represents an open plain and a value of 0.0 represents mountains or manmade structure such that the reservoir surface is fully sheltered from the wind. CE-QUAL allows WSC to vary by segment in order to set values to specific landscapes. The landscape surrounding the Wachusett Reservoir is similar, so only one value of the WSE is used for the entire area.

Previous students calibrating the model for years 2003-2006 (Mathews, 2007 and Sojkowski, 2011) determined that using a WSC of 0.626 was the best choice. In order to verify the appropriate WSE value to use, a sensitivity analysis was performed by varying the WSC values from 0.5 to 0.7; results for impacts on temperature profiles for July 2, 2007 are shown in Figure 3.22. A WSC value of 0.626 works well and is appropriate to use. An interesting note about varying the WSC is that when the reservoir is stratified, a higher WSC value results in a lower epilimnial surface temperature and a higher hypolimnion temperature than for a lower WSC value. The result of a higher WSC value is that the reservoir is slightly less stratified, i.e., there is less of a difference between top and bottom temperatures.

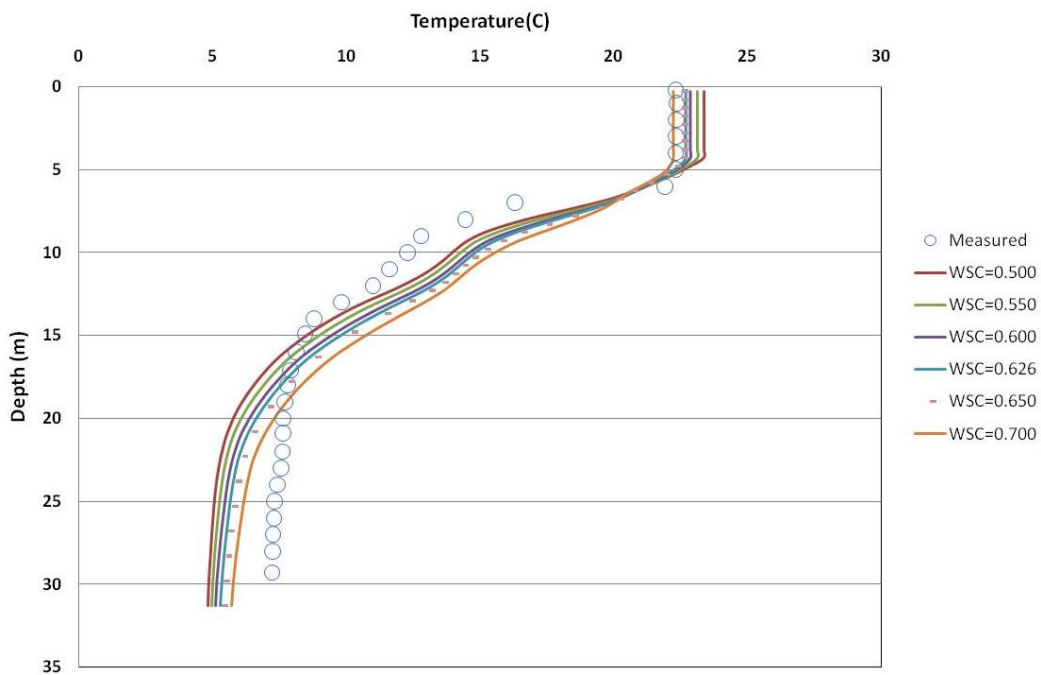


Figure 3.22: Impact of varying WSC, 7/2/2007

To illustrate the impact of the WSC on the reservoir temperature profile, the same sensitivity analysis was performed for calendar year 2008. For this analysis, however, less simulations were run but with a wider WSC value range of 0.25, 0.626, and 1.00. Figure 3.23 presents the

results of this analysis for July 3, 2008, where similar results occur as for the 2007 simulations; a higher WSC value produces lower epilimnial surface temperature with less stratification and a higher hypolimnion temperature with greater stratification for a lower WSC value. Again, 0.626 is a reasonable choice for the WSC value.

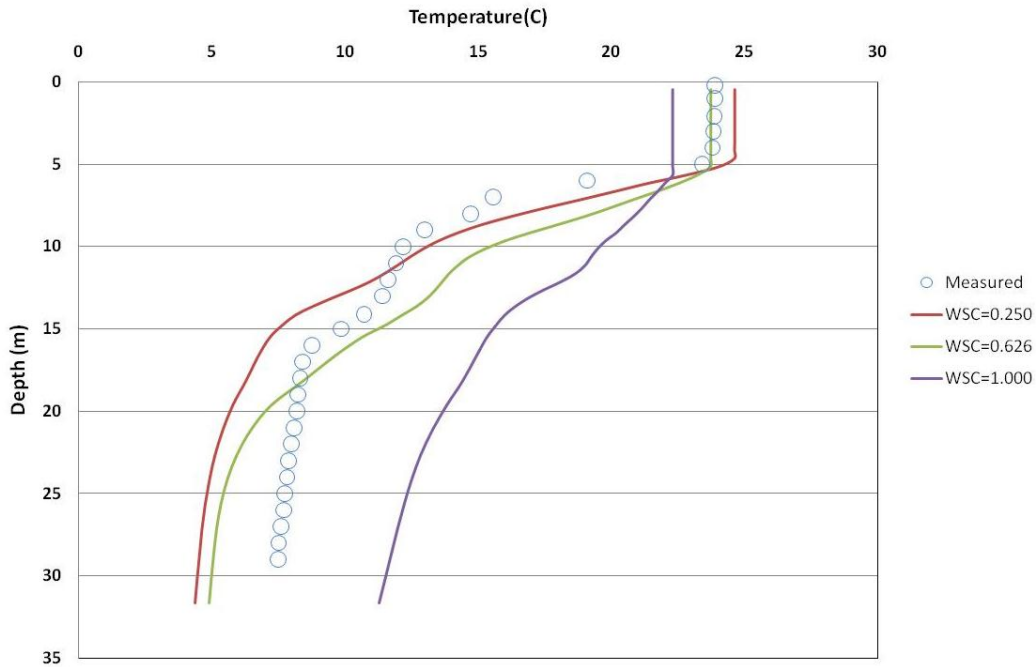


Figure 3.23: Impact of varying WSC, 7/3/2008

3.3.5 Bottom Heat Exchange Coefficient

The bottom heat exchange coefficient (CBHE) is used to calculate temperature changes at the bottom of the reservoir due to heat transfer between the reservoir and sediment interface.

Varying the CBHE can significantly change the calculated temperature of the bottom layers in CE-QUAL. This parameter is used for calibration to help accurately calculate bottom temperatures of the reservoir by allowing or inhibiting heat transfer between the sediments and bottom water column temperatures. CE-QUAL specifies a default value of 0.3 W/m²-s. A value

of zero cannot be input into CE-QUAL, so to minimize heat transfer between the reservoir and sediments, a value of $7 \times 10^{-7} \text{ W/m}^2\text{-s}$ was selected, and a maximum value of $2.0 \text{ W/m}^2\text{-s}$ was selected. Figure 3.24 shows the impacts of varying the CBHE on temperature profiles in Segment 42 for June 25, 2007. The results show a difference in bottom temperature of about 3°C between the minimum and maximum CBHE values. A higher value for CBHE increases the bottom temperature of the reservoir, while a low value decreases the bottom temperature. These results are consistent with intuition because CBHE determines the extent of heat transfer between the bottom water column and the sediment. For calibration, the sediment temperature was set to 10°C , which is consistent with realistic subsurface temperatures. As the year progresses, the difference in simulated bottom temperature for the range of CBHE values increase, as shown in Figure 3.25, where the difference in minimum and maximum bottom temperatures is about 5°C . A value of 1.0 was picked for CBHE, which resulted in the best fit for the entire year.

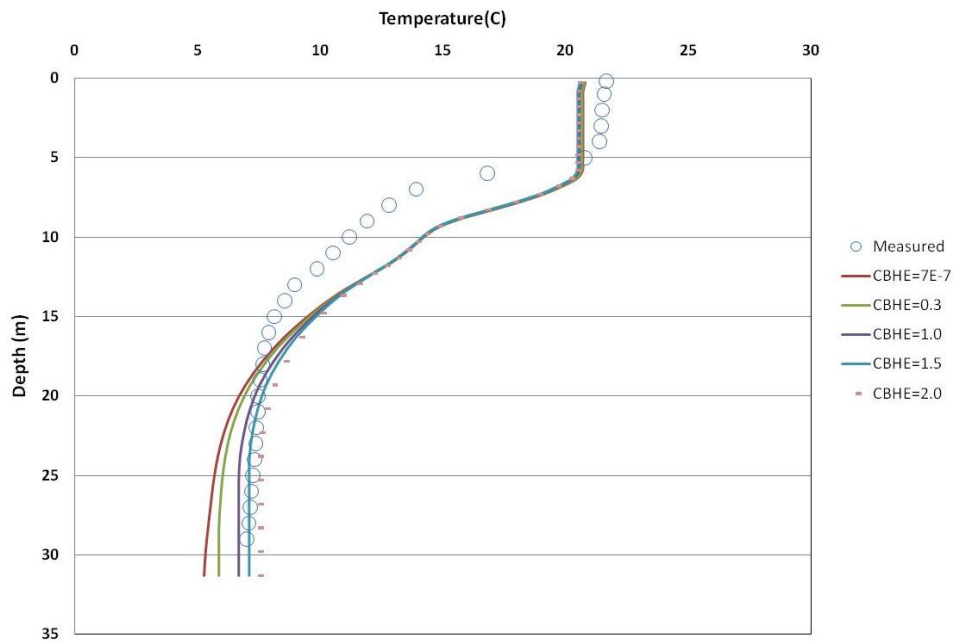


Figure 3.24: Varying CBHE, 6/25/2007

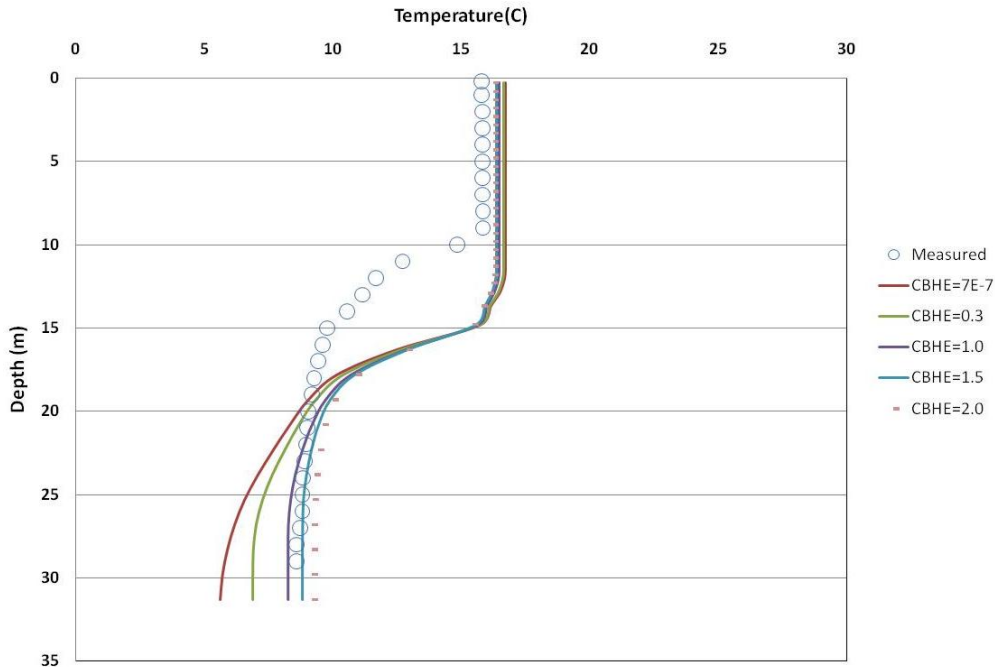


Figure 3.25: Varying CBHE, 10/15/2007

3.3.6 Sediment Temperature

It is important to assess the impact of varying the sediment temperature on model simulations.

Figure 3.26 shows the results of a sensitivity analysis of the sediment temperature for 6/25/07; a realistic range of 10 to 15°C was selected. In the summer months, a sediment temperature of 10°C resulted in a 2°C lower bottom temperature than a sediment temperature of 15°C. As shown in Figure 3.27, the difference in simulated bottom temperature increases for 11/1/07 to approximately a 4°C difference. A sediment temperature of 10°C was selected as the best fit for the entire year.

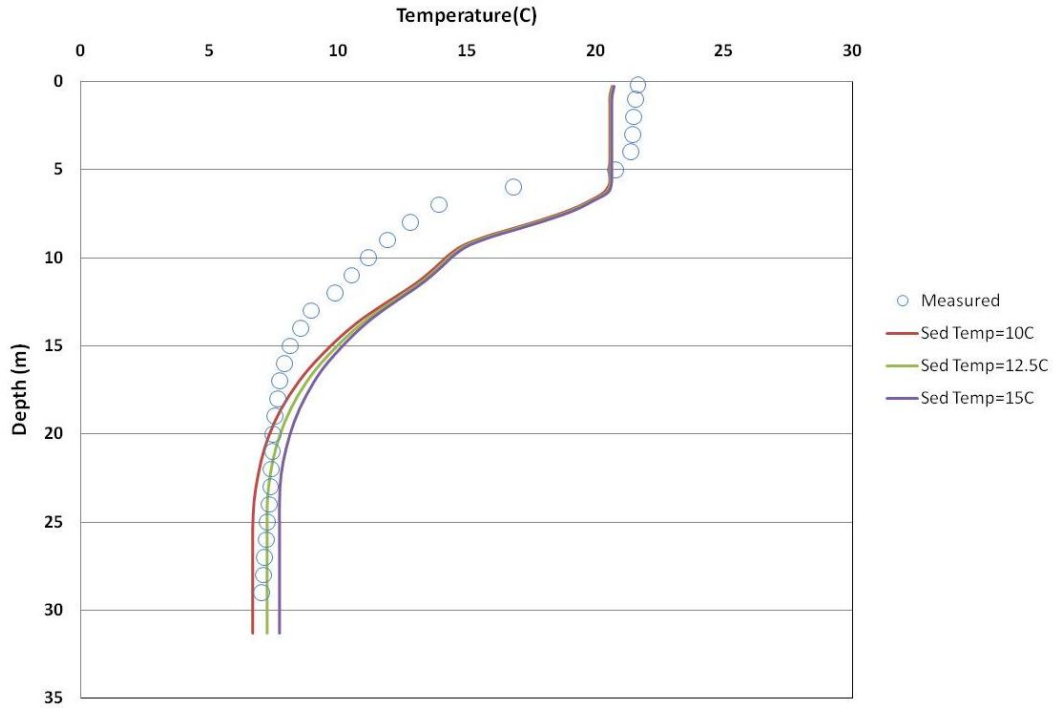


Figure 3.26: Varying sediment temperature, 6/25/2007

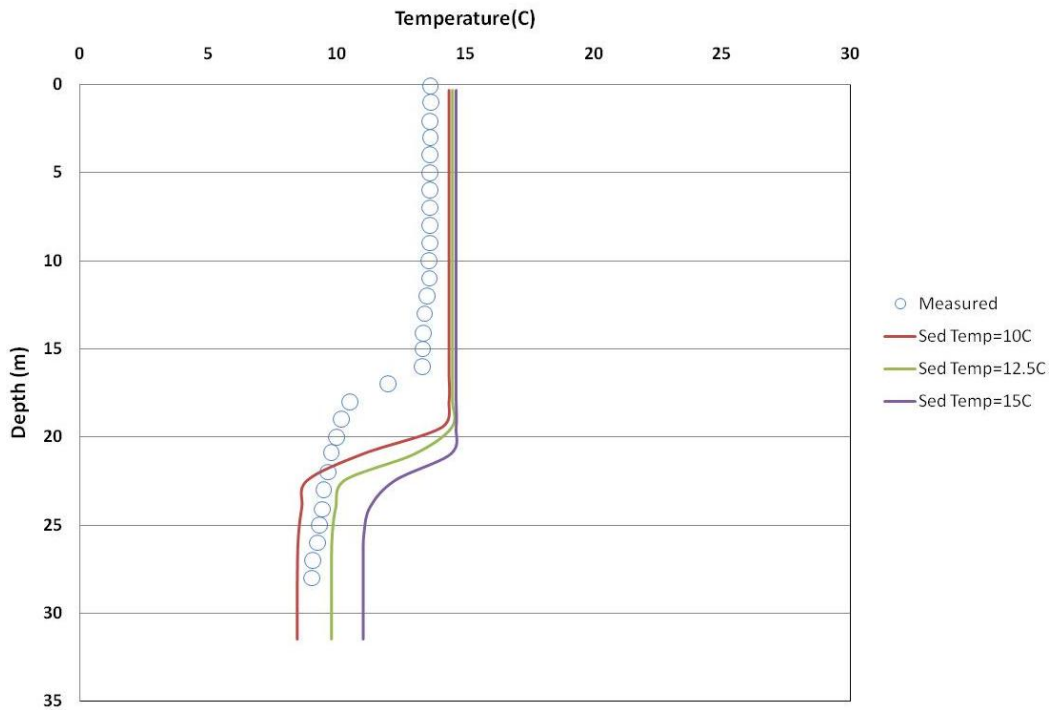


Figure 3.27: Varying sediment temperature, 11/1/2007

3.3.7 Ice On/Off

Ice cover is known to develop on the Wachusett Reservoir, however, since CE-QUAL has the ability to turn on and off the formation of ice in its calculations, the possibility for ice not to form was investigated. Historically, for this project, ice calculations have always been on. An analysis was performed to determine the impact the ice calculations have on the temperature profiles. Figure 3.28 shows results for the ice calculations on and off for March 3, 2008, resulting in about a 1°C difference. If ice formation is on, the reservoir is slightly warmer because ice shields the reservoir from the environment, where freezing weather can result in lower reservoir temperatures if ice does not form. During the warmer seasons, ice cover has no effect on the temperature of the reservoir, as shown in Figure 3.29, which is a simulation for June 9, 2008.

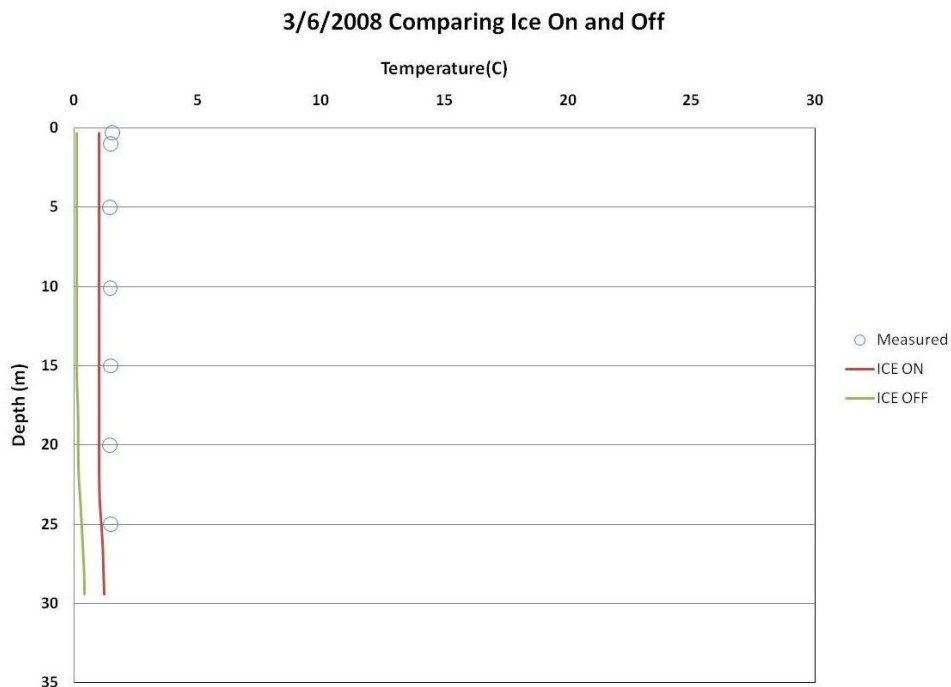


Figure 3.28: Comparison of on and off ice calculation, 3/6/2008

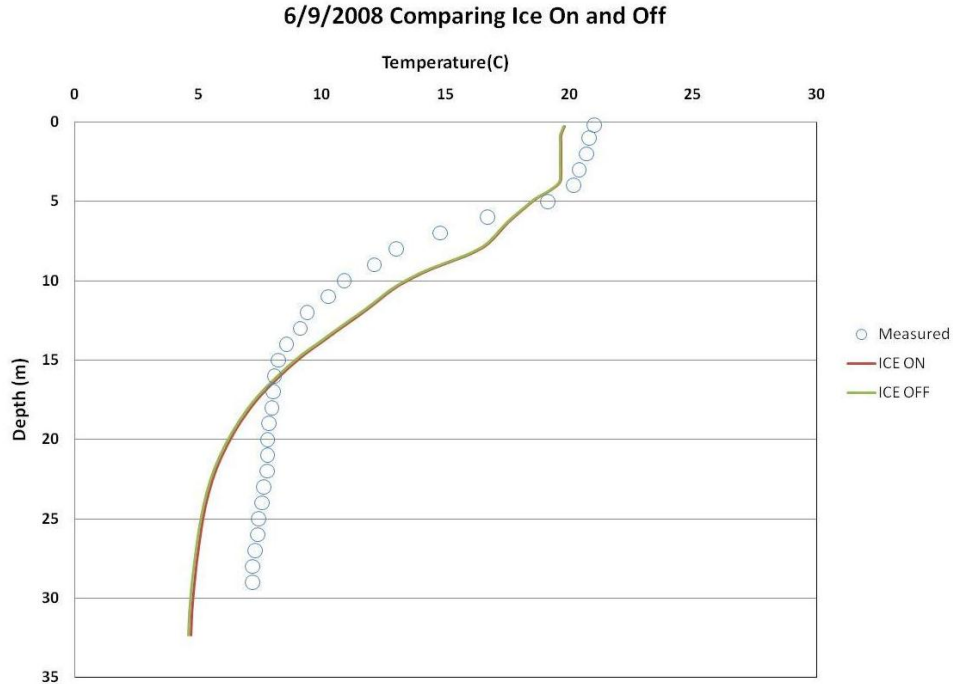


Figure 3.29: Comparison of on and off ice calculation, 6/9/2008

3.4 Final Calibration Results

This section provides the final values selected for the calibration parameters and shows the calibrated temperature and specific conductance profiles for calendar years 2007 and 2008. Table 3.3 presents the parameter values selected from the calibration process. The initial specific conductance for each year was selected in order to produce a better calibration fit and to account for possible errors in measurements and calculations. The WSC, CBHE, and sediment temperature values are the same for both years because they reflect the physical parameters of the reservoir and should not change year to year. The sediment temperature may vary slightly, however, not significantly. Ice is also turned on for each year because ice is known to form on the reservoir, and thus should be included in the calculations.

Table 3.3: Parameter Results of Final Calibration

Parameter	2007	2008
Initial Temperature (°C)	7	4
Initial Specific Conductance (µS/cm)	75	86.6
Wind Sheltering Coefficient	0.626	0.626
Bottom Heat Exchange Coefficient	1	1
Sediment Temperature (°C)	10	10
Ice On/Off	On	On

3.4.1 Temperature and Specific Conductance Profiles

Figure 3.30 to Figure 3.33 present all of the final calibrated temperature and specific conductance profiles for calendar years 2007 and 2008. The final calibration results in slight error well within acceptable values. Error is measured at top, middle, and bottom for all available measured data with top depth measured at zero meters, middle depth measured at fifteen meters, and bottom depth measured at thirty meters.

The 2007 temperature error for top, middle, and bottom depths averages -0.4, +2.1, and -0.4°C respectively; maximum errors of +1.4 and -2.2 °C for top, always higher for the middle with a maximum error of 5.9 °C, and maximum errors of +0.8 and -1.0 °C for bottom depth. The 2008 temperature error for top, middle, and bottom averages -0.4, +1.7, and -0.9 °C respectively; maximum errors of +1.3 and -2.8 °C for top depth, +4.5 and -0.4 °C for middle depth, and +1.0 and -1.6 °C for bottom depth. Both years on average underestimate the top and bottom depth temperatures, while overestimate the middle depth.

The 2007 specific conductance error for top, middle, and bottom depths averages -4.3, -0.9, and -3.3 µS/cm respectively; maximum errors of +4.2 and -39.4 µS/cm for top depth, +17.3 and -39.1

$\mu\text{S}/\text{cm}$ for middle depth, and +8.7 and -41.9 $\mu\text{S}/\text{cm}$ for bottom depth. The 2008 specific conductance error for top, middle, and bottom depths averages -2.0, -5.5, -0.1 $\mu\text{S}/\text{cm}$; maximum errors of +2.2 and -7.7 $\mu\text{S}/\text{cm}$ for top depth, +4.6 and -29.0 $\mu\text{S}/\text{cm}$ for middle depth, and +8.4 and -4.0 for bottom depth. Both years on average underestimate the specific conductance for all depths. Interestingly, 2007 has higher specific conductance errors for top and bottom depths, while 2008 has higher errors in the middle depth and lower. The high errors for the maximums are due to the first date of available data because initial conditions were selected based on results that better match data later in the year.

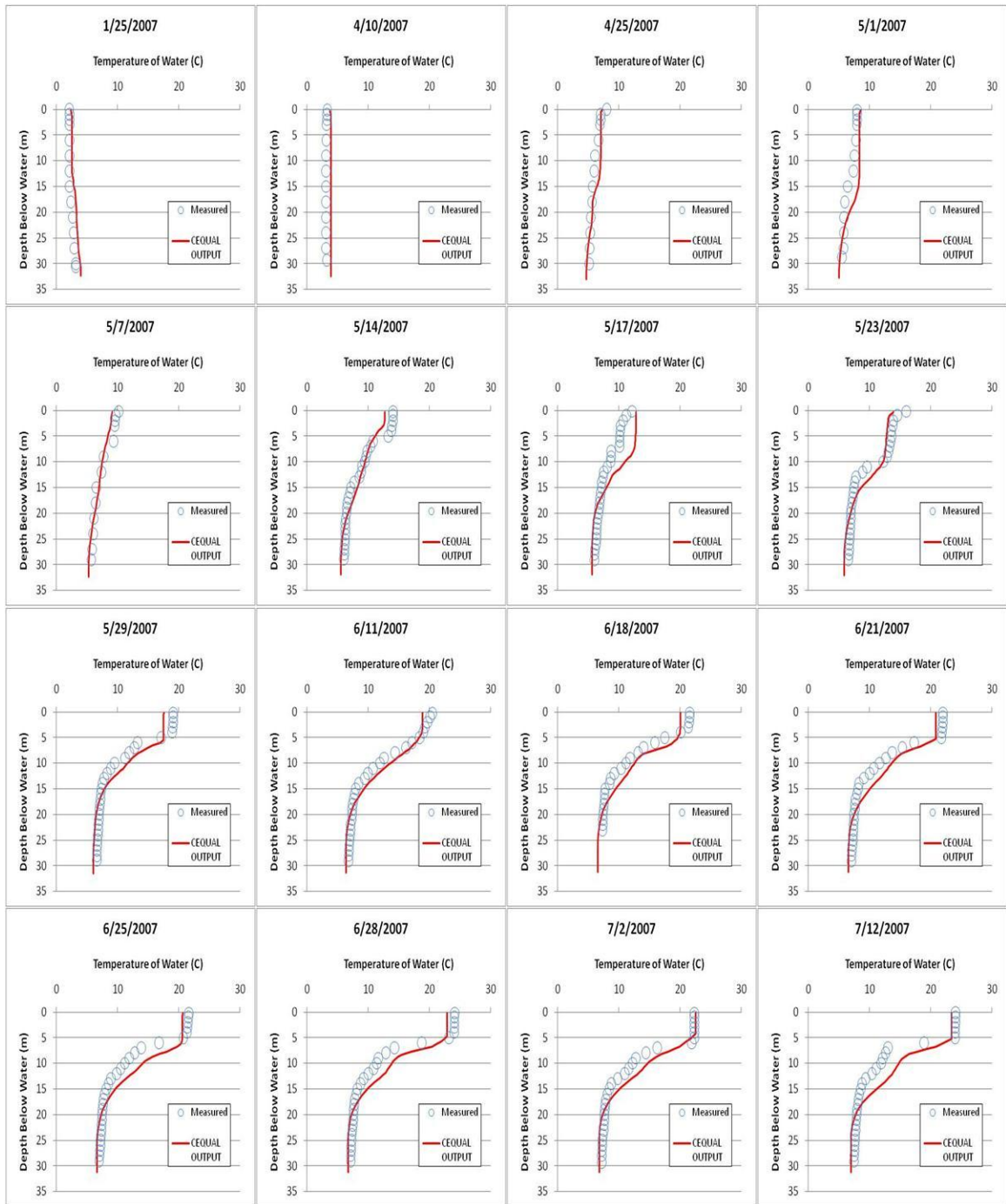


Figure 3.30: 2007 temperature calibration profiles, North Basin (Segment 42)

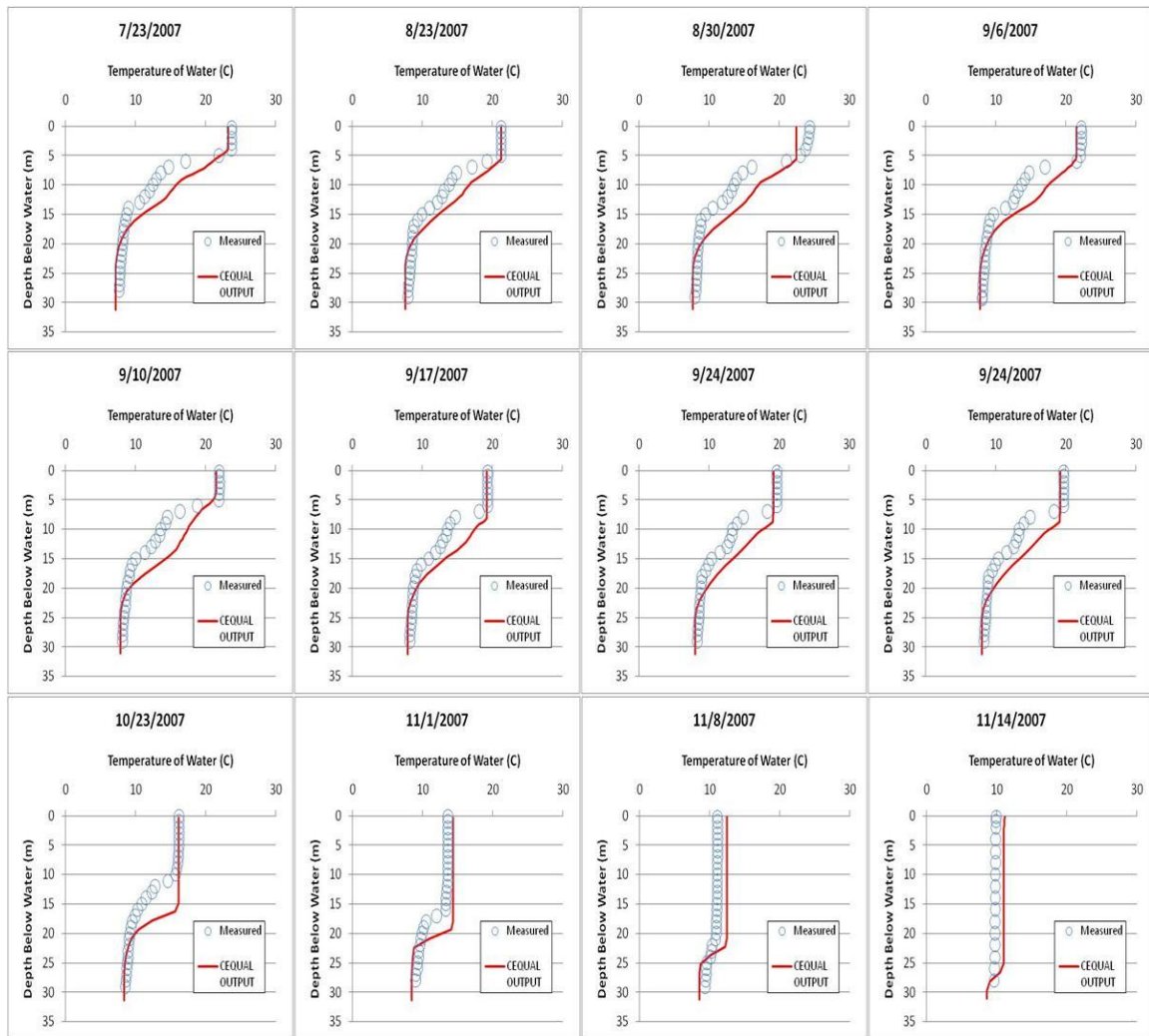


Figure 3.30 (cont.): 2007 temperature calibration profiles, North Basin (Segment 42)

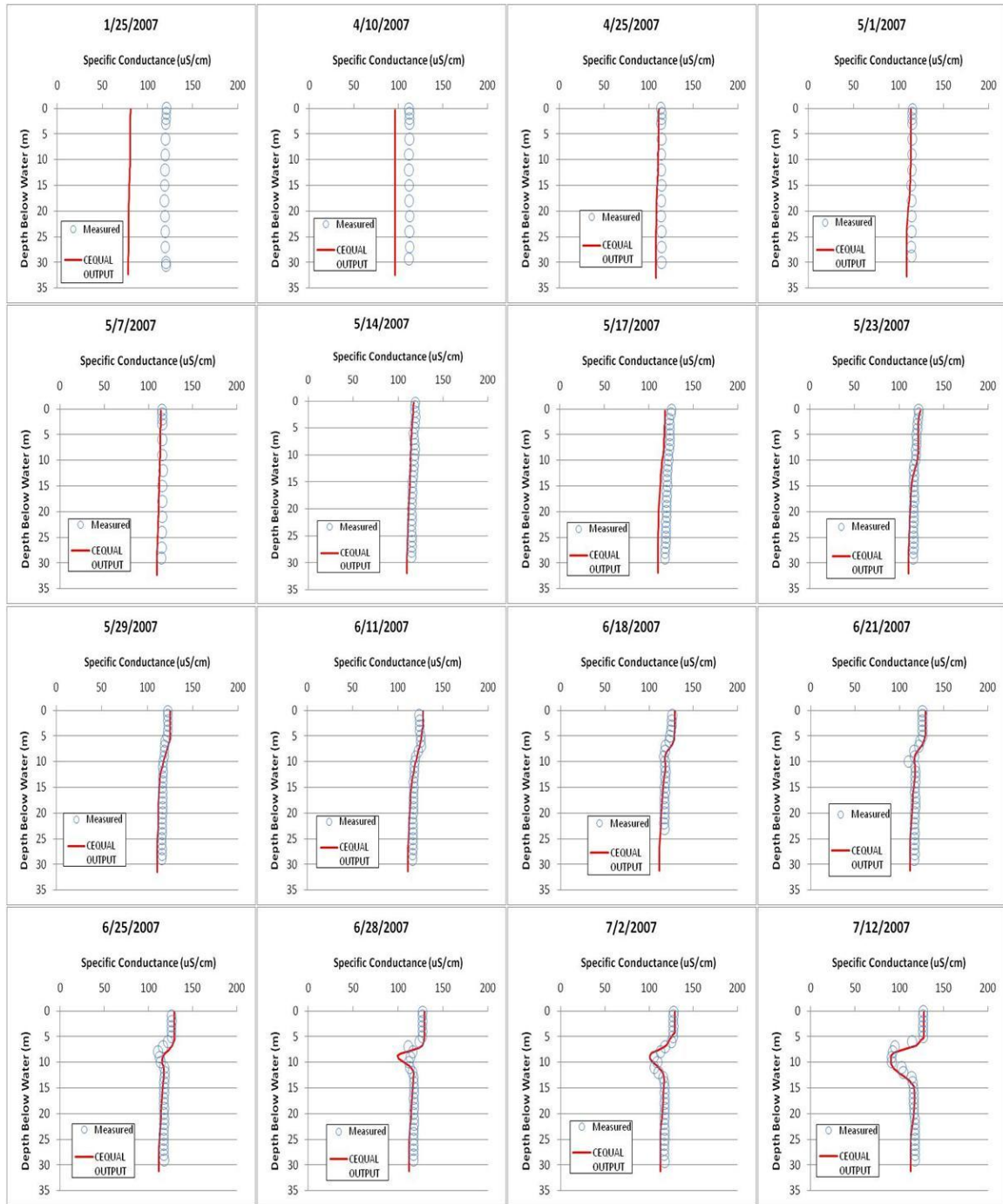


Figure 3.31: 2007 specific conductance calibration profiles, North Basin (Segment 42)

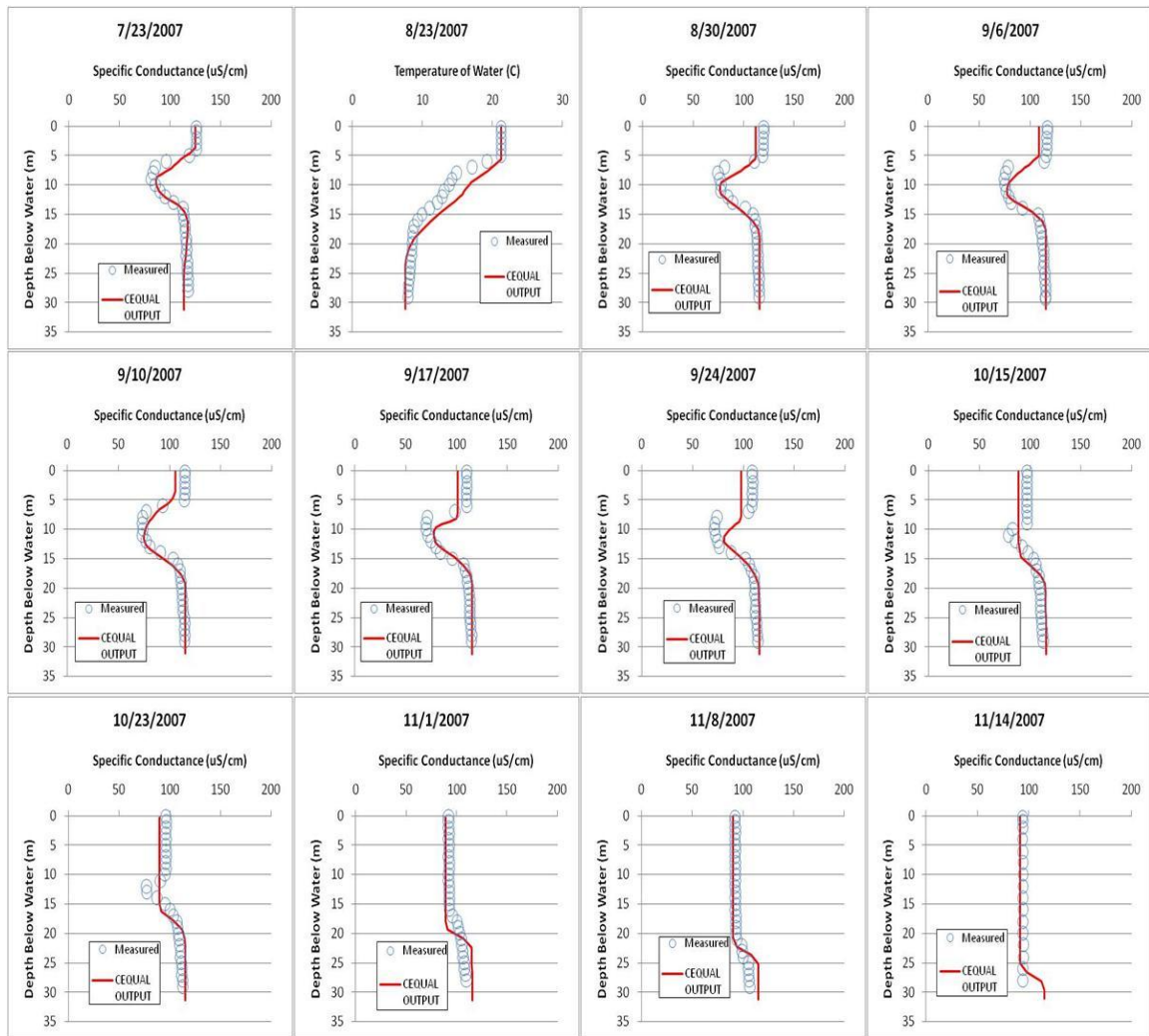


Figure 3.31 (cont.): 2007 specific conductance calibration profiles, North Basin (Segment 42)

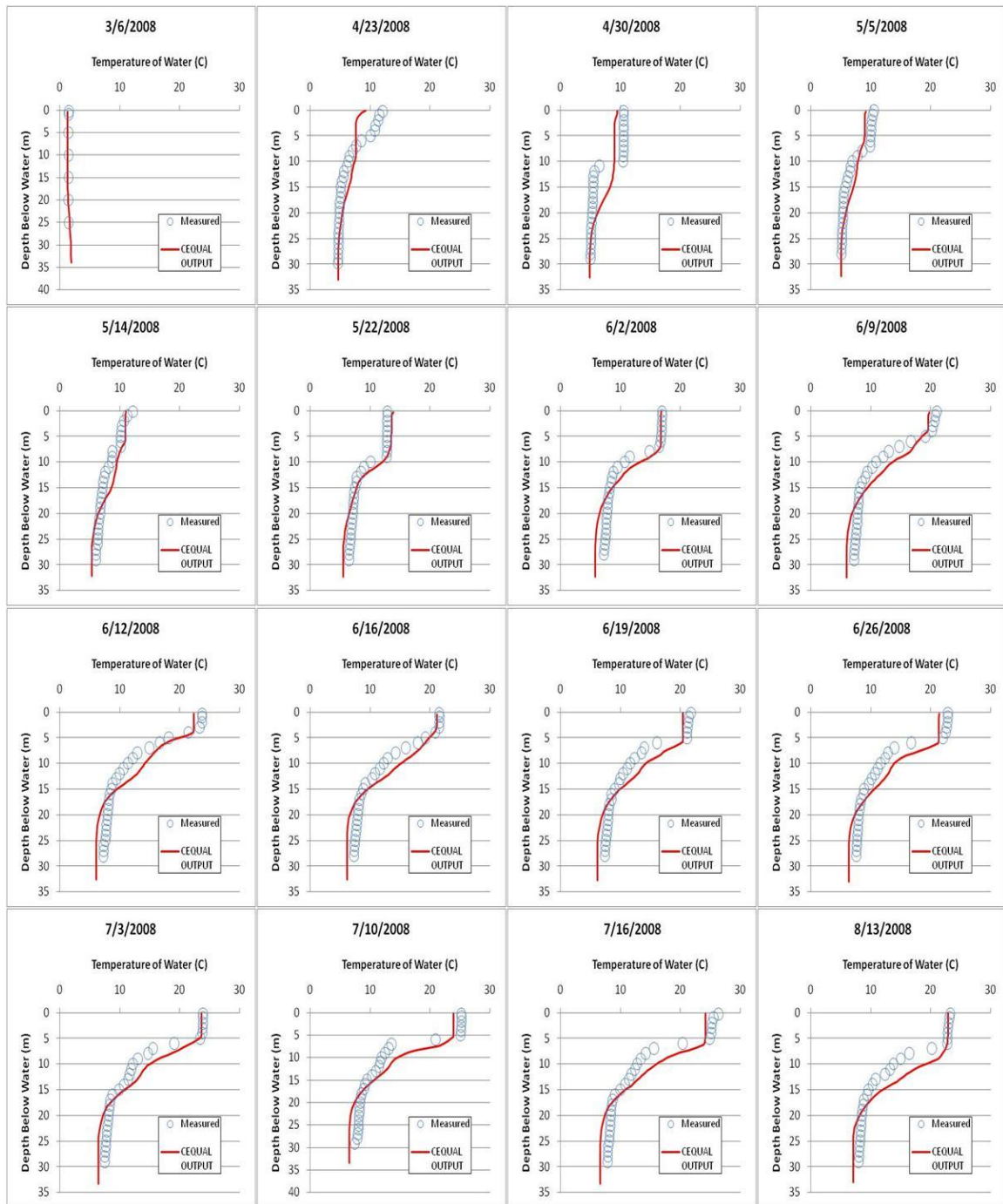


Figure 3.32: 2008 temperature calibration profiles, North Basin (Segment 42)

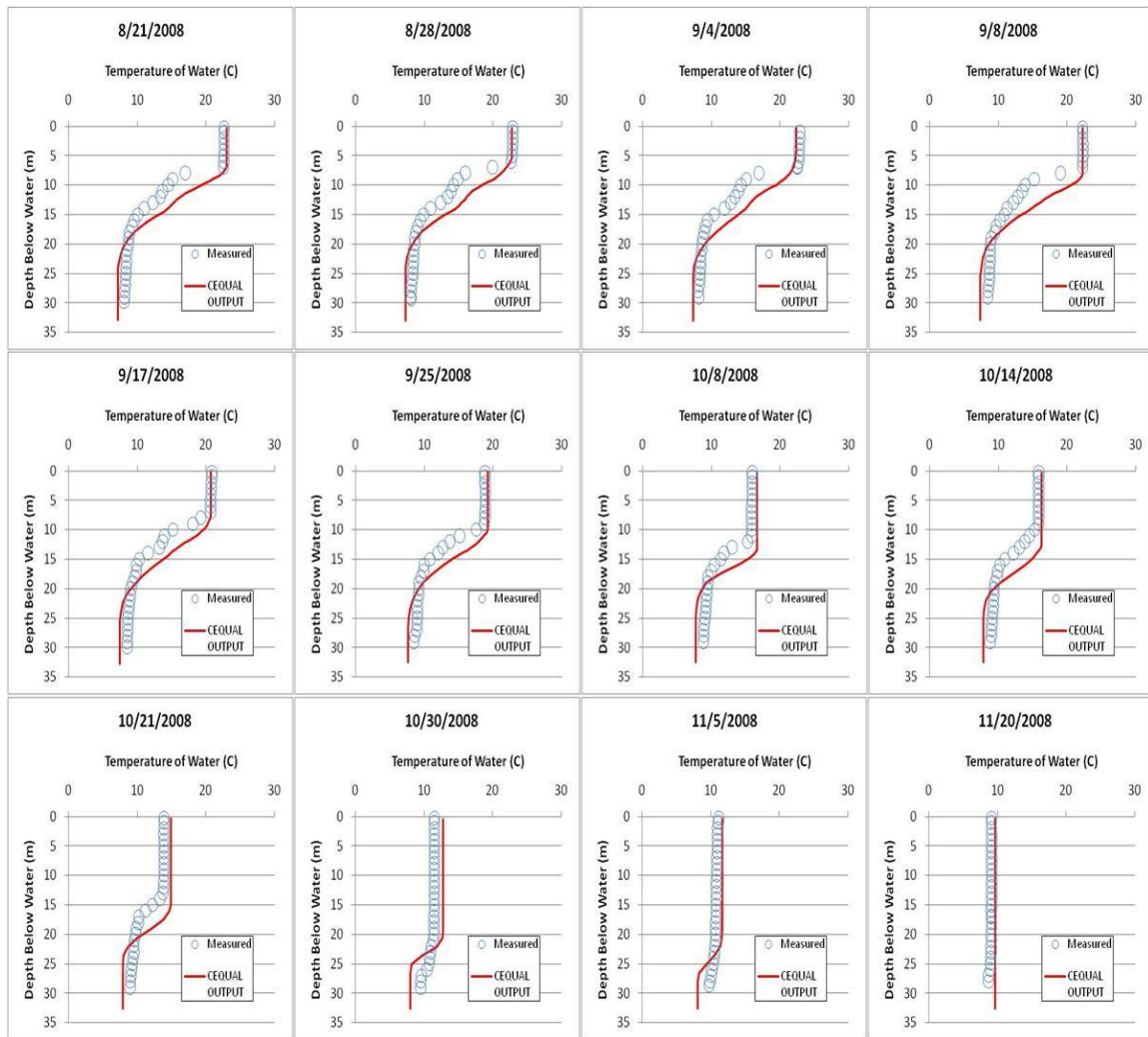


Figure 3.32 (cont.): 2008 temperature calibration profiles, North Basin (Segment 42)

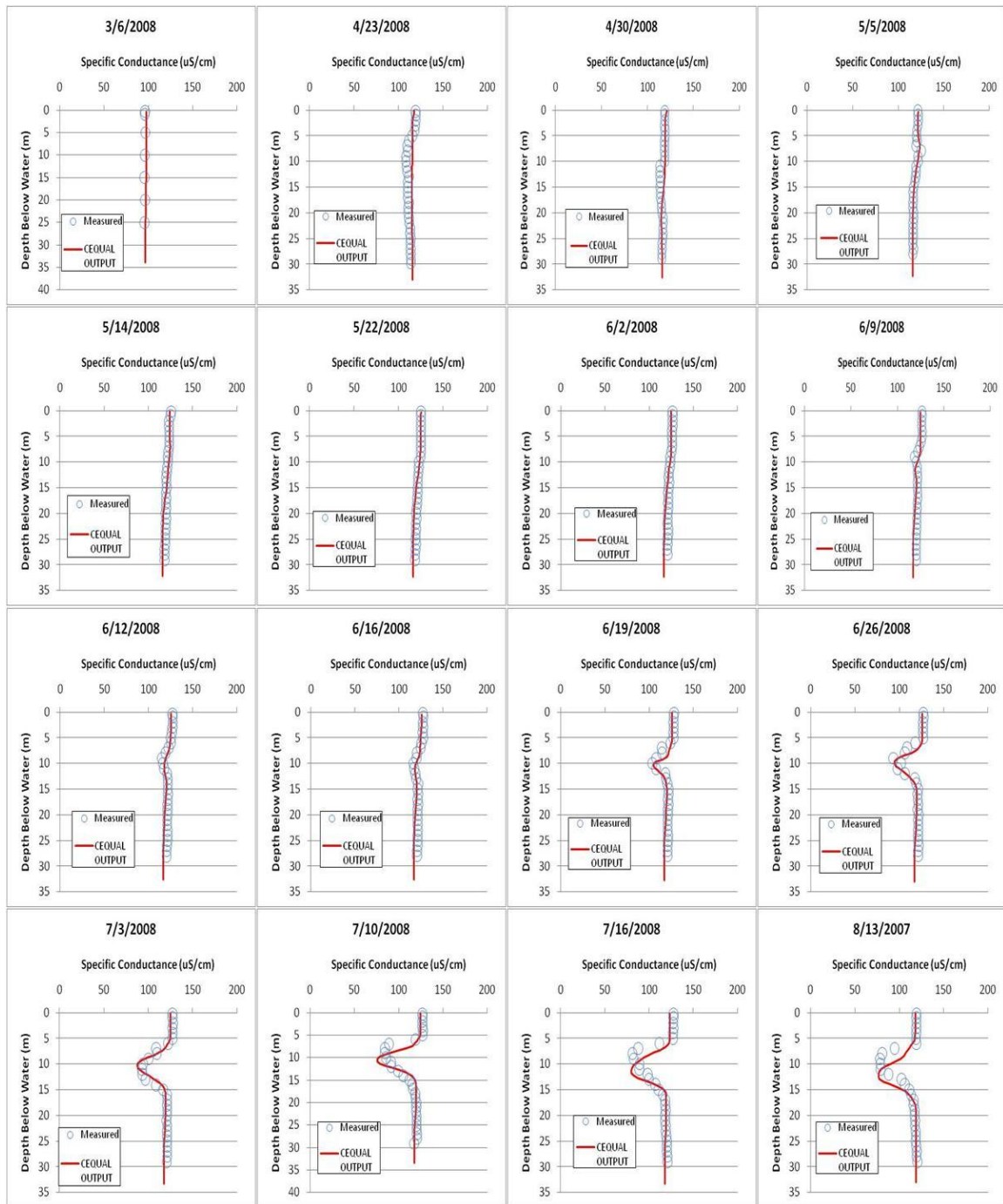


Figure 3.33: 2008 specific conductance calibration profiles, North Basin (Segment 42)

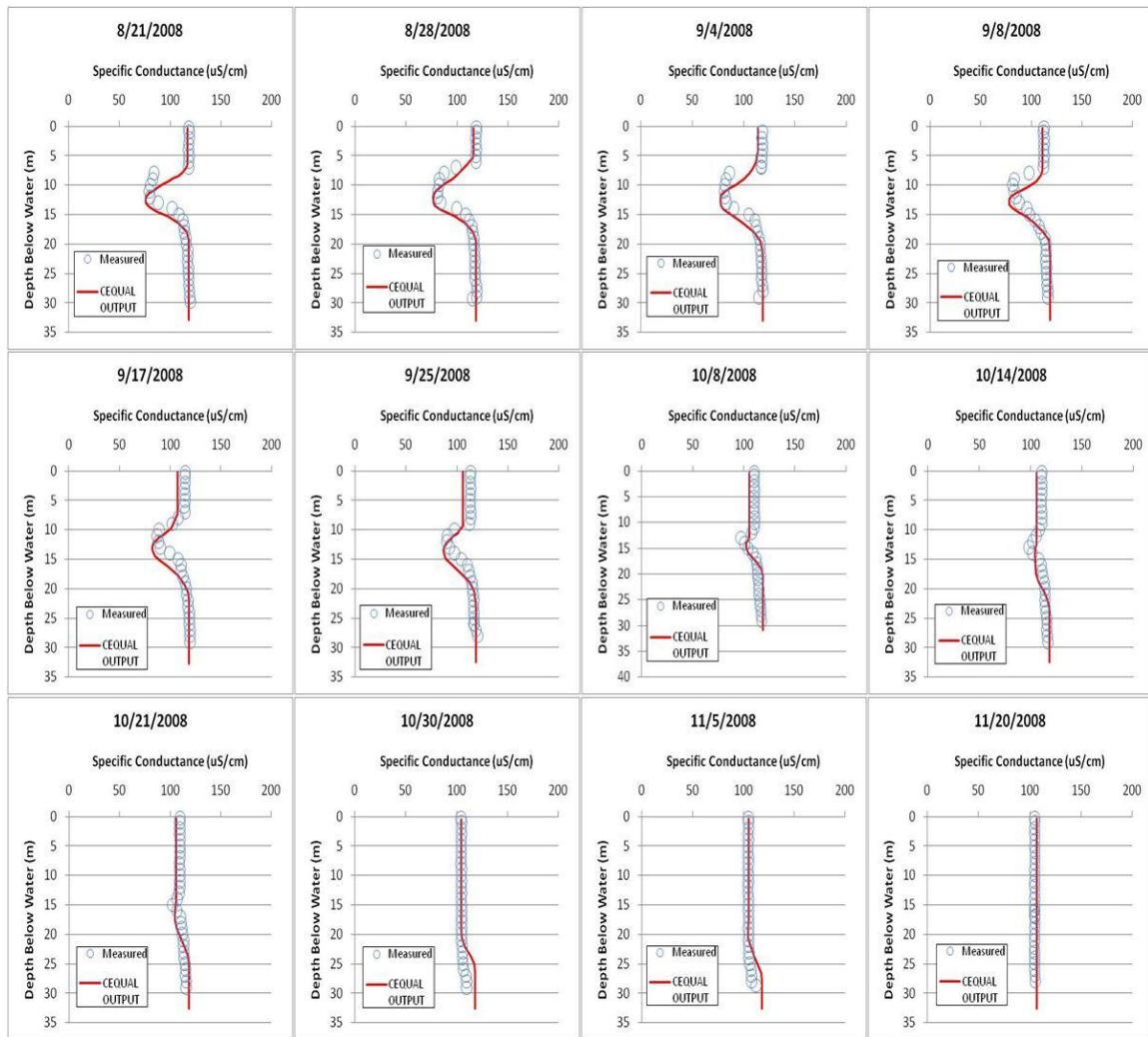


Figure 3.33 (cont.): 2008 specific conductance calibration profiles, North Basin (Segment 42)

3.5 Spill Simulation

Spill simulations were accomplished by specifying that the contaminant is a general constituent, and is a conservative, non-reactive substance that does not volatilize or degrade over time. For this study, all spills occurred at noon at the Rt. 140 bridge, Segment 7 in CE-QUAL, with a high concentration of 1×10^8 mg/L at a flow of $0.02 \text{ m}^3/\text{s}$. It should be noted that the spill concentration is high, and the flow low, to simulate a certain mass of contaminant spilled to the reservoir. Simulated contaminant concentration results are presented as relative or normalized concentrations as developed by Stauber (Stauber, 2009). The simulated concentration is divided by the calculated completely mixed concentration that would occur if the mass of the spill was mixed into the total volume of the reservoir. A relative concentration of 1.0 represents a spill that is completely mixed throughout the reservoir, while values greater than 1.0 occur when the spill is not as well mixed. Simulations have been conducted to demonstrate that the actual mass of contaminant spill has no effect on the simulated relative concentration.

CE-QUAL does not have the capability of modeling different contaminant densities directly for general constituents, however, density effects can be simulated by varying the spill temperature. By setting the spill temperature high relative to the temperature of the reservoir, the spill will act as if it had a low density, so it will tend to float on the top of the water column. If the temperature is set low compared to the reservoir temperature, the spill will tend to sink and stay at the bottom of the water column. Thus spill temperature was varied to simulate possible difference in the density or temperature of a spill.

3.5.1 Spill Date Selection

In order to examine seasonal effects for spill scenarios, specific dates, or Julian Days, were selected within each season of the year. Sojkowski (2011) used periods with four consistent days of average wind direction based on Stauber's (2009) finding that wind direction has a substantial effect on the behavior of the spill. Table 3.4 presents the days chosen for each of the six years (2003-2008) and subsequent seasons. The day selected for the spill is the first day listed in each section. It should be noted that the direction of the wind listed is the direction from which the wind is coming from, so a northwest wind listed in the table is traveling towards the southeast.

Another series of spill scenarios were selected for periods of high inflows due to storm events. These days were selected based on criteria that if the Stillwater and Quinapoxet flows were unusually high for a brief period of time, then spill day simulations for few days before, during and after the unusually high inflows were selected to assess the impact of a high inflow event on the behavior of the spill at the Cosgrove Intake.

Table 3.4: Average Daily Wind Comparison for all Six Years

2003 SPRING			2004 SPRING			2005 SPRING			2006 SPRING			2007 SPRING			2008 SPRING		
JDAY	Wind Dir	Wind Mag (m/s)	JDAY	Wind Dir	Wind Mag (m/s)	JDAY	Wind Dir	Wind Mag	JDAY	Wind Dir	Wind Mag (m/s)	JDAY	Wind Dir	Wind Mag (m/s)	JDAY	Wind Dir	Wind Mag (m/s)
117	SW	4.03	120	SW	6.67	114	SE	6.78	115	NW	6.04	119	NW	2.70	122	NW	3.45
118	SW	4.23	121	SW	6.73	115	SW	5.10	116	SW	5.28	120	NW	4.42	123	SE	2.33
119	NW	4.72	122	SW	6.65	116	SW	5.26	117	SW	4.21	121	NW	5.27	124	SE	3.11
120	SW	4.00	123	SW	6.08	117	SE	3.78	118	SE	3.82	122	SW	3.01	125	SE	3.11
Avg.		4.24	Avg.		6.53	Avg.		5.23	Avg.		4.84	Avg.		3.85	Avg.		3.00
2003 SUMMER			2004 SUMMER			2005 SUMMER			2006 SUMMER			2007 SUMMER			2008 SUMMER		
JDAY	Wind Dir	Wind Mag (m/s)	JDAY	Wind Dir	Wind Mag (m/s)	JDAY	Wind Dir	Wind Mag (m/s)	JDAY	Wind Dir	Wind Mag (m/s)	JDAY	Wind Dir	Wind Mag (m/s)	JDAY	Wind Dir	Wind Mag (m/s)
237	SW	4.30	230	SE	2.56	233	SW	8.27	222	SW	4.67	222	SE	2.53	227	SW	1.77
238	SW	3.84	231	SW	4.21	234	NW	9.54	223	NW	5.01	223	NW	2.79	228	SW	1.98
239	SW	5.28	232	SW	4.79	235	NW	8.21	224	NW	4.59	224	NW	2.55	229	NW	2.44
240	SW	3.38	233	SW	3.63	236	NW	7.25	225	NW	4.32	225	NW	3.70	230	SW	4.84
Avg.		4.20	Avg.		3.80	Avg.		8.32	Avg.		4.65	Avg.		2.89	Avg.		2.76
2003 FALL			2004 FALL			2005 FALL			2006 FALL			2007 FALL			2008 FALL		
JDAY	Wind Dir	Wind Mag (m/s)	JDAY	Wind Dir	Wind Mag (m/s)	JDAY	Wind Dir	Wind Mag (m/s)	JDAY	Wind Dir	Wind Mag (m/s)	JDAY	Wind Dir	Wind Mag (m/s)	JDAY	Wind Dir	Wind Mag (m/s)
311	NW	3.40	319	NW	6.47	323	SW	3.32	318	SE	4.36	318	SW	4.59	314	SW	4.75
312	NW	7.21	320	NW	4.48	324	SW	4.99	319	SE	3.20	319	SW	5.40	315	SW	3.78
313	NW	4.61	321	NW	2.96	325	SW	3.47	320	SE	5.66	320	NW	8.25	316	SW	4.84
314	SW	4.00	322	SW	2.42	326	SE	6.98	321	SW	7.28	321	NW	5.55	317	NW	2.91
Avg.		4.81	Avg.		4.08	Avg.		4.69	Avg.		5.12	Avg.		5.94	Avg.		4.07

4 RESULTS

The purpose of this section is to present and discuss the results of the CE-QUAL W2 modeling work. This section presents results for modeled years 2003-2008 using CE-QUAL W2 v.3.6. Model years 2003 and 2004 were developed by Matthews (2007) in CE-QUAL W2 v.3.5 and later converted to CE-QUAL v.3.6 by Sojkowski (2011). Model years 2005 and 2006 were developed by Sojkowski (2011). The impacts of season of year, Quabbin transfer, daily variation of spill day, high inflow events, and wind on the contaminant spill behavior are presented by considering the relative magnitude of the spill concentration at the Cosgrove Intake as a function of time after the spill occurs. The following graphs are displayed on either a Julian day or a "Days After" temporal scale. The "Days After" scale displays a time scale where time zero represents the time of the spill and subsequent times are presented as days after the spill occurred. It is important to note that the mean hydraulic residence time (volume/outflow) of the Wachusett Reservoir is approximately 200 days.

4.1 Seasonal Influence

Contaminant spills are modeled on a seasonal basis as the hydrology, temperature and stratification of the Wachusett Reservoir vary seasonally. The seasons have a profound effect on the behavior of the contaminant spill arriving at the Cosgrove Intake as shown in Figure 4.1, which shows simulated relative Cosgrove Intake contaminant concentration for each of the 2007 Spring, Summer, and Fall cold spills over the entire calendar year. The relative concentrations for the Spring and Fall spills peak at approximately 1.0, whereas in Summer the peak is much higher at nearly 3.0. The reservoir stratification (temperature gradients) in the Summer and

hydraulics cause greater variability and higher concentrations. The 2007 results are typical of all modeled years with respect to seasonal impacts; this aspect is explored later in this report. The elapsed time between the spill data and appearance of the contaminant at Cosgrove, and the concentration variability, are of great interest; the effects of seasons are well illustrated in Figure 4.1.

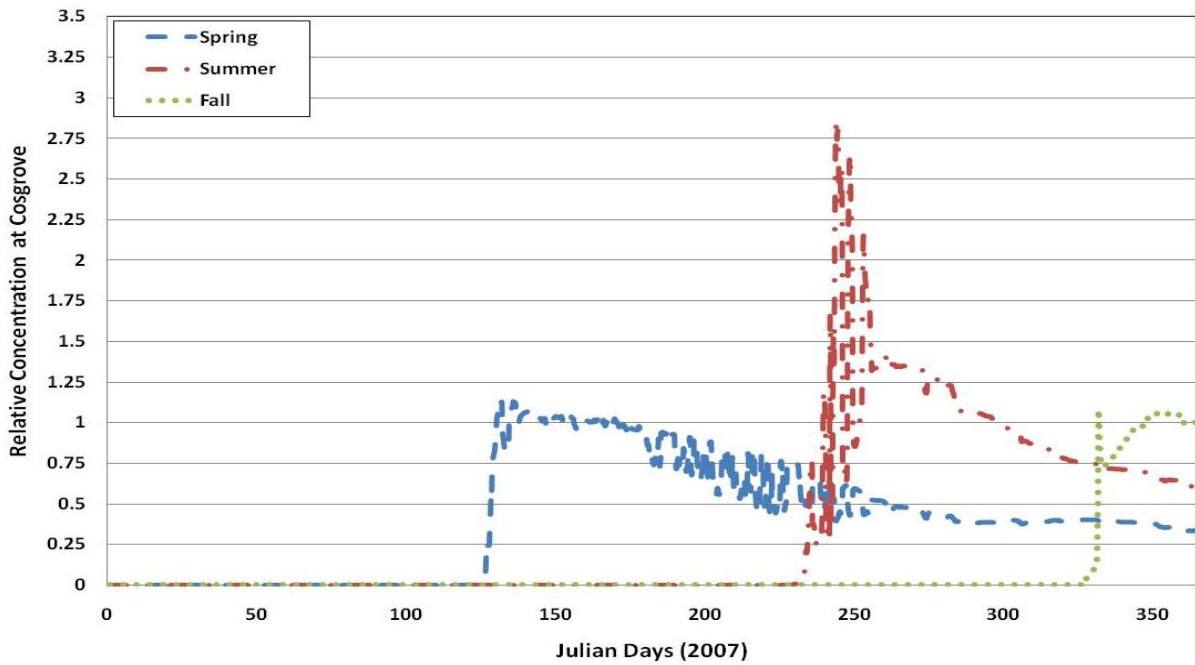


Figure 4.1: Relative contaminant concentration at the Cosgrove Intake for 2007 Spring, Summer, and Fall cold spills for the entire year

4.1.1 Spring Season Spills

During the Spring season, when the reservoir is not stratified, there are also normally higher precipitation events and snow melt that increase the tributary flows, adding to the complexity of the reservoir hydrodynamics. Spring spills typically have the shortest Cosgrove arrival time, ranging from two to five days (Sojkowski, 2011). Typically, spill temperature does not affect the behavior of the concentration at the Cosgrove Intake, but for modeled year 2007, the warm spill

arrives about two days earlier than a medium or cold spill, as shown in Figure 4.2. It is believed that meteorological conditions are the main reason for the differences between the warm and colder spills as the warm spill is initially located at the top of the water column. During the day of the spill, the wind came from the northwest direction, thus in the direction of the Cosgrove. More analysis of wind impact is presented later in this report.

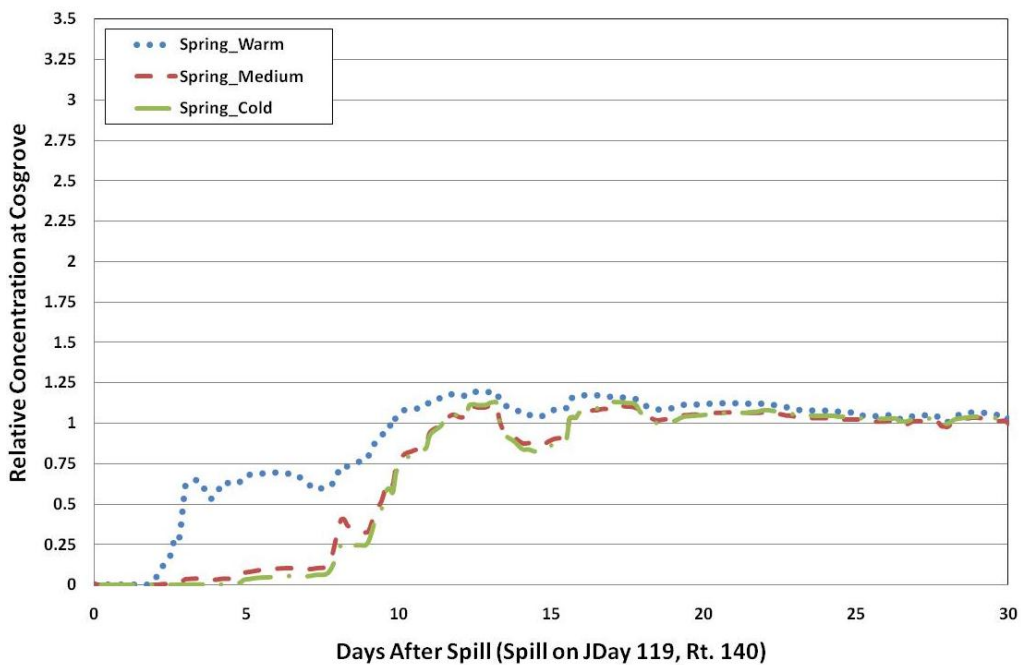


Figure 4.2: Relative contaminant concentration behavior at Cosgrove Intake for 2007 Spring, spill temperature variations for spill at Rt. 140 Bridge on Julian Day 119

Modeled year 2008 is a more typical result with no difference in the concentration behavior at the Cosgrove with varying spill temperatures as seen in Figure 4.3; the arrival time is about five days. An unusual characteristic for Spring 2008 is that there is an increase in contaminant concentration from 5 to 8 days after the spill, then the concentration decreases sharply until about 9 days after the spill, and finally increases again to a relative concentration of 1.25, and slowly

decreases to a value of 1.0. Calendar year 2008 had unusual Quabbin transfer activity early in the year, followed by high Stillwater and Quinapoxet inflows, which may have contributed to this behavior. Also, the spill occurred at the end of the high inflows, which may have impacted transport.

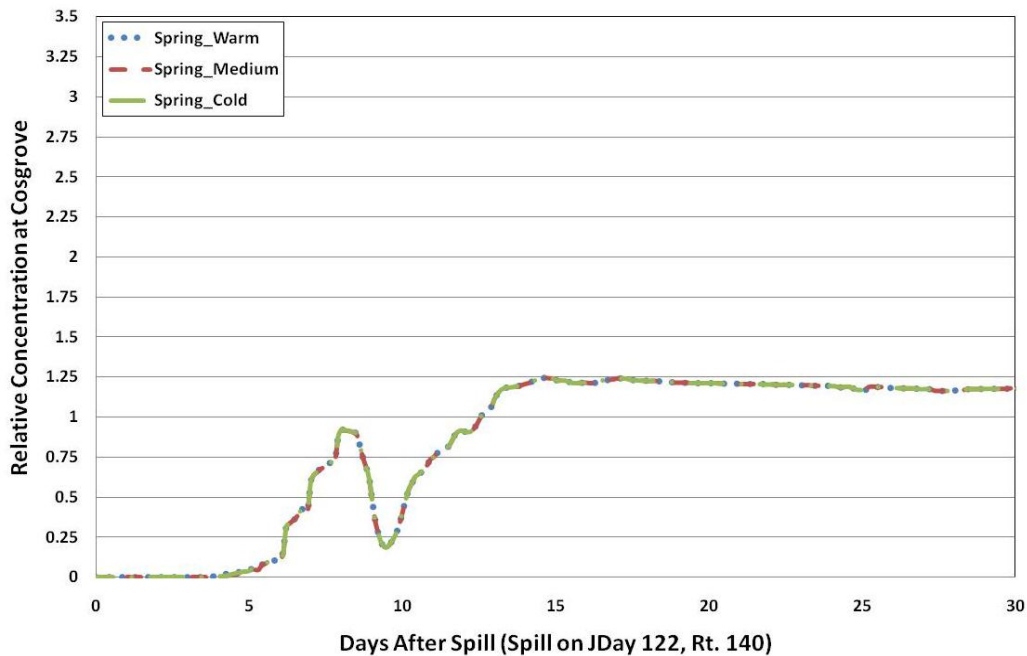


Figure 4.3: Relative contaminant concentration behavior at Cosgrove Intake for 2008 Spring, spill temperature variations for spill at Rt. 140 Bridge on Julian Day 122

There are now six simulated years for the Spring season for use in assessing typical patterns, as shown in Figure 4.4 to Figure 4.6. A Cosgrove arrival time frame of two to five days for warm and medium spills, and three to five days for a cold spill is established, consistent with results from Stauber (2009) and Sojkowski (2011). It can be seen in Figure 4.4 to Figure 4.6 that for simulated years 2005, 2006, and 2008, the contaminant arrives at five days the after the spill occurs, with no dependence on where (based on temperature) the contaminant is located in the

water column. Simulated year 2003 has unusual behavior for warm and medium spills, with an almost delayed CFSTR behavior where the bulk of the contaminant reaches the Cosgrove at the same time two days after the spill occurred and decreases over time. Simulated year 2004 shows an arrival time of three days after the spill and has the same behavior for cold, medium, and warm spills, with an arrival time of about 3 days and a gradual increase to a relative concentration value of 1.0. Simulated year 2007 has arrival times approximately two and a half days after a warm spill, with behavior similar to simulated Spring 2003. Medium and cold spills for Spring 2007 are very similar with an arrival time of about five days with a gradual increase in relative concentration to a value of 1.0. The difference between warm and colder spills indicates that the warm behavior is impacted by meteorological conditions; this is explored further in later sections of this report.

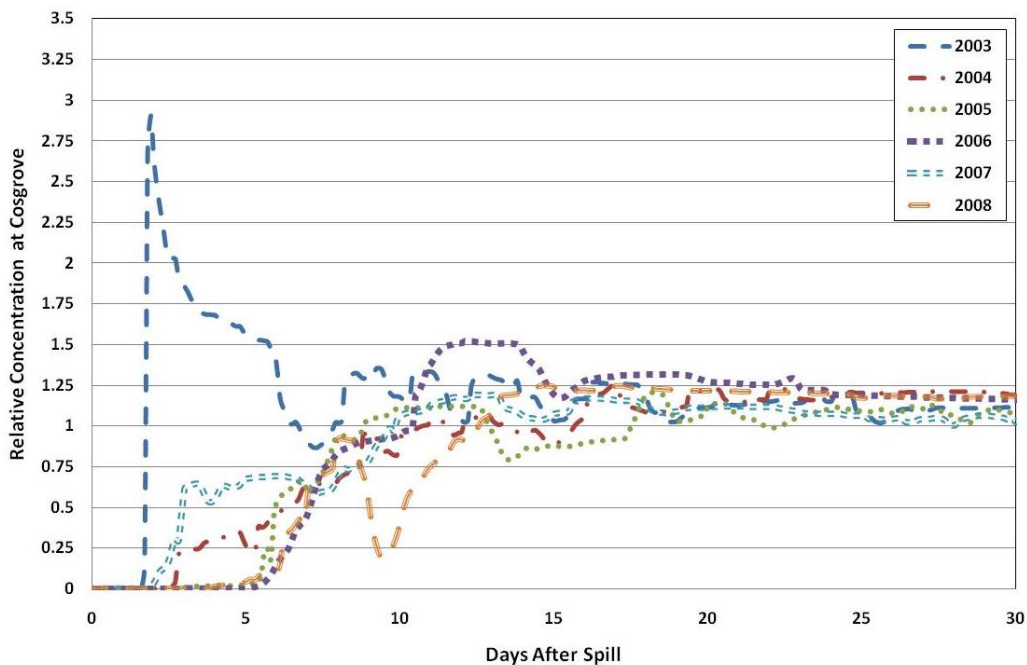


Figure 4.4: Relative contaminant concentration behavior at Cosgrove Intake for Spring model years 2003-2008 with warm spill at the Rt. 140 Bridge

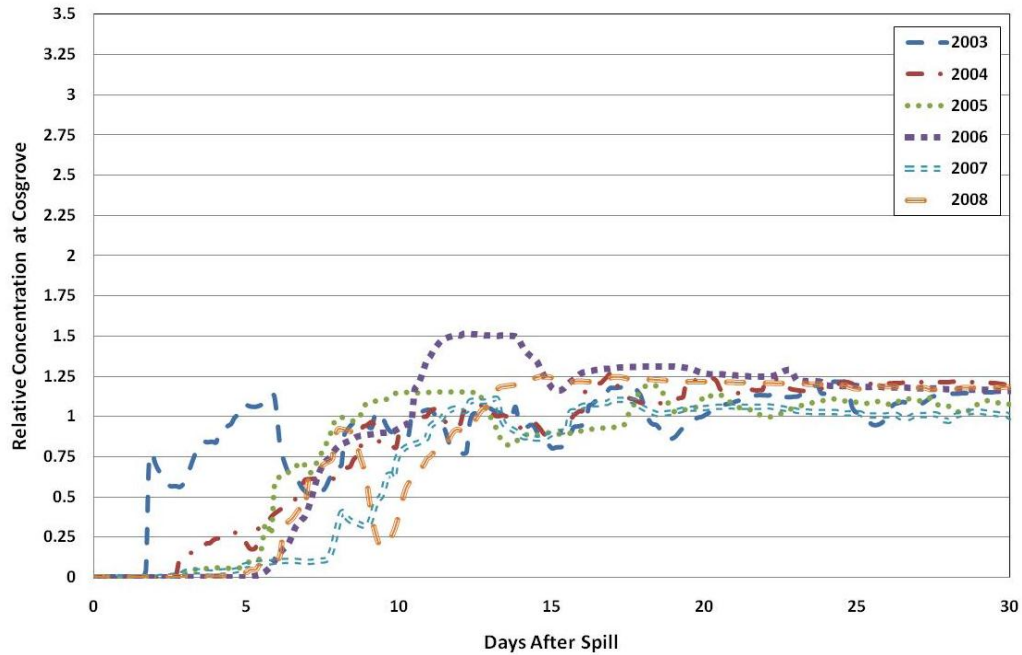


Figure 4.5: Relative contaminant concentration behavior at Cosgrove Intake for Spring model years 2003-2007 with medium spill at the Rt. 140 Bridge

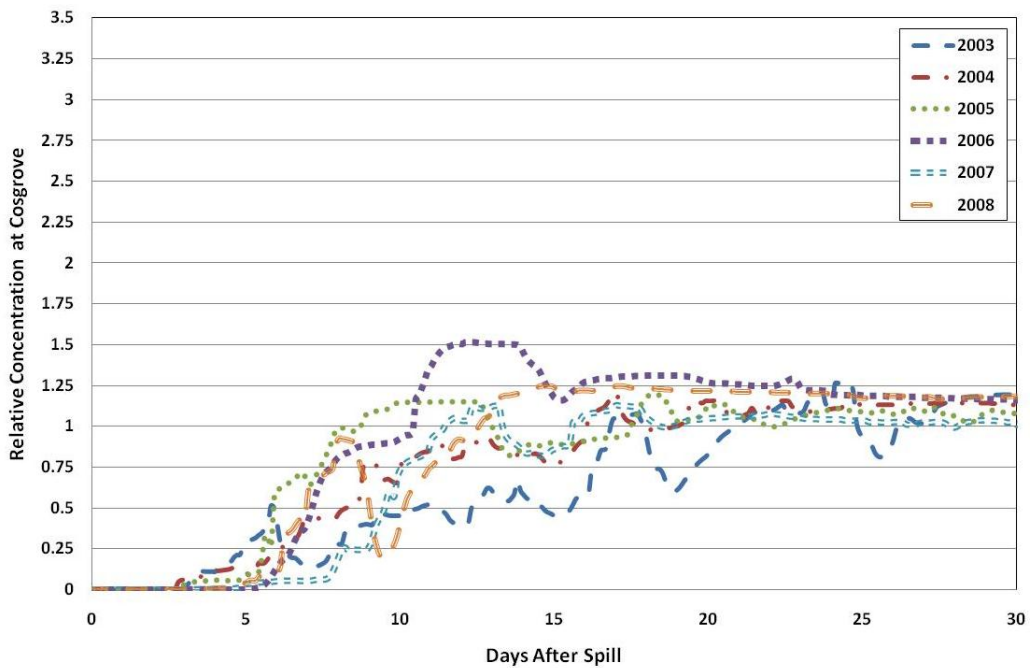


Figure 4.6: Relative contaminant concentration behavior at Cosgrove Intake for Spring model years 2003-2008 with cold spill at the Rt. 140 Bridge

4.1.2 Summer Season Spill

The Summer season is characterized by warmer temperatures, reduced tributary inflows, a stratified reservoir with large temperature gradients, and increase in water demand. To maintain Wachusett reservoir levels while meeting water demands under these conditions, the Quabbin transfer is initiated, which causes an interesting effect within the reservoir known as the Quabbin interflow. Sojkowski (2011) discovered that the Quabbin Interflow has a significant influence on the behavior of the contaminant; this is discussed in later sections of this report.

With low inflows, higher demands, and the Quabbin interflow on, the Wachusett Reservoir has complex hydrodynamics, which can be seen in the behavior of the spill contaminant at the Cosgrove Intake shown in Figure 4.7 and Figure 4.8. Figure 4.7 shows the behavior of the spill contaminant at the Cosgrove Intake for warm, medium, and cold spill temperatures for simulated Summer 2007, while Figure 4.8 presents the same for simulated Summer 2008. Both years have similar behaviors, with high concentration variability for medium and cold spills, while the warm spills have earlier arrival times with a dampening effect on the concentration variability. Due to the difference between warm and colder spills, there is an indication that meteorological conditions dictate behavior for warm spills, while the complex hydrodynamics are responsible for the response for colder spills. Summer 2007 and 2008 have initial low concentrations arriving at five to six days after a warm spill occurs, while medium and cold spills have an arrival time of about ten days after the spill.

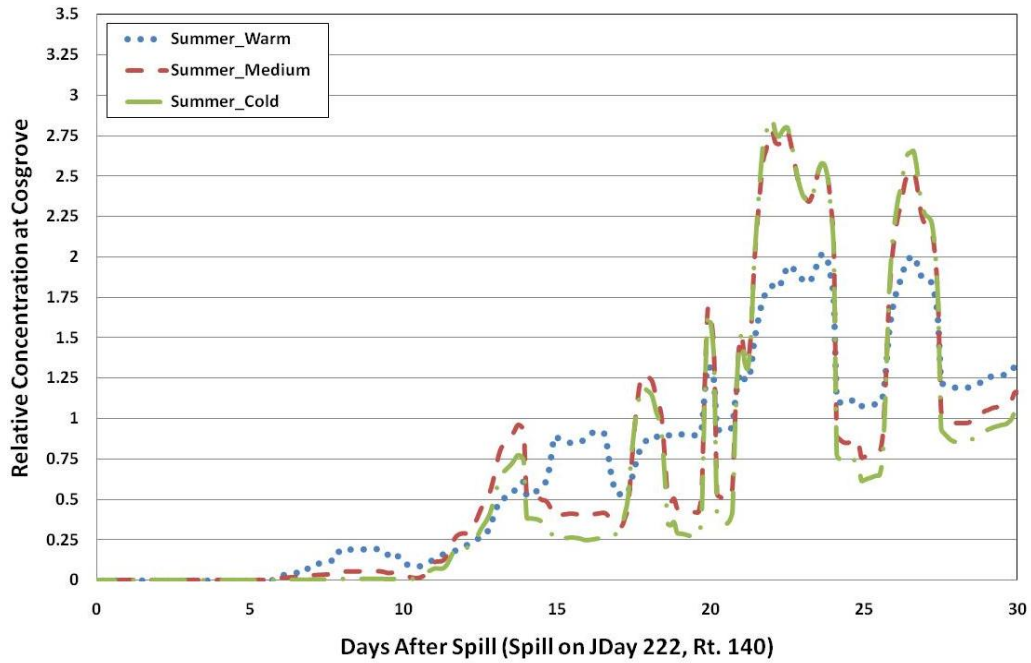


Figure 4.7: Relative contaminant concentration behavior at Cosgrove Intake for 2007 Summer, spill temperature variations for spill at Rt. 140 Bridge on Julian Day 222

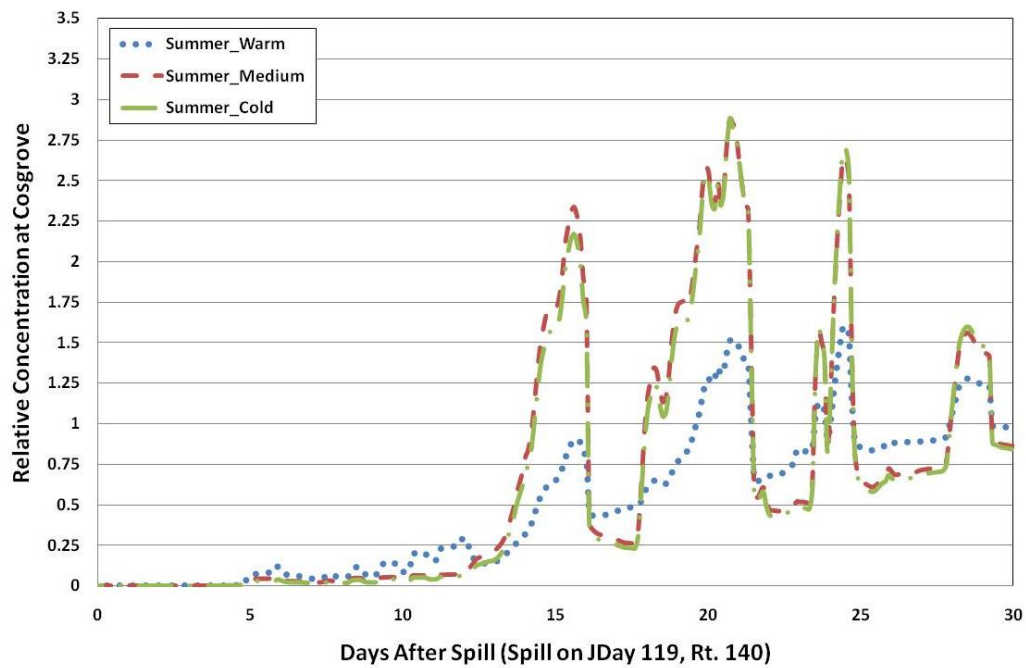


Figure 4.8: Relative contaminant concentration behavior at Cosgrove Intake for 2008 Summer, spill temperature variations for spill at Rt. 140 Bridge on Julian Day 227

The seasonal pattern for Summer spills for all six simulated years is shown in Figure 4.9 to Figure 4.11, which present results for simulated Summer years 2003 to 2008 for warm, medium, and cold spills. Typically a warm spill has less concentration variability and lower concentration magnitude than medium and cold spills. A warm spill has an arrival from five to fourteen days after the spill, while medium and cold spills arrive time ten to fifteen days after the spill occurs, which is consistent with the timeframe found by Sokjowski (2011). The difference between spills that remain on top of the water column and the spills that transport at lower levels suggest that meteorological conditions greatly impact the surface spills and that the complex overall hydrodynamics of the reservoir greatly impact the spills located at lower levels in the water column. The relative concentration magnitudes vary from nearly 1.5 to 3.0 for the peaks and 0.5 to 2.0 for minimum in the variability, showing the Summer variability for all years. One influence explored later in this report is the Quabbin interflow.

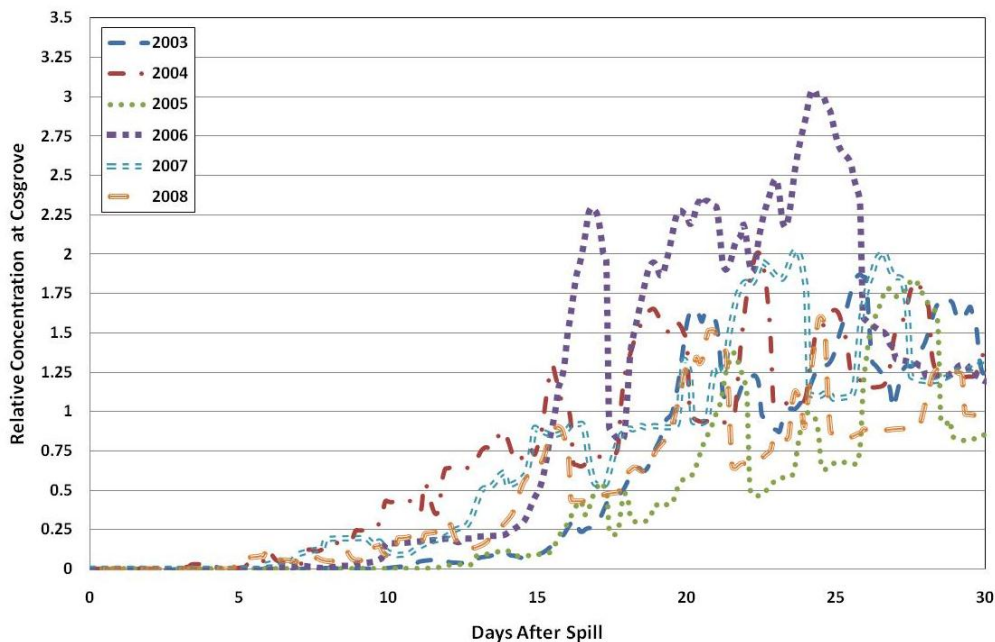


Figure 4.9: Relative contaminant concentration behavior at Cosgrove Intake for Summer model years 2003-2008 with warm spill at the Rt. 140 Bridge

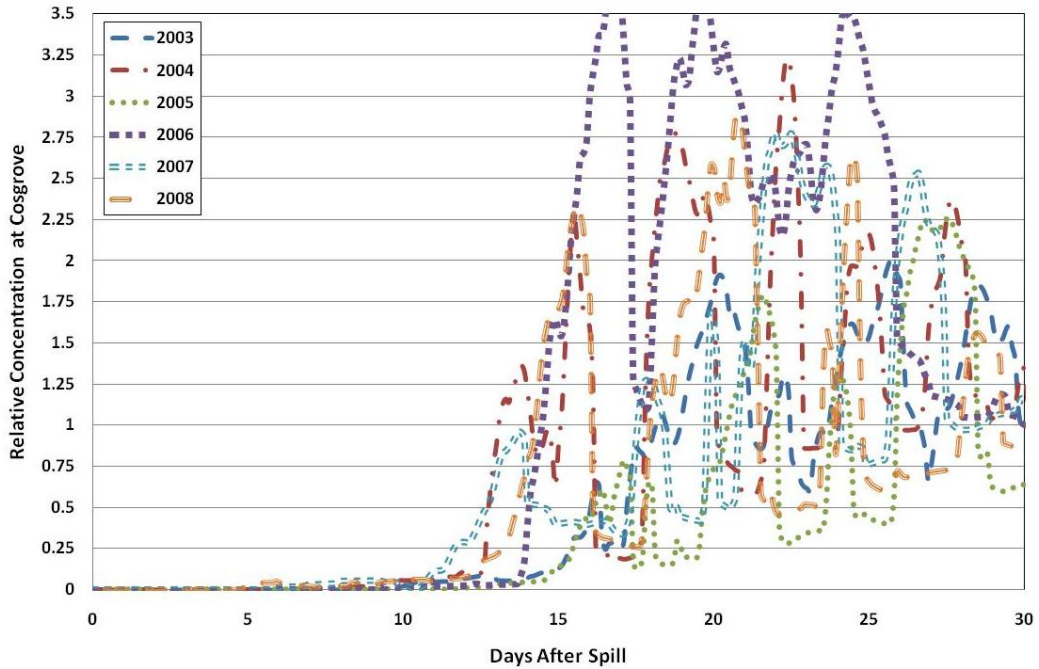


Figure 4.10: Relative contaminant concentration behavior at Cosgrove Intake for Summer model years 2003-2008 with medium spill at the Rt. 140 Bridge

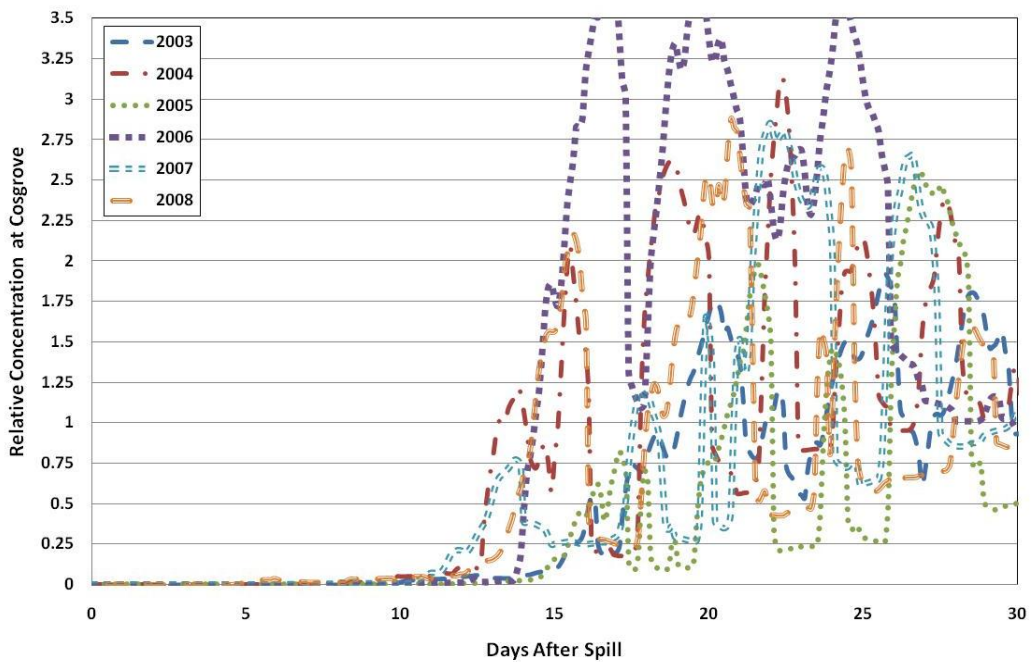


Figure 4.11: Relative contaminant concentration behavior at Cosgrove Intake for Summer model years 2003-2008 with cold spill at the Rt. 140 Bridge

4.1.3 Fall Season Spill

The Fall season captures the destratification of the reservoir and temperatures typically become colder and more uniform. Quabbin Aqueduct usually has no flow, and water demand, inflows, outflows, and precipitation are somewhat low. Figure 4.12 and Figure 4.13 present the spill results for the 2007 and 2008 Fall seasons, respectively. When the spill occurs, the reservoir typically has a small temperature gradient (if not uniform temperature) therefore the behavior of the spill does not depend on where it is located (i.e. temperature) within the water column. The 2007 results show an arrival time of nine days after the spill. There is a spike in relative concentration to a value of 1.0 at approximately fourteen days after the spill occurs and then concentration decreases to a value of 0.75 shortly after, followed by a steady increase to a value of 1.0, which is an unusual Fall behavior. The 2008 results show an arrival time of six days with a slow, almost linear with time, increase in concentration at the Cosgrove Intake which indicates that there are lower velocities within the reservoir and the contaminant is more slowly dispersed throughout the reservoir. Sojkowski (2011) determined that the arrival times for the Fall season were between seven and ten days after the spill, so the results for 2007 and 2008 indicate that the full arrival timeframe may be broader, from six to ten days.

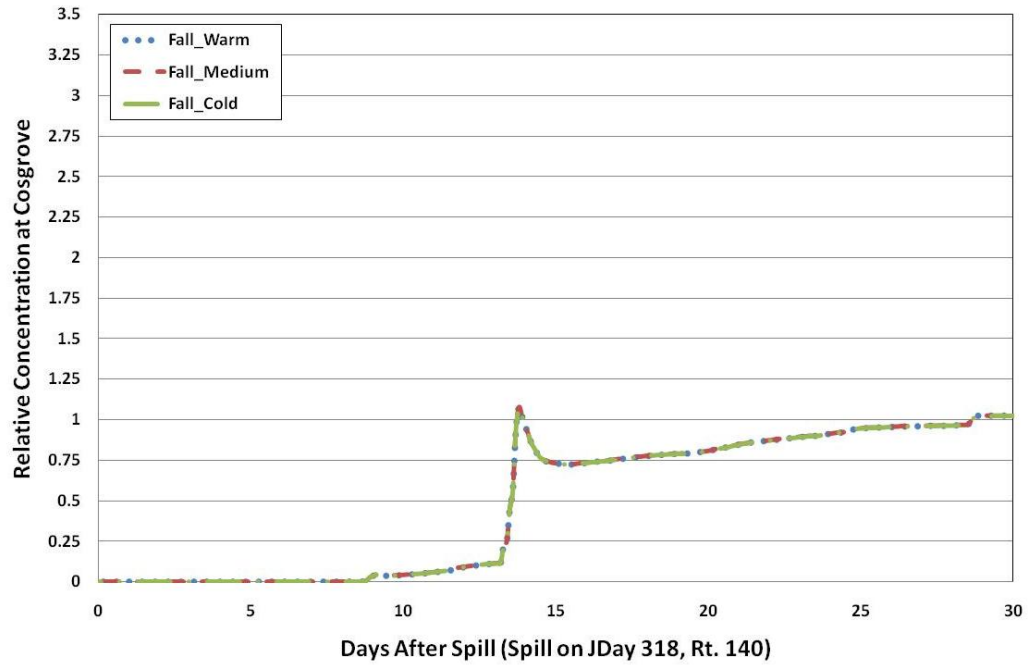


Figure 4.12: Relative contaminant concentration behavior at Cosgrove Intake for 2007 Fall, spill temperature variations for spill at Rt. 140 Bridge on Julian Day 318

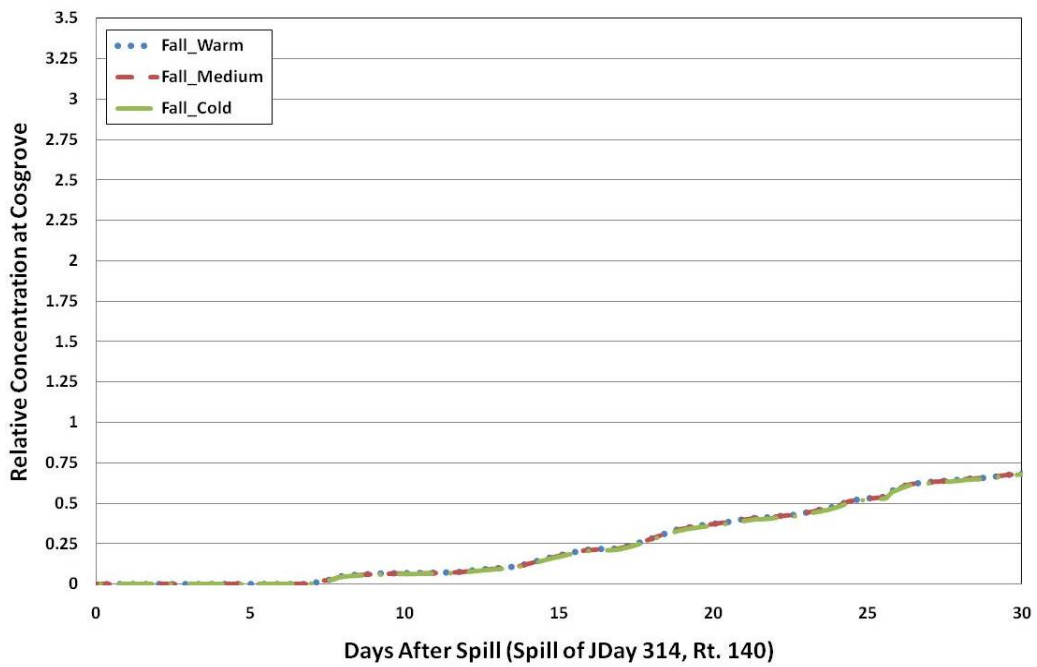


Figure 4.13: Relative contaminant concentration behavior at Cosgrove Intake for 2008 Fall, spill temperature variations for spill at Rt. 140 Bridge on Julian Day 318

The results for Fall season spills for five years, as shown in Figure 4.14 to Figure 4.16, establish the Fall seasonal pattern for the simulated years for warm, medium, and cold spills. It should be noted that there is no simulation for 2003 because during the Fall of that year there was construction at the connection of Cosgrove Intake to the new Carroll Water Treatment Plant so the Wachusett Aqueduct was being implemented as the main withdrawal to supply the Boston metropolitan area. An arrival time frame of four to ten days emerges with no dependence on the temperature of the spill as there is no difference in behavior of the contaminant spill for warm, medium, and cold spills; indicating that the Wachusett Reservoir temperature and velocities are relatively uniform with depth. The year to year behavior varies, which is due to the particular hydrodynamics of the time, not due to meteorological conditions (which do have significant influence in the Spring and Summer seasons).

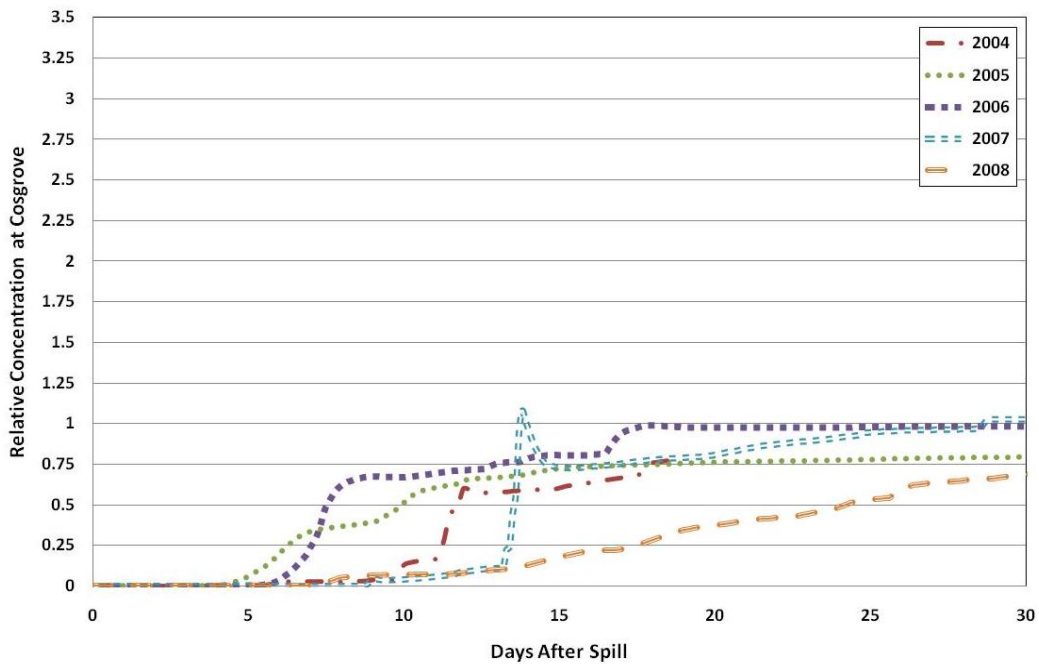


Figure 4.14: Relative contaminant concentration behavior at Cosgrove Intake for Fall model years 2004-2008 with warm spill at the Rt. 140 Bridge

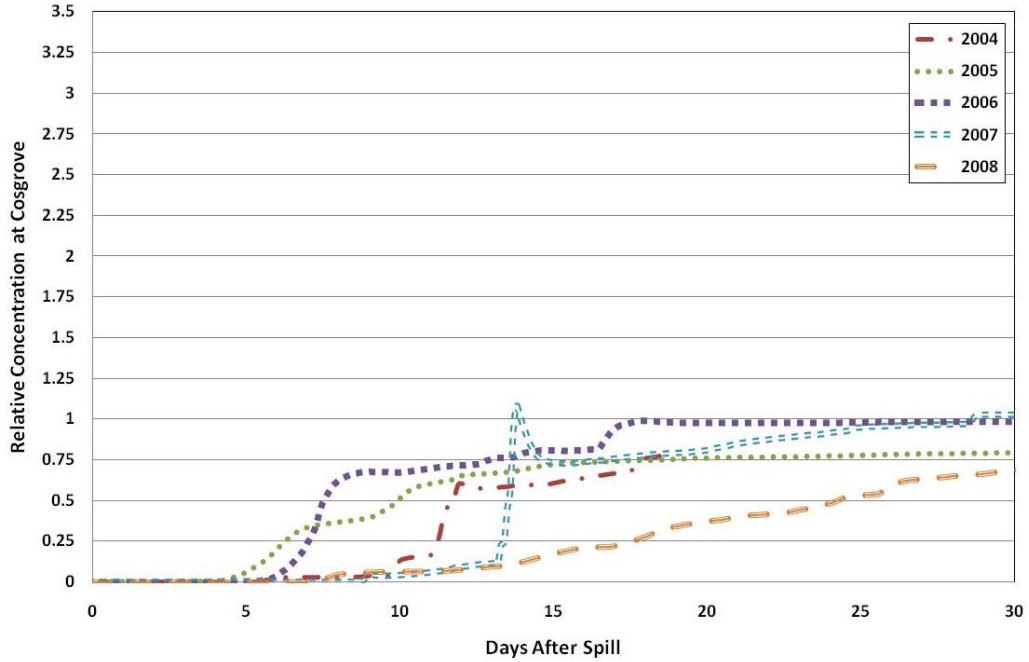


Figure 4.15: Relative contaminant concentration behavior at Cosgrove Intake for Fall model years 2004-2008 with medium spill at the Rt. 140 Bridge

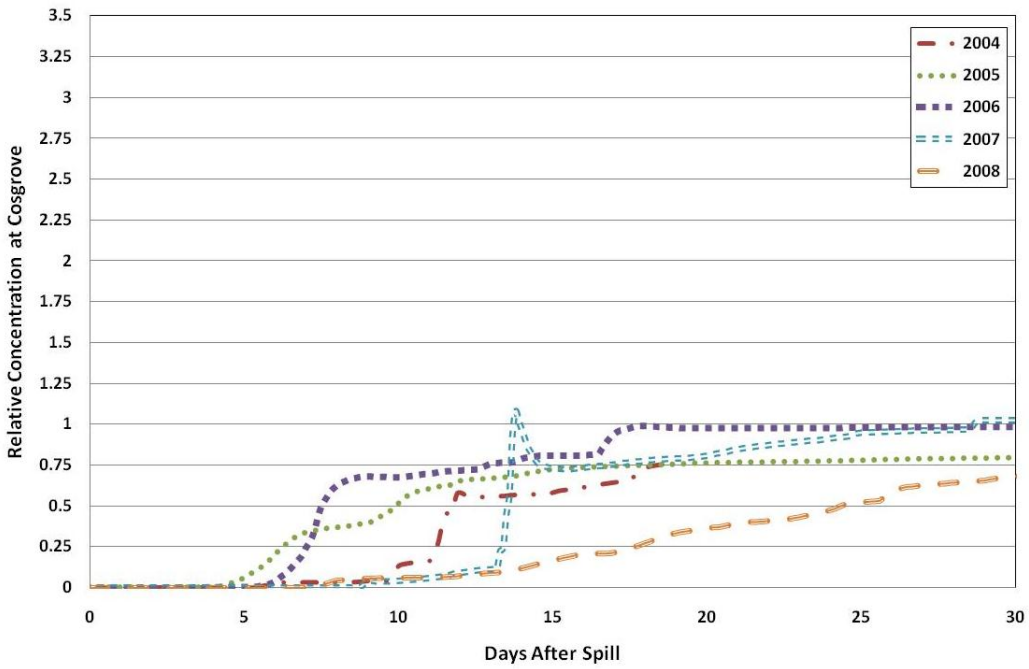


Figure 4.16: Relative contaminant concentration behavior at Cosgrove Intake for Fall model years 2004-2008 with cold spill at the Rt. 140 Bridge

4.2 Quabbin Transfer Influence

The Quabbin Aqueduct is used to supply water to Wachusett maintain desired water surface elevation and also sometimes to alter water quality by increasing discharge to the Nashua River, typically during the summer and early fall months. An interesting event happens when the Quabbin water flows through the reservoir during periods of stratification; this is known as the Quabbin Interflow. The Quabbin interflow is essentially Quabbin water flowing through the Wachusett Reservoir at a specific depth. This can be observed in the specific conductance depth profiles because the Quabbin water specific conductance is relatively low compared to overall Wachusett Reservoir water. Due to the cold temperature of the Quabbin water, it is found to transport mainly at a depth of five to fifteen meters below the water surface. Sojkowski (2011) explored the influence of the Quabbin transfer on spill behavior for 2003 to 2006; his results showed that turning the Quabbin transfer off during the summer (when it is normally on) dampens the variability of the contaminant concentration arriving at the Cosgrove Intake. He also noted that there is little difference when changing the state of the Quabbin transfer during the Spring and Fall seasons; these seasons are not explored for 2007 and 2008.

The influence of the Quabbin transfer is presented in Figure 4.17 to Figure 4.20, which show results for changing the state of the Quabbin transfer for simulation years 2007 and 2008 warm and cold spills during the Summer. The “Quabbin_Actual_On” legend means that the real state of the transfer is on and flowing into the Wachusett Reservoir at the time of the spill, whereas “Quabbin_Turned_Off” means that the model input file was altered to simulate the Quabbin transfer being shut off in response to the spill. The Quabbin transfer is “turned off” twelve hours after the spill to simulate actual reaction time and is kept off for a twenty day period. Results for

2007 show similar arrival times with no dependence on the state of the Quabbin transfer. When the Quabbin transfer was “turned off”, the magnitude of the maximum concentration is greater than when it is “actually on”, however, variability is dampened, which is the important attribute to note. These results are not consistent with past results for years 2003 to 2006, which indicates that there may be other factors responsible for the 2007 behavior. Simulated 2008 results (Figure 4.19 and Figure 4.20) are more similar to those for 2003 to 2006 where the concentration variability at the Cosgrove is dampened when the Quabbin transfer was “turned off” for both warm and cold spills. There is no difference in arrival times, however, there is a significant difference in the behaviors at the Cosgrove Intake. These results are consistent with results from Sojkowski (2011).

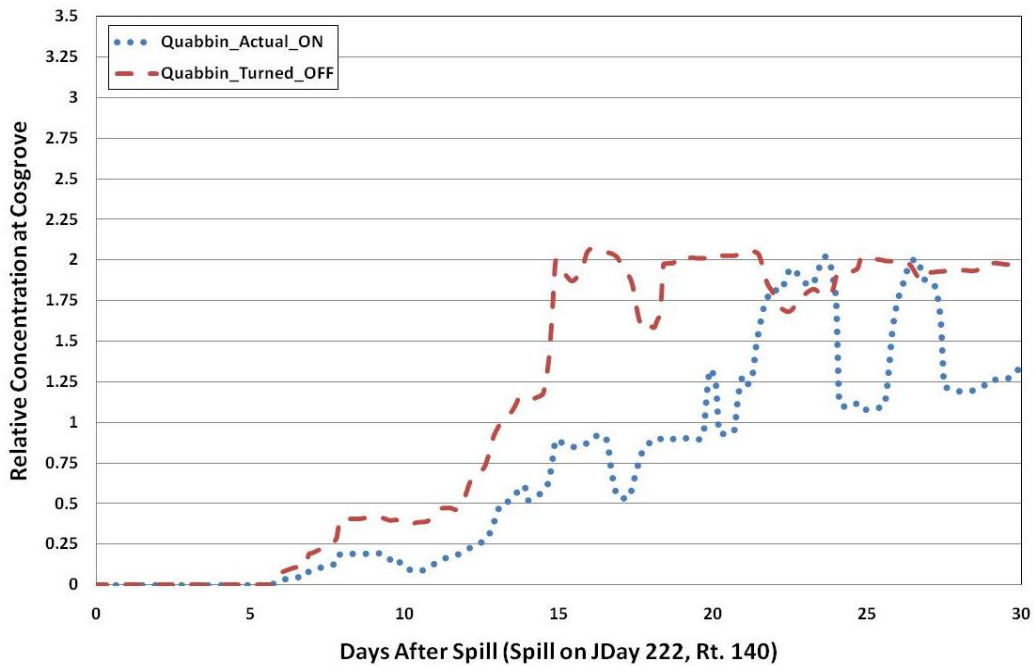


Figure 4.17: Relative contaminant concentration behavior at Cosgrove Intake for Summer model year 2007 warm spill by varying the state of the Quabbin Transfer

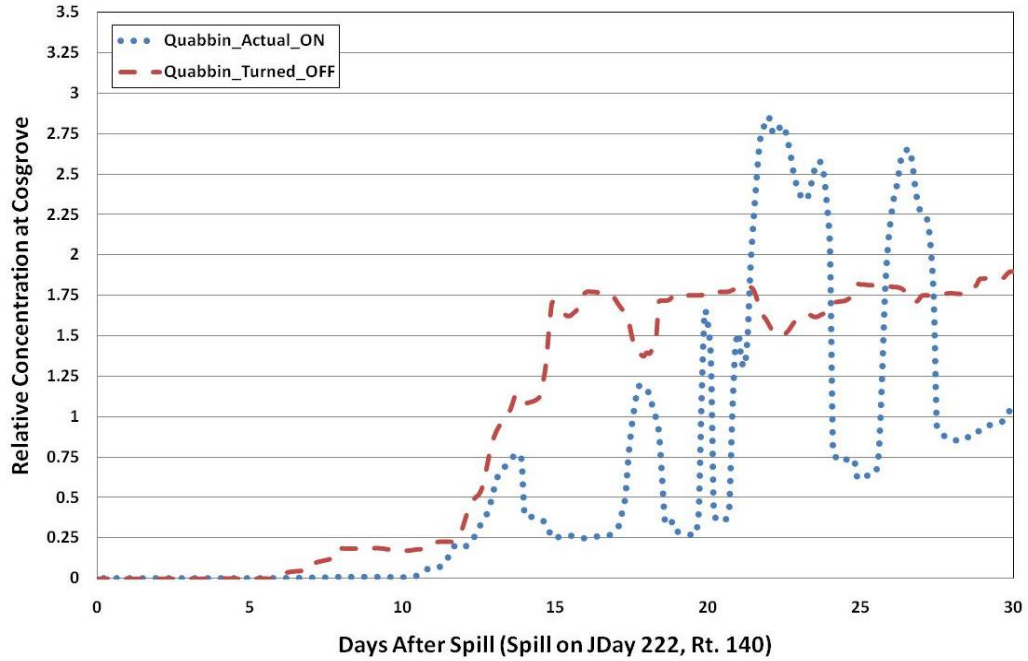


Figure 4.18: Relative contaminant concentration behavior at Cosgrove Intake for Summer model year 2007 cold spill by varying the state of the Quabbin Transfer

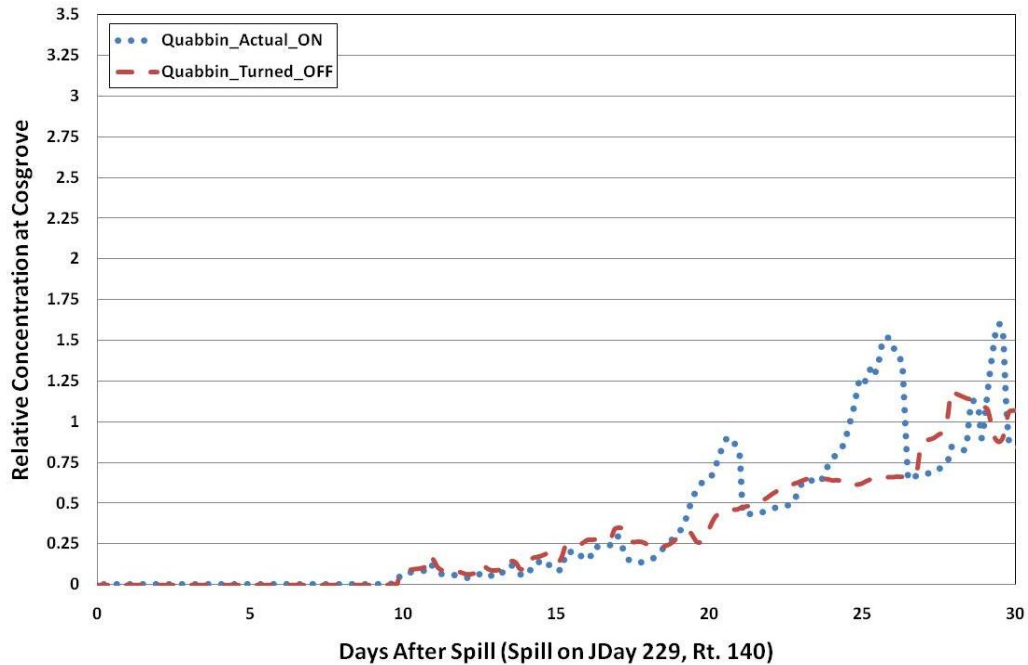


Figure 4.19: Relative contaminant concentration behavior at Cosgrove Intake for Summer model year 2008 warm spill by varying the state of the Quabbin Transfer

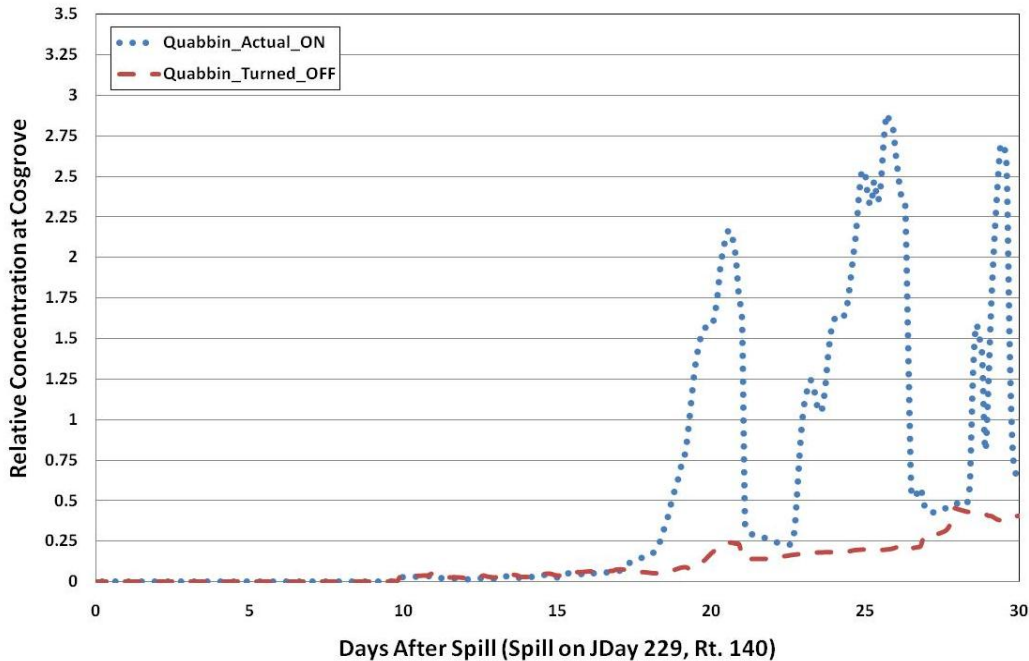


Figure 4.20: Relative contaminant concentration behavior at Cosgrove Intake for Summer model year 2008 cold spill by varying the state of the Quabbin Transfer

4.3 Daily Variability in Spill Behavior

Seasonal impacts on spill behavior have been examined by selecting one day within a season for the spill for multiple years. This section provides results to investigate the variability at arrival time for spills occurring week to week within a twenty day seasonal period. Figure 4.21 to Figure 4.23 present results of day of spill variation for Spring, Summer, and Fall seasons. The figures present the behavior of relative Cosgrove concentrations for five different spill dates within a twenty day period. The spill dates are selected in five day intervals, starting ten days before and going to ten days after the previously investigated yearly seasonal spill date. The solid line in the graphs are the results from the seasonal yearly plots presented in Section 4.1. Figure 4.21 presents results for a Spring 2005 warm spill. The arrival time is very similar for all cases at about four to six days after the spill occurred and the behavior after arrival are relatively similar as well. The spill that occurred on Julian day 104 has a couple of peaks when it first

arrives at the Cosgrove, most likely due to meteorological conditions; this behavior is not seen for spills on subsequent dates.

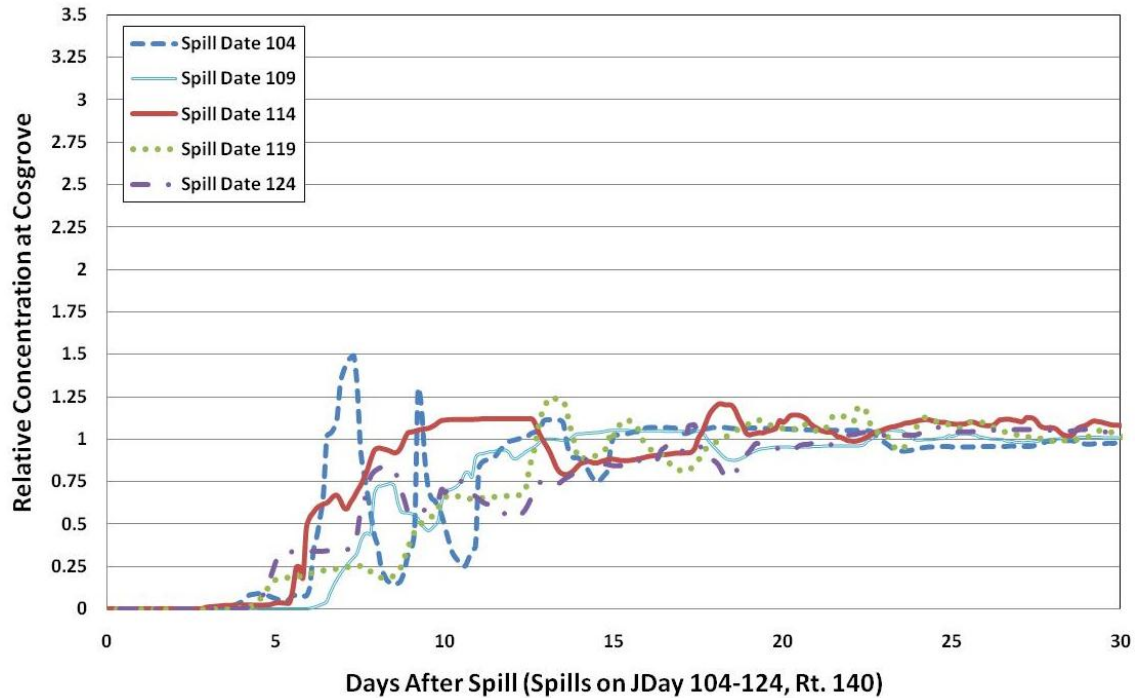


Figure 4.21: Relative contaminant concentration behavior at Cosgrove Intake for Spring model year 2005 warm spill; varied spill date ten days before and after original date in five day intervals

Summer 2008 day of spill variation results are presented in Figure 4.22. Arrival times are similar at eight to ten days, however, the behavior patterns and concentration magnitudes vary considerably. The spills which occurred on Julian day 219 and 224 are more variable than the other days which suggests that some event occurs within that period of time to increase the variability. The spills which occurred on Julian day 229, 234 and 239 are less variable with a steady increase in concentration. The results help enforce the prior seasonal results that show that the summer spills have extremely variable Cosgrove concentrations, but arrival times are similar due to similar meteorological conditions over the twenty day period.

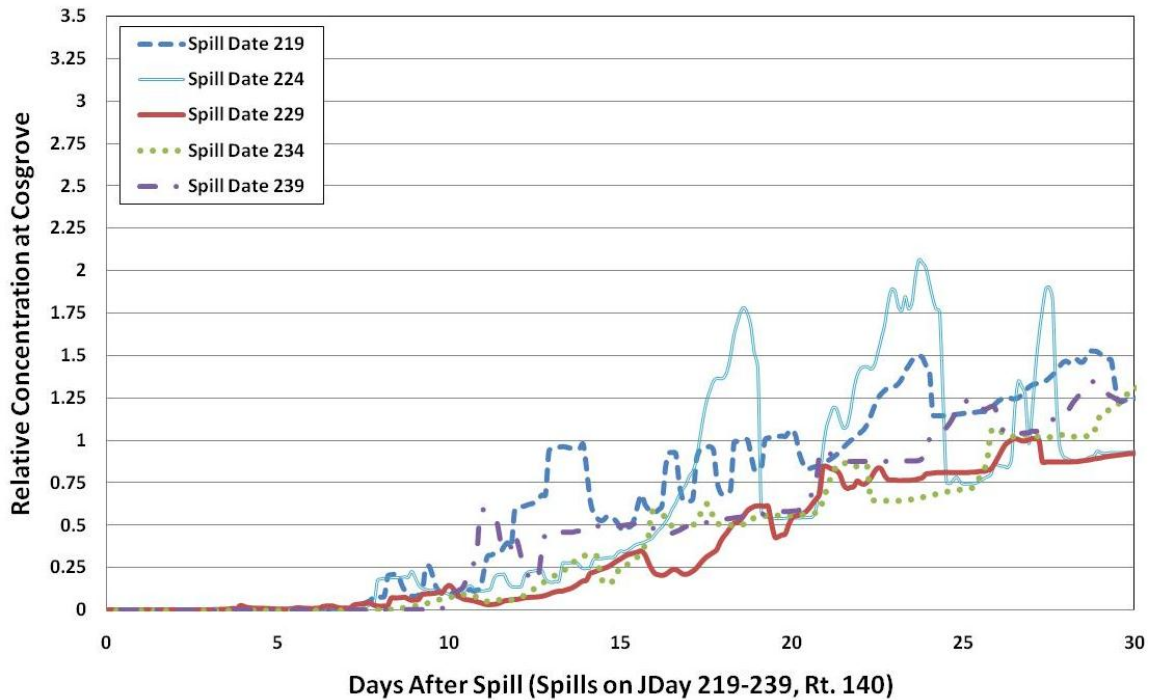


Figure 4.22: Relative contaminant concentration behavior at Cosgrove Intake for Summer model year 2008 warm spill; varied spill dates, ten days before and after original date in five day intervals

Fall 2006 day of spill variation results are presented in Figure 4.23. Concentration behavior similar to a delayed CFSTR, and arrival times, are very similar, with an arrival time of about five days. The similar behavior and magnitudes for the five day interval spill dates enforces the belief that there are uniform hydrological conditions throughout the reservoir that do not vary drastically day to day in the Fall season.

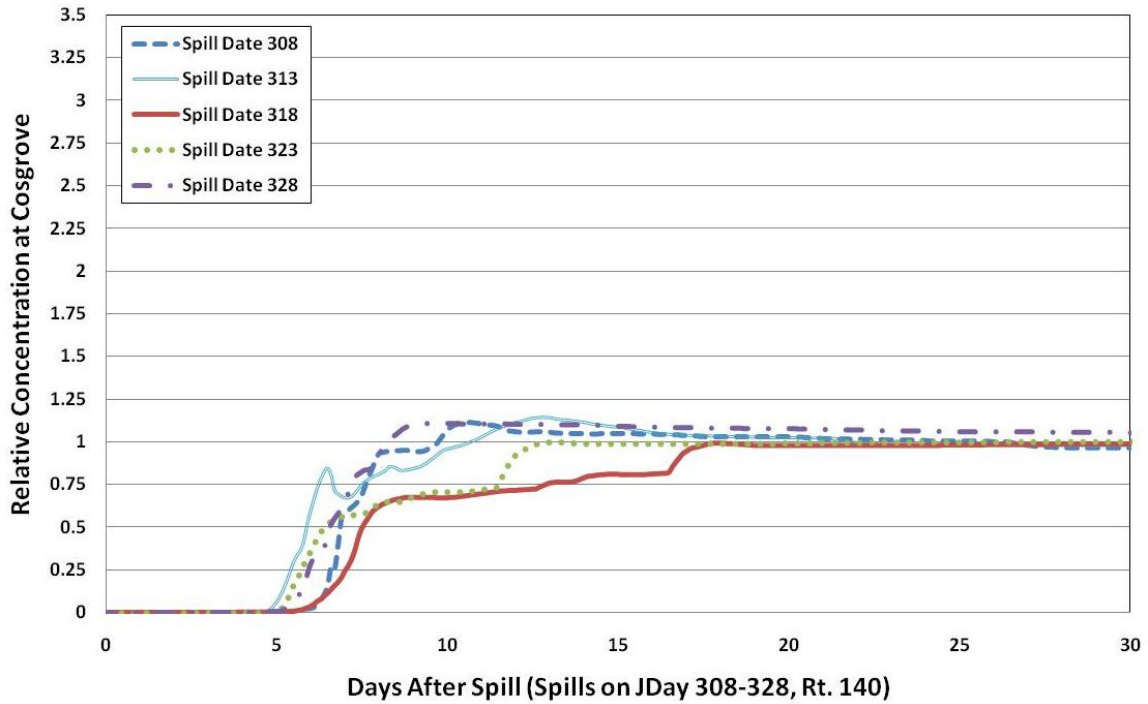


Figure 4.23: Relative contaminant concentration behavior at Cosgrove Intake for Fall model year 2006 warm spill; varied spill dates, ten days before and after original date in five day intervals

Not all the years show similar arrival times and behaviors for the five day variation in day of spill, as shown in Figure 4.24 and Figure 4.25. The following examples are warm spills, and are considered special cases, as discussed in further sections, but are presented in order to demonstrate that arrival time and behavior can vary significantly for spill date variations of only several days. Figure 4.24 presents results for Spring 2003, where the arrival times and behaviors vary drastically between the various spill dates. The arrival time varies from two to seven days, which is a larger timeframe than resulted from the seasonal pattern established by results for all six years. Figure 4.25 presents results for Summer 2007, where arrival times and behaviors vary drastically. The arrival time varies from four to ten days, which is within the timeframe established by the seasonal patterns. Since this is a warm spill, it seems that there is some

meteorological event that is influencing the behaviors of the spills. The Summer season has potential for the extremely variable weather which may be responsible for the behavior.

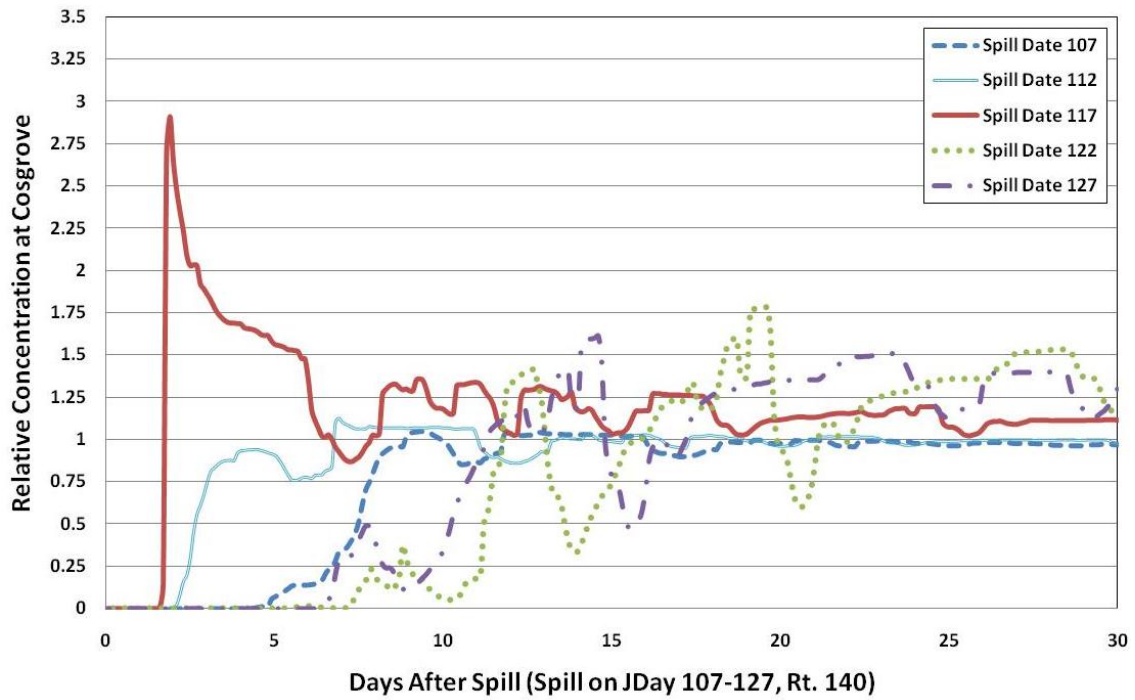


Figure 4.24 Relative contaminant concentration behavior at Cosgrove Intake for Spring model year 2003 warm spill; varied spill date, ten days before and after original date in five day intervals

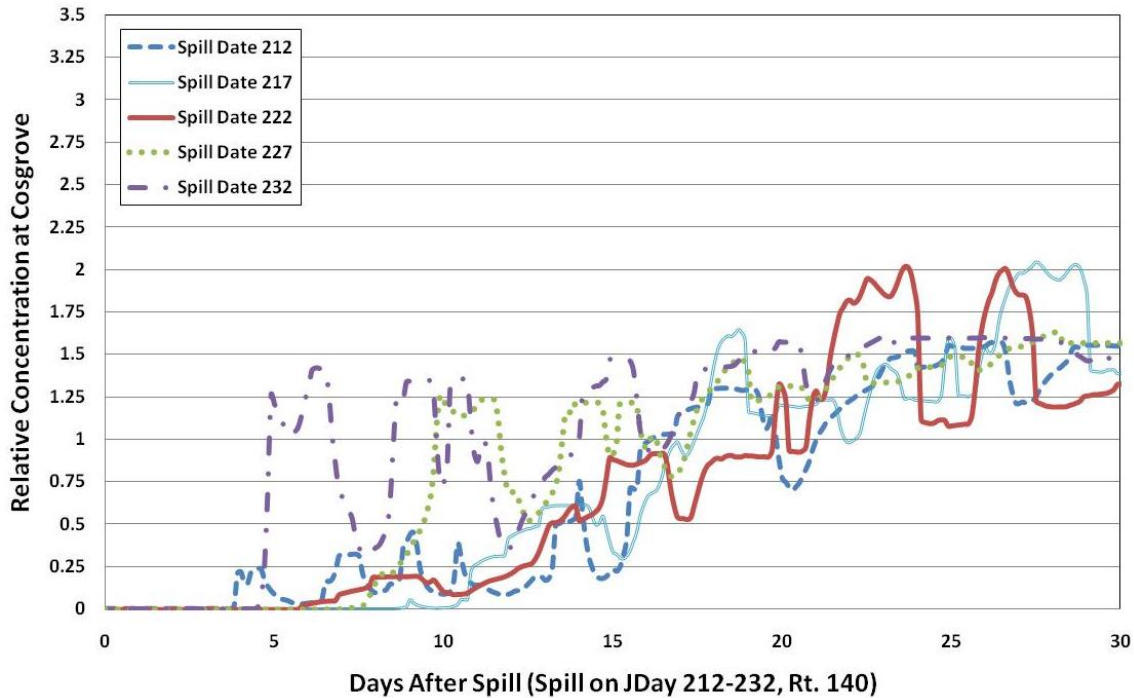


Figure 4.25: Relative contaminant concentration behavior at Cosgrove Intake for Summer model year 2007 warm spill; varied spill date ten days before and after original date in five day intervals

4.4 High Inflow Influence

The purpose of this section is to present results that examine the impact of high inflow events on the spill behavior at the Cosgrove Intake. High inflow events are determined by unusually high inflows for short periods of time in the Quinapoxet and Stillwater Rivers. This is an area of interest because high inflow events correlate to high precipitation events or storms, causing unfavorable driving conditions and accidents may be more likely. The following are case studies for three different storms.

The first case study is for a high inflow event that occurred on Julian day 173 in the Spring of 2003; results for the spill analysis are presented in Figure 4.26. The results are similar to those presented in the day of spill section of this report, however, these figures present results for spills

that occurred two days before to two days after the high inflow event with one day spill occurrence intervals. As the spill occurs in later dates, the arrival time becomes earlier (i.e. a spill that occurs on Julian day 171 has an arrival time of 13 days and a spill that occurs on Julian Day 172 has an arrival time of twelve days). The arrival times range from nine to thirteen days. The concentration behavior is extremely variable and there does not seem to be any similarity to the behavior or arrival time at all. A new view of this data is needed to see if a similarity to the spill behaviors exist.

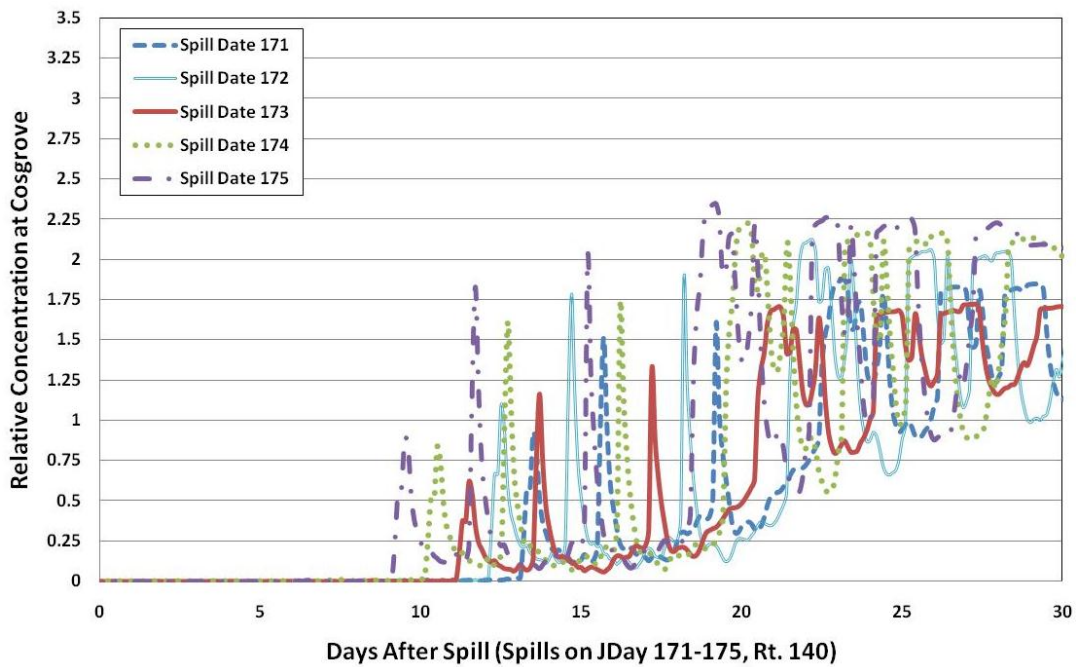


Figure 4.26: Relative contaminant concentration behavior at Cosgrove Intake for Summer model year 2003 warm spill; varied spill date, two days before and after original date in one day intervals to evaluate high inflow events with “Days After Spill” time

Interestingly, the arrival times and concentration variability are all very similar, as seen in Figure 4.27, which displays the same results as Figure 4.26, but on a Julian Day time scale instead of a

days after spill basis. All the spills arrive on Julian day 184 with identical behaviors, except for the magnitudes of the concentrations. The results suggest that the storm influences the movement of the contaminant within the reservoir. The spills that occur prior to the high inflow event are transported when the high inflows enter the reservoir, while the spill that occurs during and after the high inflow event have the reservoir has increased velocities. It should be noted that outflow from the Cosgrove Intake and Nashua River also increased during that time period, which may contribute to increased net transport velocities within the reservoir.

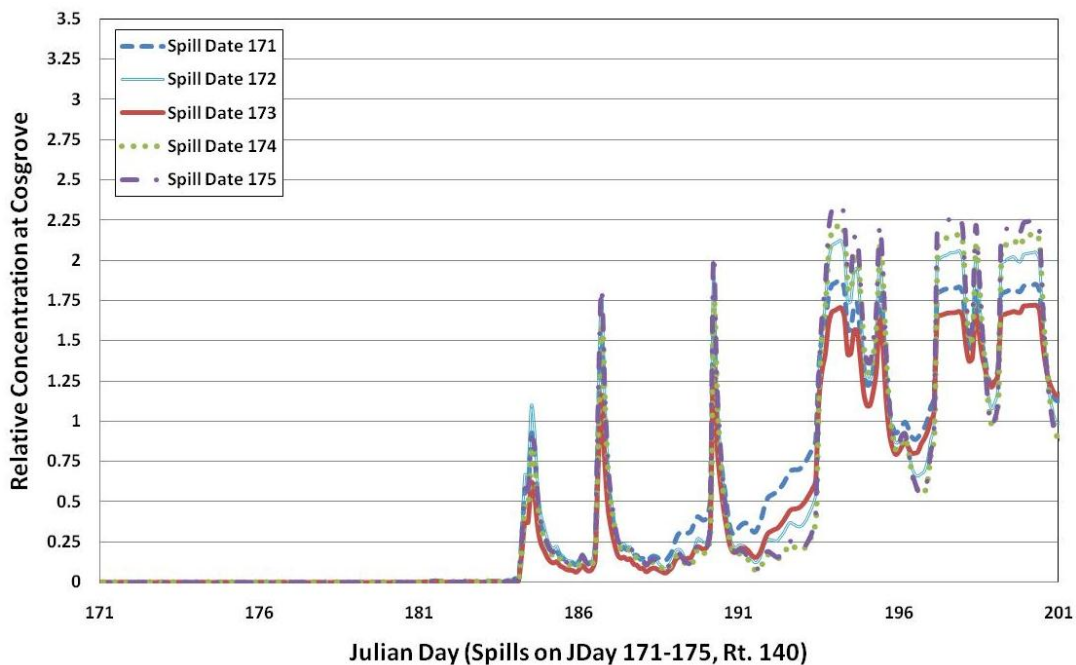


Figure 4.27: Relative contaminant concentration behavior at Cosgrove Intake for Summer model year 2003 warm spill; varied spill date, two days before and after original date in one day intervals to evaluate high inflow events with “Julian Day” time

The same Spring 2003 high inflow event is evaluated for a cold spill and the results are presented in Figure 4.28. Arrival times are more similar, around thirteen to fifteen days and there appears

to be a correlation between the spills for the concentration peaks for the spills that occur before and during the high inflow event. The peaks look offset by about a day and a pattern emerges if the same data are plotted on a Julian day time scale rather than a days after spill time scale, as presented in Figure 4.29. All the spills have very similar contaminant behavior to the spill that occurs on the day of the high inflow event, with the peaks and valleys occurring at the same Julian day. The high inflows may be responsible for dampening out the magnitudes of the spill, which could be due to the high velocities at the deeper section of the reservoir due to the increase of inflows to the reservoir.

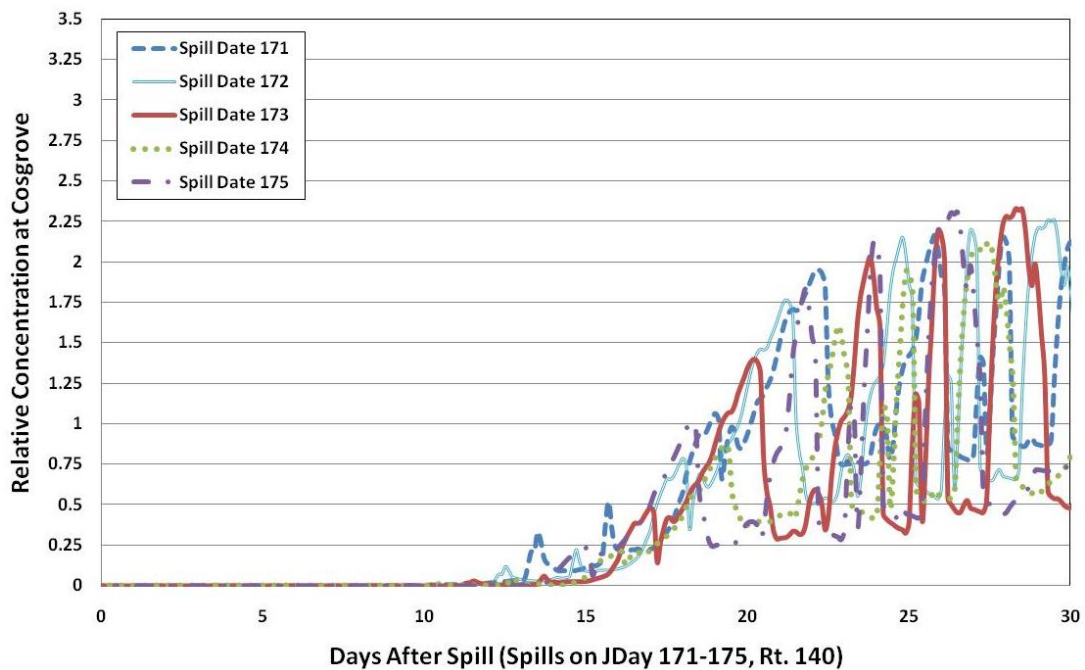


Figure 4.28: Relative contaminant concentration behavior at Cosgrove Intake for Summer model year 2003 cold spill; varied spill date, two days before and after original date in one day intervals to evaluate high inflow events in “Days After Spill” time

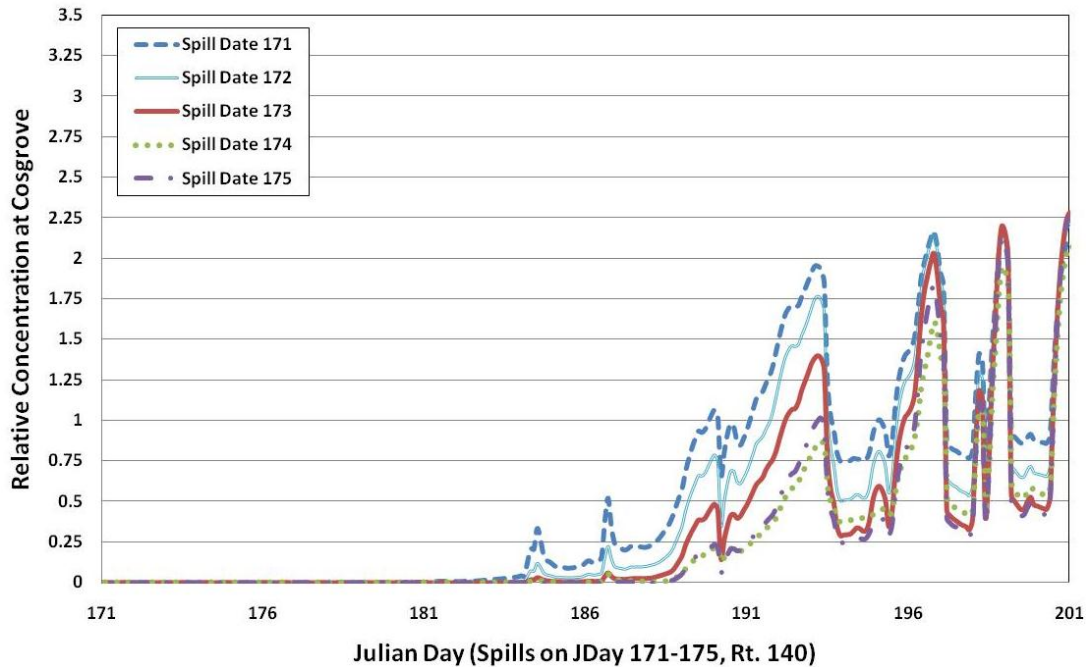


Figure 4.29: Relative contaminant concentration behavior at Cosgrove Intake for Summer model year 2003 cold spill; varied spill date, two days before and after original date in one day intervals to evaluate high inflow events in “Julian Day” time

The second case study examined is a high inflow event that occurred for five days in the Spring of 2005 from Julian day 88 to 93. Only a warm spill is evaluated because colder spills have more similar responses to high inflow events, as shown for the Spring 2003 high inflow event. The results from evaluating the Spring 2005 high inflow event are presented in Figure 4.30. Spills on Julian days 87 and 94 occur one day before and one day after the high inflow event to capture the full spectrum of the high inflow influence. A similar result as for the previous case emerge as for spills that occur on later subsequent dates, the arrival times become shorter (i.e. a spill that occurs on Julian day 87 has an arrival time of seven days and a spill that occurs on Julian day 88 has an arrival time of six days). Interestingly, at the end of the high inflow event, the spill arrival time increases, indicating that the high inflow event has less of an impact on the behavior of the contaminant spill.

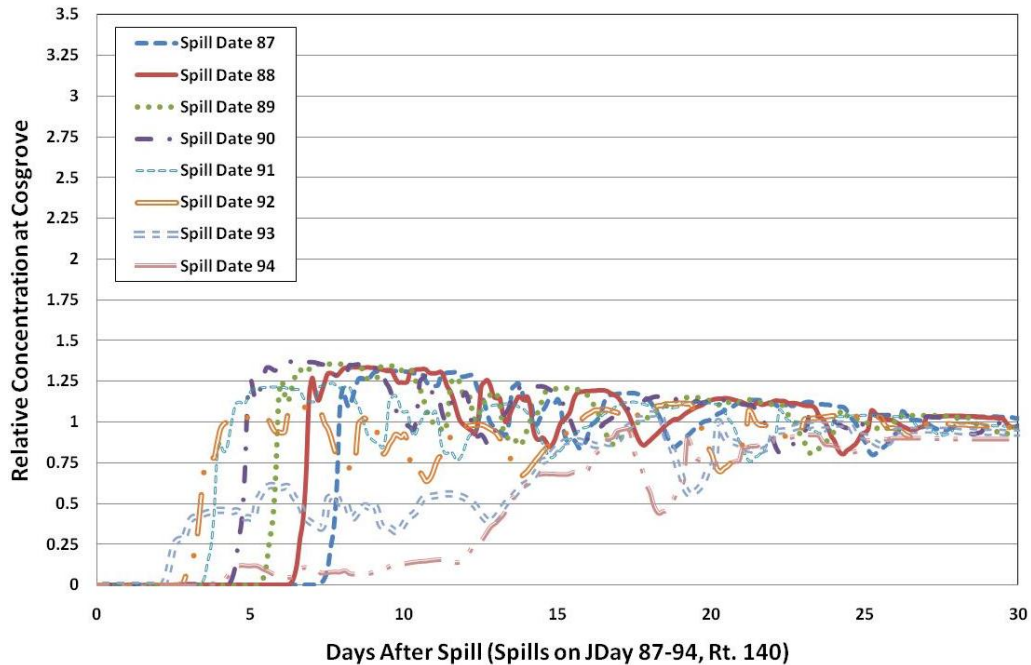


Figure 4.30: Relative contaminant concentration behavior at Cosgrove Intake for Spring model year 2005 warm spill; varied spill date before, during, and after original date in one day intervals to evaluate high inflow events with “Days After Spill” time (high inflows Julian day 88-93)

Similar to the previous case, when plotted on a Julian day scale (Figure 4.31), most of the spills arrive on Julian day 95, indicating that the high inflow event influences the behavior of the contaminant. The spills on Julian day 92 to 94 occur during the end of the high inflow event and there is noticeable difference in the behavior and arrival date. This attribute is consistent with the previous case in that the arrival time for spills that occur at the end of the high inflow event is shorter than for previous days, however, the spill arrives at a later Julian day (i.e. a spill that occurs on Julian day 93 has the earliest arrival time of two days, but arrives a day after all the previous spills arrive). Perhaps the momentum of the high inflow event, which is responsible for the early arrival times, is decreased and the spills are essentially following the increased flux of water from the high inflow event.

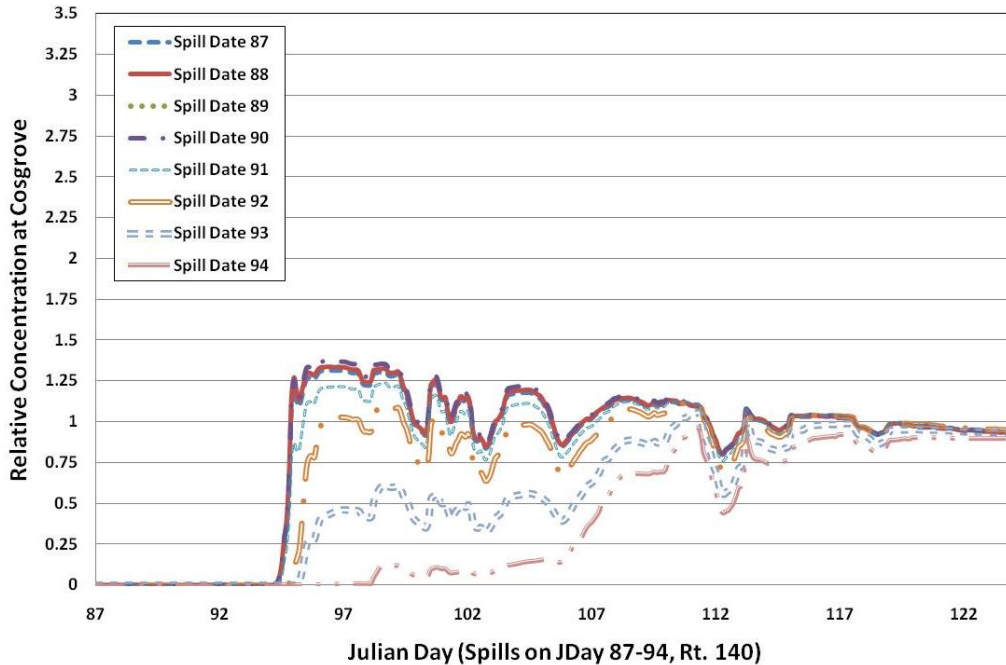


Figure 4.31: Relative contaminant concentration behavior at Cosgrove Intake for Spring model year 2005 warm spill; varied spill date before, during, and after original date in one day intervals to evaluate high inflow events with “Julian Day” time (high inflows Julian day 88-93)

The last case study examined is a high inflow event that occurred over a period of three days in the early months of 2008 from Julian day 65 to 66 followed by another high inflow event on Julian day 69. The results from evaluating the early 2008 high inflow event are presented in Figure 4.32. Spills on Julian days 64 and 70 occur before and after the high inflow events, while the spills on Julian days 67 and 68 fall in between the two high inflow events. The behavior patterns are very similar with a steady increase to a relative concentration value of 1.0. The similar pattern emerges as the spills that occur later in time have shorter arrival times and if plotted on a Julian day time scale, (Figure 4.33), most of the spills arrive on Julian day 70. Spills at the end of the high inflow (Julian days 69 and 70) have the shortest arrival times, however arrive a couple of days after the date of arrival of the spills that occur on Julian days 64 to 67.

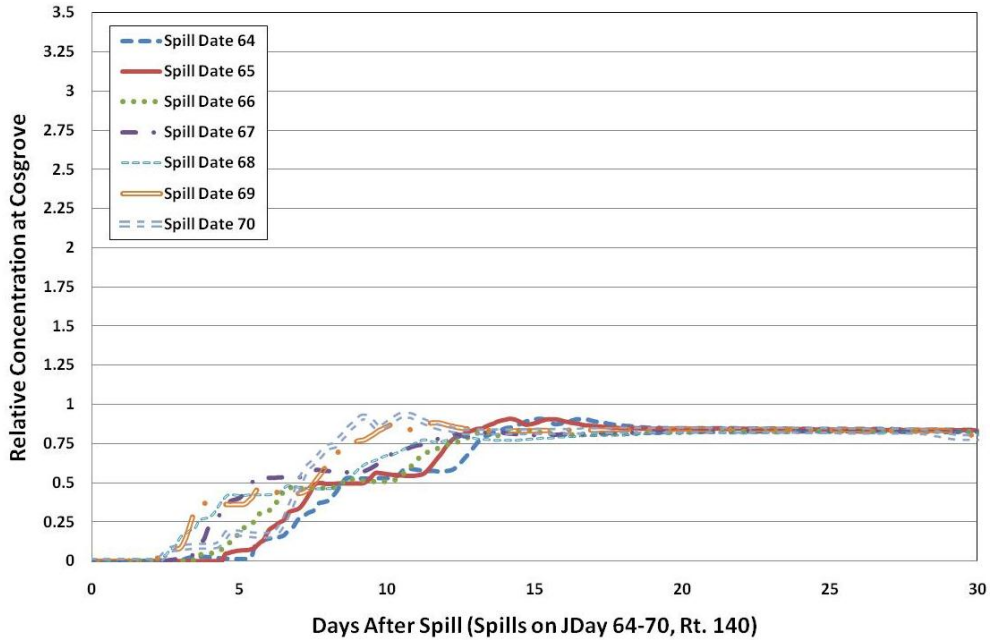


Figure 4.32: Relative contaminant concentration behavior at Cosgrove Intake for model year 2008 warm spill; varied spill date before, during, and after original date in one day intervals to evaluate high inflow events with “Days After Spill” time (high inflows Julian day 65-69)

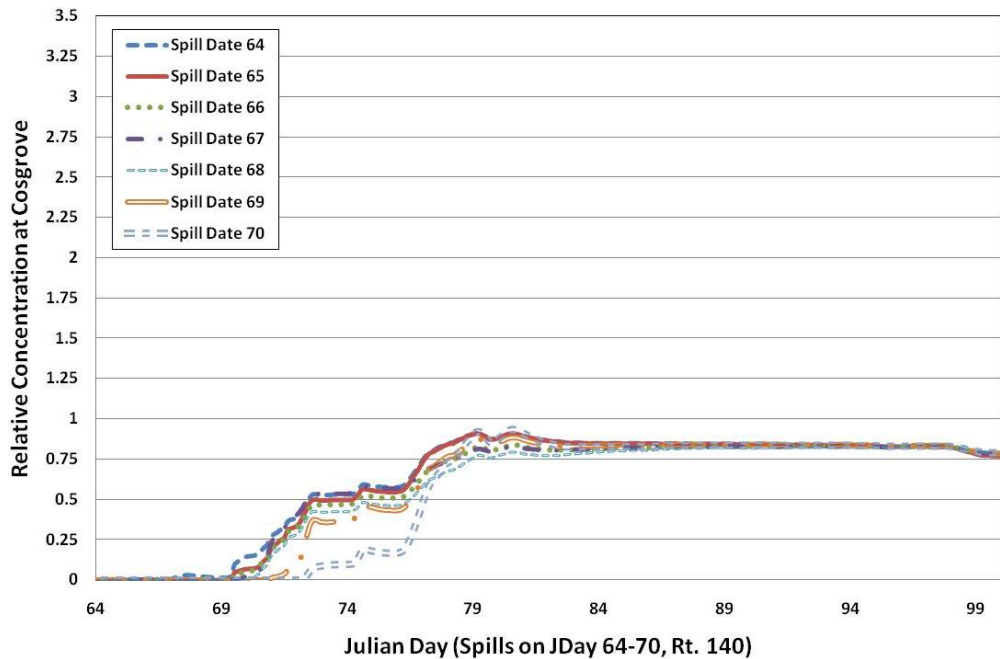


Figure 4.33: Relative contaminant concentration behavior at Cosgrove Intake for model year 2008 warm spill; varied spill date before, during, and after original date in one day intervals to evaluate high inflow events with “Julian Day” time (high inflows Julian day 65-69)

4.5 Wind Influence

Wind over the Wachusett Reservoir is a force of nature that cannot feasibly be altered by humans, however, it is important to know the impact of wind on the spill concentration at the Cosgrove Intake. Stauber (2009) identified that wind has a significant impact on the behavior of a warm spill that is located on top of the water column. She determined that the direction of the wind greatly impacts arrival time and magnitudes for Spring and Summer warm temperatures. A similar study was conducted for this report, however, wind speed was set to zero for selected periods of time after the spill, instead of varying wind direction, in order to identify the impact of the wind on the concentration at the Cosgrove Intake. The model years selected were based on the yearly seasonal warm spill results, where unusual early arrival times can be distinguished. Warm spills should theoretically be affected most by wind because a warm spill is located on top to the water column. Modeled year 2003 Spring is unlike any other year with a large increase in Cosgrove concentration at two days after the spill, while modeled year 2007 Spring has a short arrival time, but with not nearly as much mass arriving at once. The warm 2003 and 2007 Spring spills are used to analyze the effects of wind on the arrival time of the spill contaminant at the Cosgrove Intake.

4.5.1 Modeled Year 2003 Spring Warm Spill

Various time periods were selected for setting zero wind speed in order to assess the concentration response at the Cosgrove Intake. Figure 4.34 presents a comparison of concentration at the Cosgrove Intake for modeled year 2003 in the Spring season by setting wind to zero for selected periods within the first two days following the spill. Recall that the spill

occurs at noon on the day of the spill, in this case Julian day 117. The most profound effect is found by removing wind for Julian days 117.0 to 118.9, the first two days after the spill occurs, which increases the arrival time of the spill by one day and significantly decreases the magnitude of the concentration at the Cosgrove Intake. Further investigation as to what the driving force behind the unusual early arrival time included setting wind to zero for smaller increments of time within the first two days after the spill. Setting the wind to zero for Julian day 117.5 to 118.5 resulted in a very similar result as found for removing the wind for 117.0 to 118.0, which indicates that the wind speed from Julian day 118.5-119.0 has little effect on the spill behavior. In order to investigate further, an even narrower time period of one half a day was selected for zero wind. Simulations setting wind to zero for Julian days 117.5 to 118.0 and 117.75 to 118.25 resulted in a decrease in magnitude of the spill concentration, but had no impact on the initial arrival time at the Cosgrove. Interestingly, however, setting zero wind for Julian days 118.0 to 118.5 resulted in similar results as zero wind for one day after the spill (Julian day 117.5 to 118.5), which indicates that the driving force for slowing down the arrival time is within that window of time.

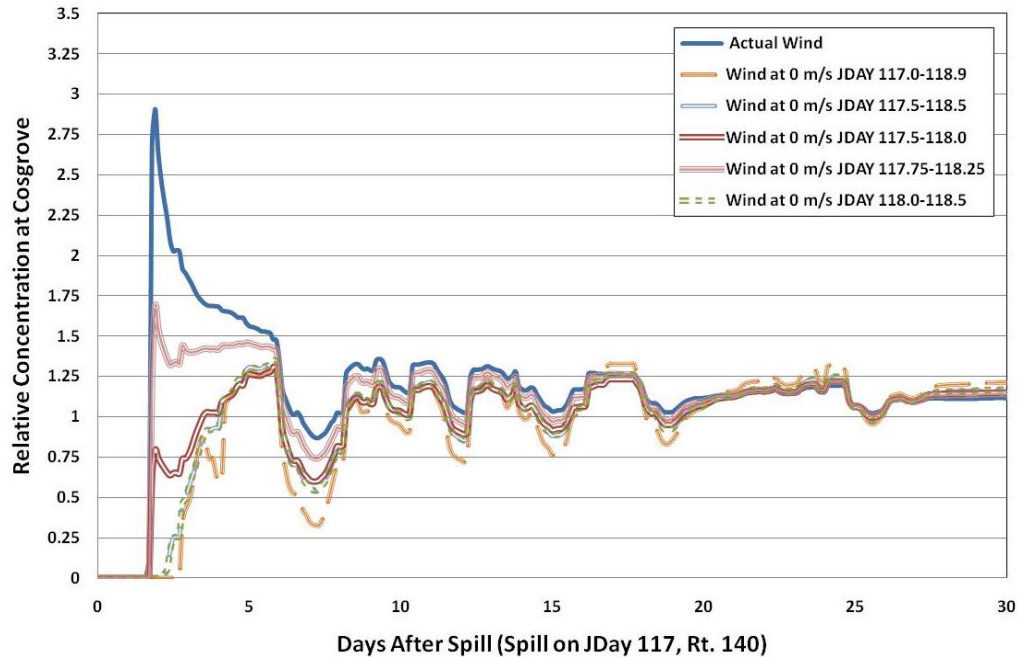


Figure 4.34: 2003 Spring comparison of contaminant concentration behavior at Cosgrove by varying wind speed with spill on Julian Day 117

Investigating the wind speed and direction for the two days after the spill help identify the driving force behind the early arrival time of the spill at the Cosgrove intake. Figure 4.35 presents the “wind rose” for Julian days 117.5 to 118.9, where the axis units are in meters per second and the direction is the actual direction of the wind, not where the wind is coming from. Setting wind to zero for Julian days 117.0 to 118.9 delays the arrival time by about a day, however the wind rose data do not give any insight as to why. Further investigation found that removing wind speed for Julian day 118.0 to 118.5 resulted in similar results as removing wind speed for the entire two days after the spill. The wind rose shows that during Julian day 118.0 to 118.5 the wind is primarily an easterly wind. Based on this it is intuitive that the arrival time at Cosgrove is earlier because that is the direction of the Cosgrove Intake from the spill location at the Route 140 bridge.

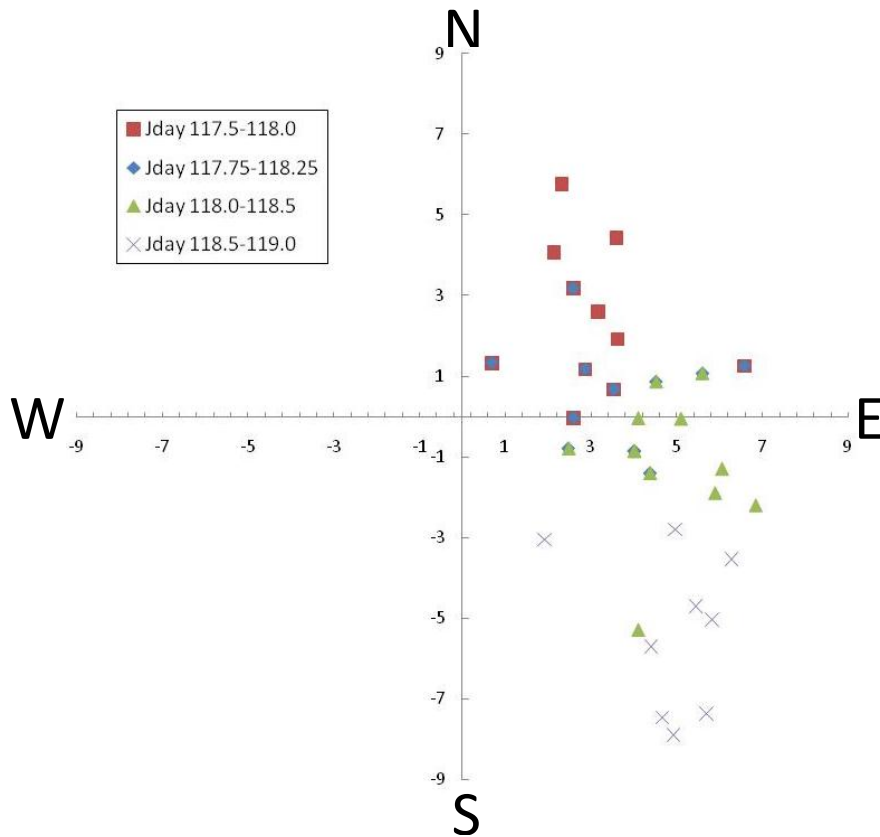


Figure 4.35: Wind Rose (m/s) for Julian Day 117.5 to 118.9

4.5.2 Modeled Year 2007 Spring Warm Spill

The Spring 2007 warm spill simulation resulted in an unusually short arrival time of two days, similar to the Spring 2003 warm spill. An analysis was conducted similar to the prior analysis of the Spring 2003 spill by selecting specific periods of time to force zero wind in order to identify the wind influence; results are presented in Figure 4.36. The spill occurs on Julian day 119, and the time period of interest is two and one half days after the spill, or Julian days 119.5 to 121.9. The first test was to set wind to zero for Julian day 119.5 to 121.9 which resulted in an increase in arrival time from two days to about four and one half days, which indicates that wind is the key factor behind the early arrival time. However, other sections of time were selected to set the wind to zero and there is no twelve hour period of time that affects the arrival time significantly as was found for the Spring of 2003.

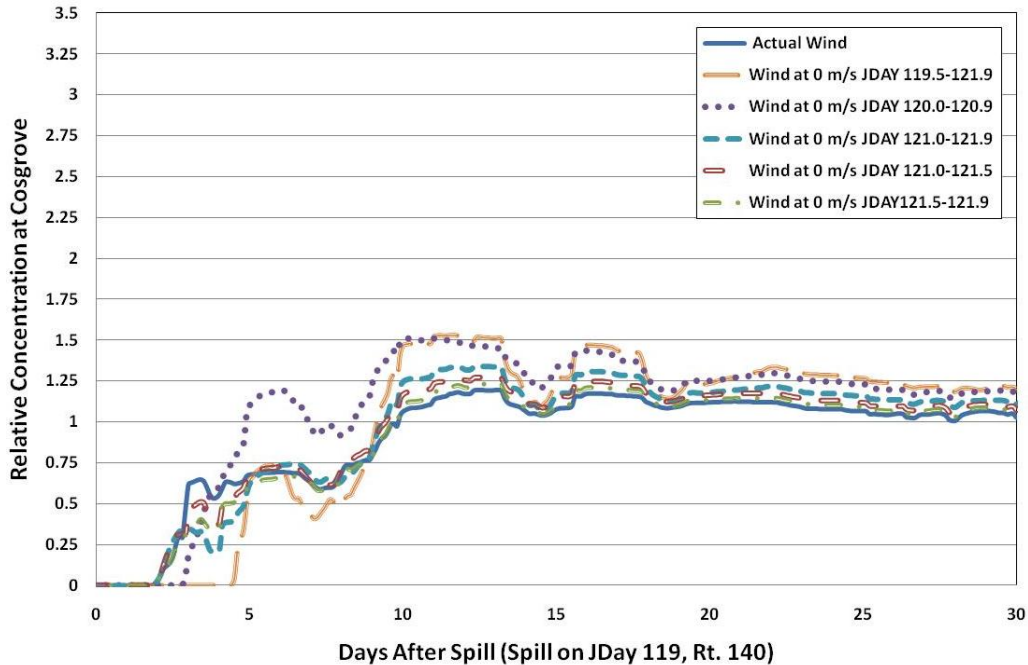


Figure 4.36: 2007 Spring comparison of contaminant concentration behavior at Cosgrove by varying wind speed with spill on Julian day 119

In order to find out why there is no one short period of time that influences the spill behavior significantly, a modified wind rose was produced as for the Spring 2003 case, with the wind direction showing the actual direction the wind is traveling. The wind is in a general easterly direction, however, there are variations north and south quite a bit. Under investigation, however, it can be seen that from Julian day 120.0 to 120.5 the direction is a south east direction, which would be in the direction from the spill location to the South Basin. From Julian day 120.5 to 121.0 there is a general easterly direction, which is the direction from the beginning to the middle of the South Basin. Under further inspection, the wind direction on Julian day 121.0 to 121.5 is in a northeast direction, which is the direction the contaminant would need to travel from the South Basin to the North Basin. The Wachusett Reservoir makes a semi “U” shape, and the combination of wind directions and speeds could be the cause of the early arrival times.

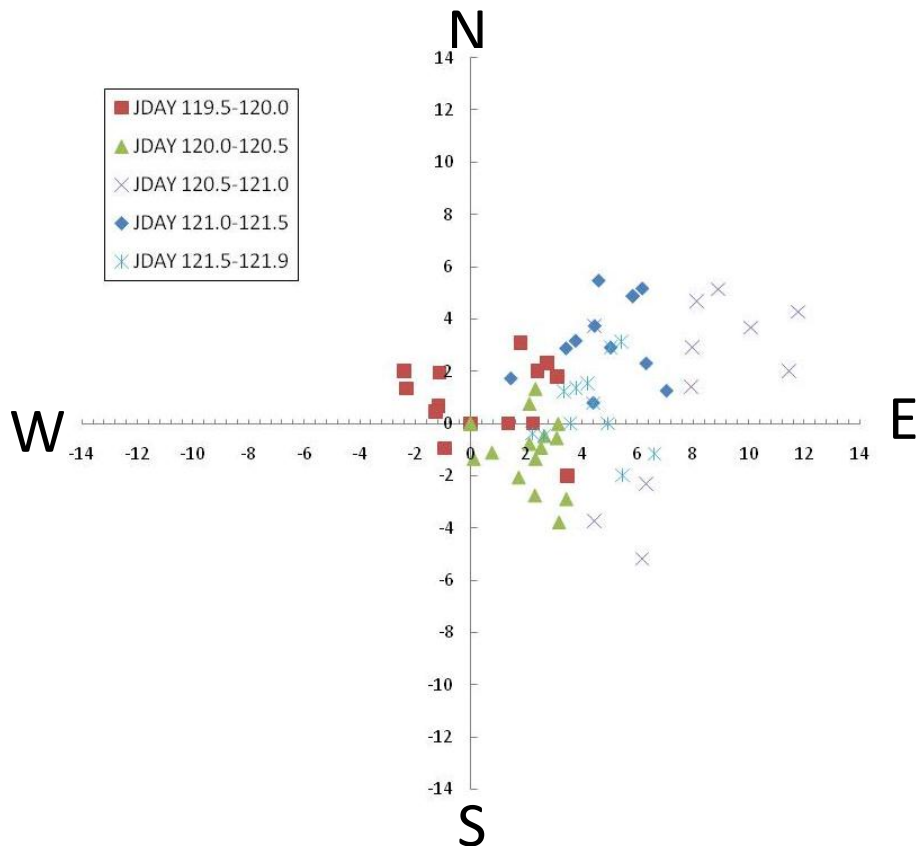


Figure 4.37: Wind Rose (m/s) for Julian Day 119.5 to 121.9

5 SUMMARY, CONCLUSIONS AND RECOMMENDATIONS

5.1 Summary

CE-QUAL W2 Models were successfully generated for calendar years 2007 and 2008 by matching water surface elevations as well as temperature and specific conductance measurements within the Wachusett Reservoir. Error between measured and calculated water surface elevations was minimized by an optimization model in the water balance that adjusts inflow calibration factors to minimize the sum of square residuals. CE-QUAL W2 parameters were adjusted to minimize error between temperature and specific conductance profiles measured in the North Basin by MWRA. This was accomplished by a sensitivity analysis of specific parameters, which included varying a single parameter and comparing the results to other simulations that varied the same parameter, thus finding results that minimized error.

Contaminant spill scenarios were modeled using CE-QUAL W2 and behavior at the Cosgrove Intake was analyzed for calendar years 2003 to 2008 under a variety of conditions. The various scenarios included density of the contaminant, seasonal trends, Quabbin transfer, daily variation, high inflow events, and wind influence. Every spill scenario occurred at the Rt. 140 Bridge because it was determined to be at high risk site for vehicles, and the contaminant was modeled as a conservative tracer (non-reactive). Simulated contaminant concentrations at the Cosgrove Intake were analyzed to determine arrival time and behavior patterns under the various conditions for all modeled years.

5.2 Conclusions

The various scenarios included density of the contaminant, seasonal trends, Quabbin transfer, daily variation, high inflow events, and wind influence. It was determined that the density of the contaminant had an effect in the Spring and Summer seasons, with no effect in the Fall season with respect to arrival time and behavior at the Cosgrove Intake. A spill that transports on the top of the water column (low density/high temperature spill) typically arrives earlier in the Spring and Summer seasons due to exposure to meteorological conditions, while a contaminant spill that travels in the middle and bottom of the water column (medium and high density/medium and low temperature spills) typically has arrival times later than a warm spill with similar behavior due to the hydrological conditions within the reservoir.

The newly modeled years 2007 and 2008 were added to update the seasonal patterns developed by Sojkowski (2011), establishing a Spring arrival time of two to five days after the spill, a Summer arrival of five to fourteen days, and a Fall arrival of four to ten days. The seasonal patterns were assessed by selecting one day for each season and year to represent the entire season for the selected year. To determine variability within a season, daily variations were evaluated in order to identify differences in behavior if spills occurred over a twenty day time period; it was found that some years may have similar arrival times and behaviors, while other years/seasons were found to have quite variable arrival times and behavior due to the meteorological and hydrological conditions during the time period. It was found that the arrival time window for seasons could be lengthened by one to two days, however, the results never led to a shorter arrival time.

The Quabbin transfer was found to have a significant impact on the behavior of the contaminant spill during the summer months, where the variability in spill concentration at the Cosgrove Intake is dampened when the Quabbin Aqueduct is shut off twelve hours after the spill occurs, however, little to no impact on the arrival time period was found.

High inflow events correlate to storm events and were investigated because of the increase risk of a tanker truck accident. The results indicate that the high inflow events dictate when the spill will arrive and how it will behave with minor dependence on the spill date in a five day period around the date of the storm.

Wind was determined to have a significant role in the arrival time of surficial spills; given the appropriate meteorological conditions, wind can produce arrival times as early as two days after the spill occurs.

5.3 Recommendations

Future work should include further exploration of each of the scenarios investigated by this report for additional years to develop and strengthen the knowledge obtained by this continuing project. Additional work could include modeling of Giardia cysts due to increase concentrations measured recently in tributaries and at the Cosgrove Intake. In addition, it is recommended that DCR and MWRA increase the frequency of measured temperature and specific conductance data and take measurements in the South Basin for better calibration of the CE-QUAL W2 model.

REFERENCES

- Massachusetts Water Resources Authority (MWRA) (2006) "Metropolitan Boston's Water System History" (<http://www.mwra.state.ma.us/04water/html/hist1.htm>).
- Massachusetts Water Resources Authority (MWRA) (2009), "Your Drinking Water 2008" Public Report.
- Cole T.M. and S. A. Wells (2008) "CE-QUAL-W2: A two-dimensional, laterally averaged, Hydrodynamic and Water Quality Model, Version 3.6," Department of Civil and Environmental Engineering, Portland State University, Portland, OR.
- Bowen, J. D., and Hieronymus, J. W. (2003) "A CE-QUAL-W2 Model of Neuse Estuary for Total Maximum Daily Load Development" *J. Water Resour. Plng. and Mgmt.*, 129 (4), 283-293.
- Lung, W., and Bai, S. (2003) "A Water Quality Model for the Patuxent Estuary: Current Conditions and Predictions Under Changing Land-use Scenarios" *J. Estuary and Coasts*, 26(2), 267-279.
- Kuo, J., Liu, W., Lin, R., Lung, W., Yang, M., Yang, C., and Chu, S. (2003) "Water Quality Modeling for the Feitsui Reservoir in Northern Taiwan", *J. American Water Resources Association*, 39(3), 671-687.
- Liu, W., and Chen, W. (2008) "Impact of Phosphorus Load reduction on Water Quality in a Stratified Reservoir-Eutrophication Modeling Study" *Environ Monit Assess*, 159 (4), 393-406.
- Camp, Dresser and McKee (CDM) (1995) "Wachusett Reservoir Water Treatment Plan EIR Conceptual Design Task 2.3: Wachusett Reservoir Draft Modeling Report," submitted to Massachusetts Water Resources Authority.
- Joaquin A.L. (2001) "Modeling the Effect of Quabbin Transfers on Wachusett Reservoir Composition", M.S. Thesis, University of Massachusetts, Amherst Department of Civil and Environmental Engineering.
- Tobiason J.T., Ahlfeld D.P., Joaquin A. and Mas D. (2002) "Water Quality in MDC Reservoirs. Project 1: Wachusett Reservoir Water Quality Modeling", University of Massachusetts, Amherst Department of Civil and Environmental Engineering, prepared for Metropolitan District Commission, West Boylston, MA.

Kennedy M.G. (2003) “Three-Dimensional Numerical Modeling of Hydrodynamics and Transport in a Reservoir”. M.S. Thesis, University of Massachusetts, Amherst. Department of Civil and Environmental Engineering.

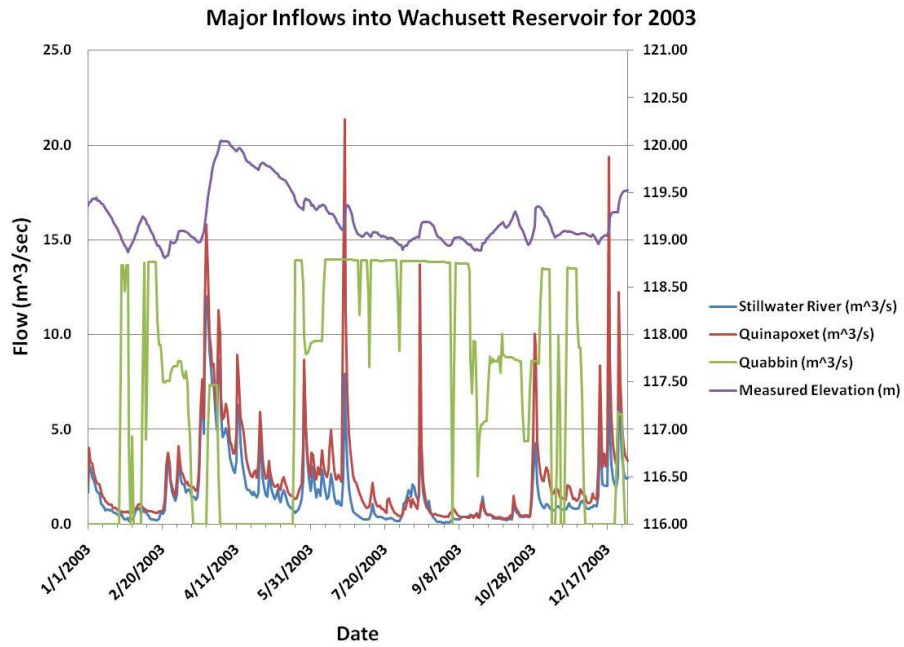
Buttrick D.R. (2005) “Modeling Natural Organic Matter in an Unfiltered Surface Water Supply”, M.S. Thesis, University of Massachusetts, Amherst. Department of Civil and Environmental Engineering.

Matthews T.P. (2007) “Modeling Fate and Transport of Fecal Coliform in Wachusett Reservoir”, M.S. Thesis, University of Massachusetts, Amherst Department of Civil and Environmental Engineering.

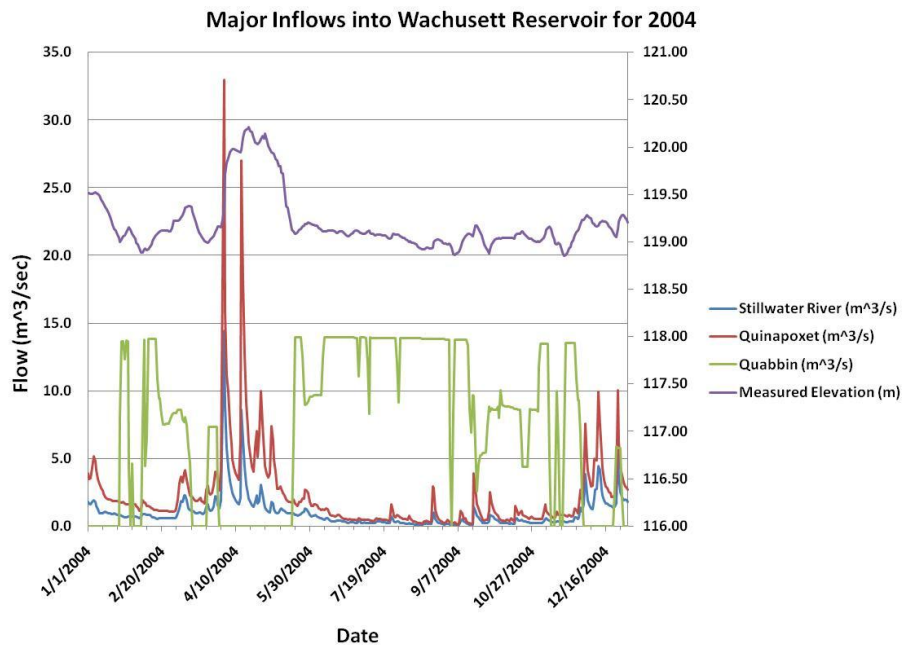
Stauber C.L. (2009) “Contaminant Spill Modeling for Wachusett Reservoir”, M.S. Thesis, University of Massachusetts, Amherst Department of Civil and Environmental Engineering.

Sojkowski B.R. (2011) “2-D Spill Modeling in the Wachusett Reservoir with CEQUAL-W2 for years 2003-2006”, M.S. Thesis, University of Massachusetts, Amherst Department of Civil and Environmental Engineering.

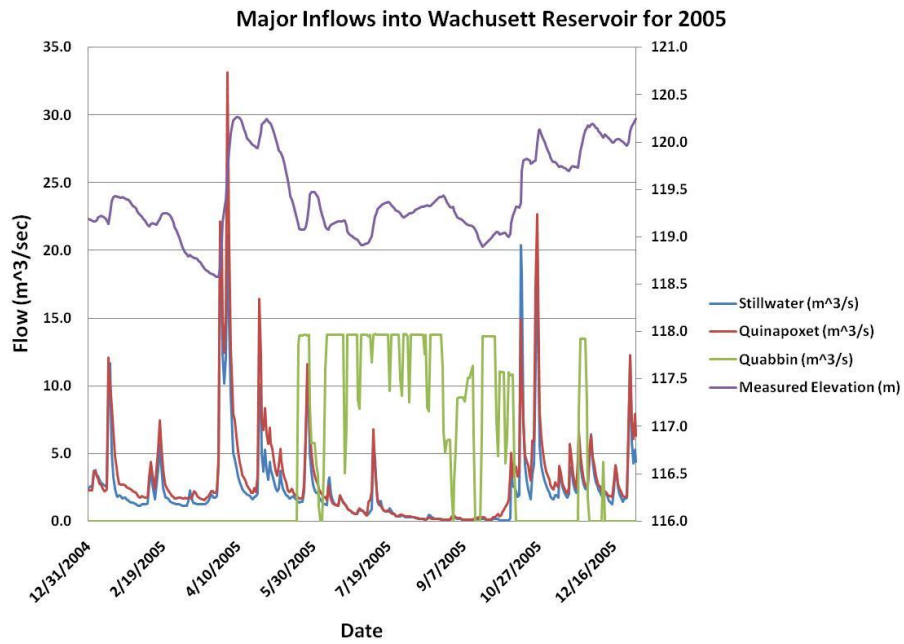
APPENDIX A - TIME SERIES OF MAJOR INFLOWS/OUTFLOWS



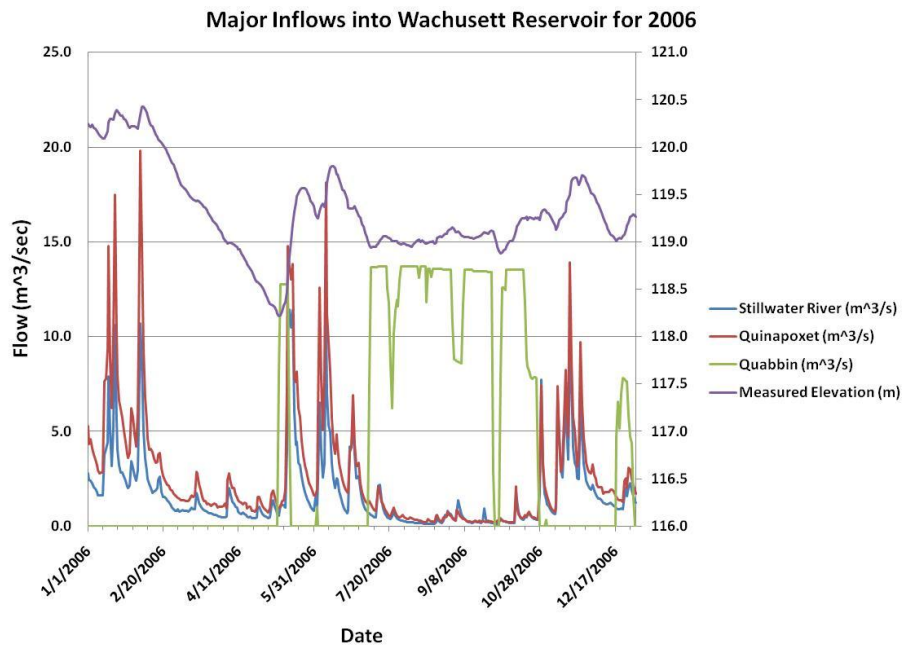
A. 1: Major Inflows into the Wachusett Reservoir for 2003



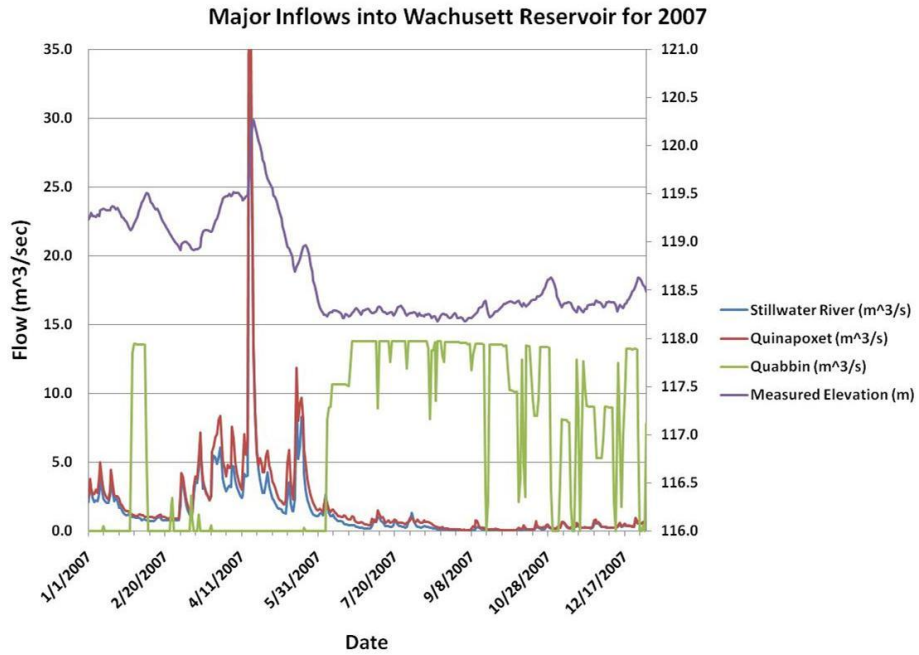
A. 2 Major Inflows into the Wachusett Reservoir for 2004



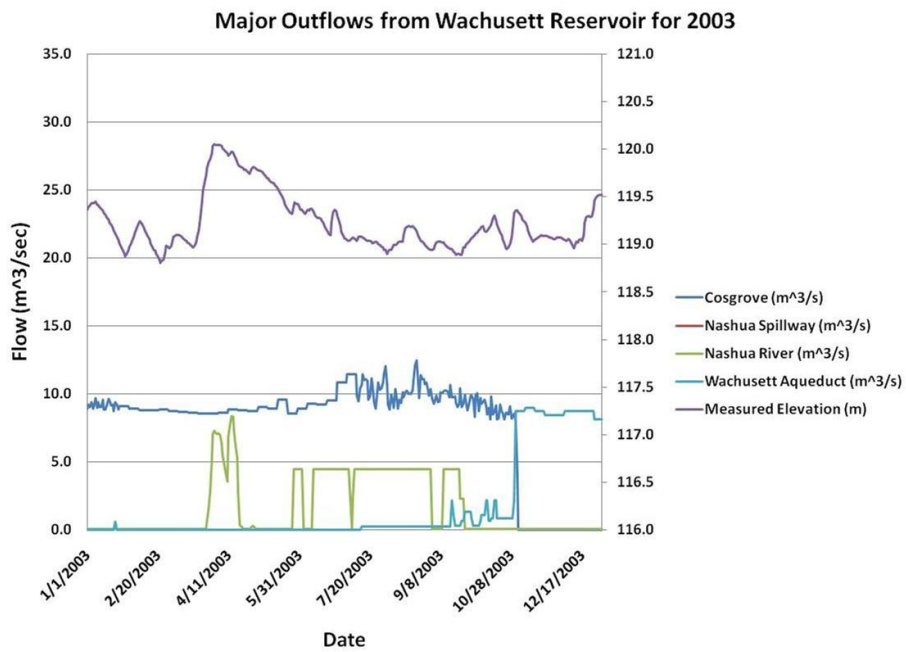
A. 3: Major Inflows into the Wachusett Reservoir for 2005



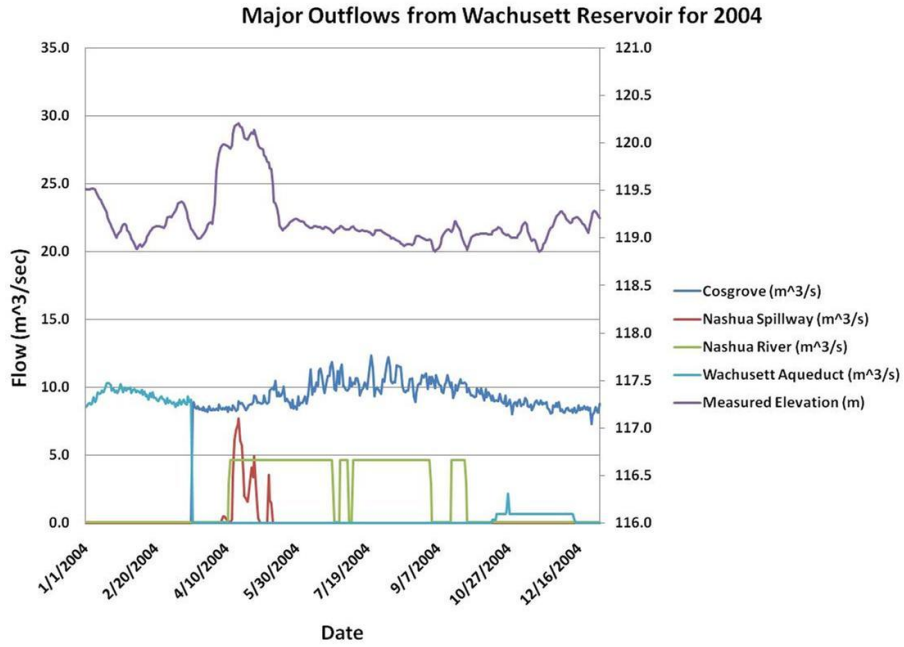
A. 4: Major Inflows into the Wachusett Reservoir for 2006



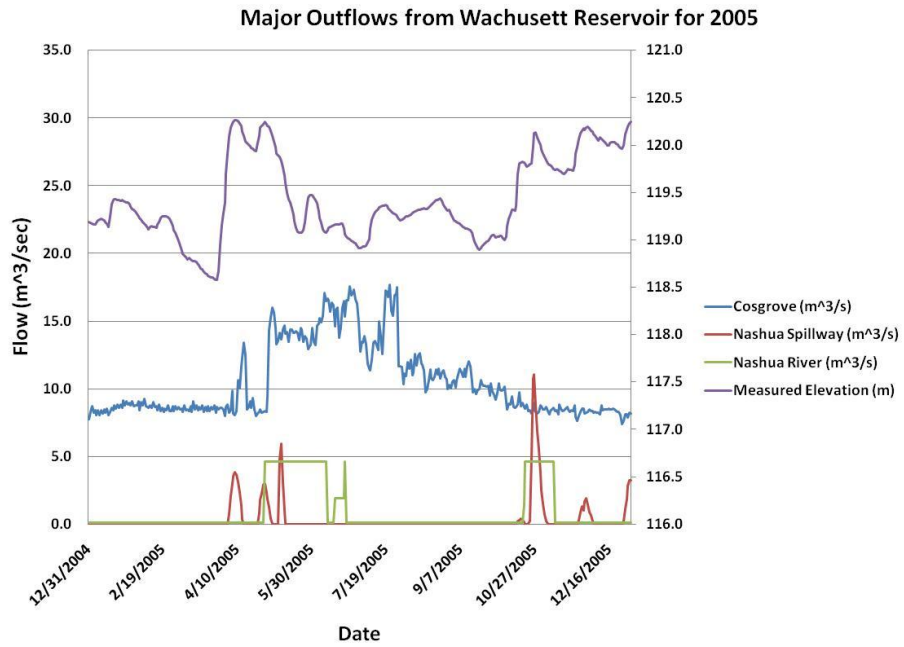
A. 5: Major Inflows into the Wachusett Reservoir for 2007



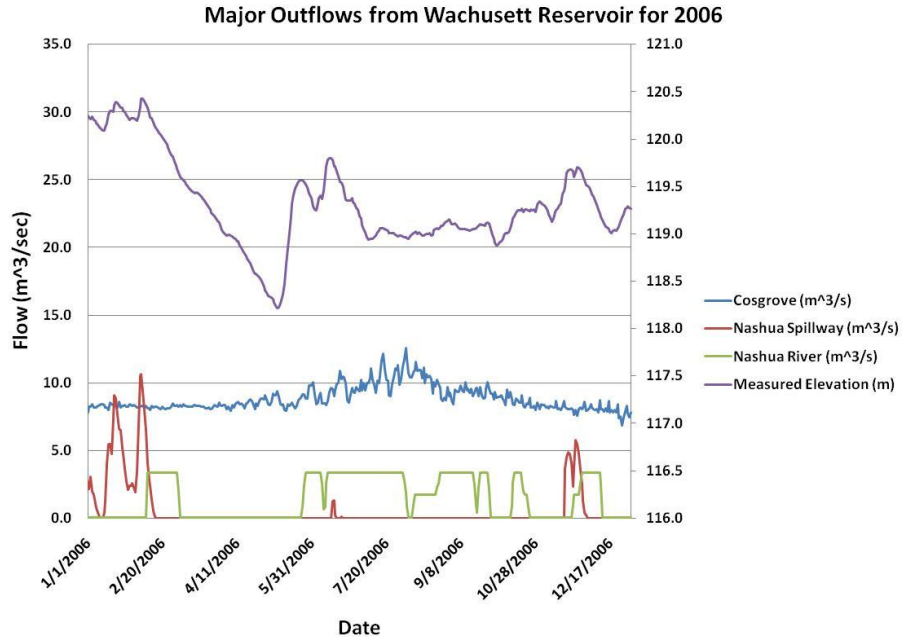
A. 6: Major Outflows into the Wachusett Reservoir for 2003



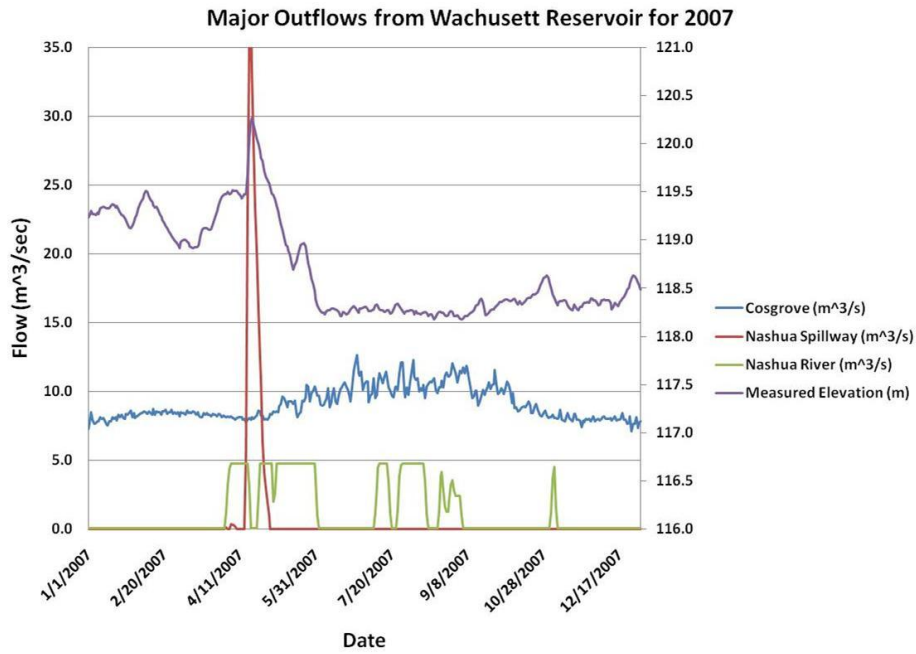
A. 7: Major Outflows into the Wachusett Reservoir for 2004



A. 8: Major Outflows into the Wachusett Reservoir for 2005

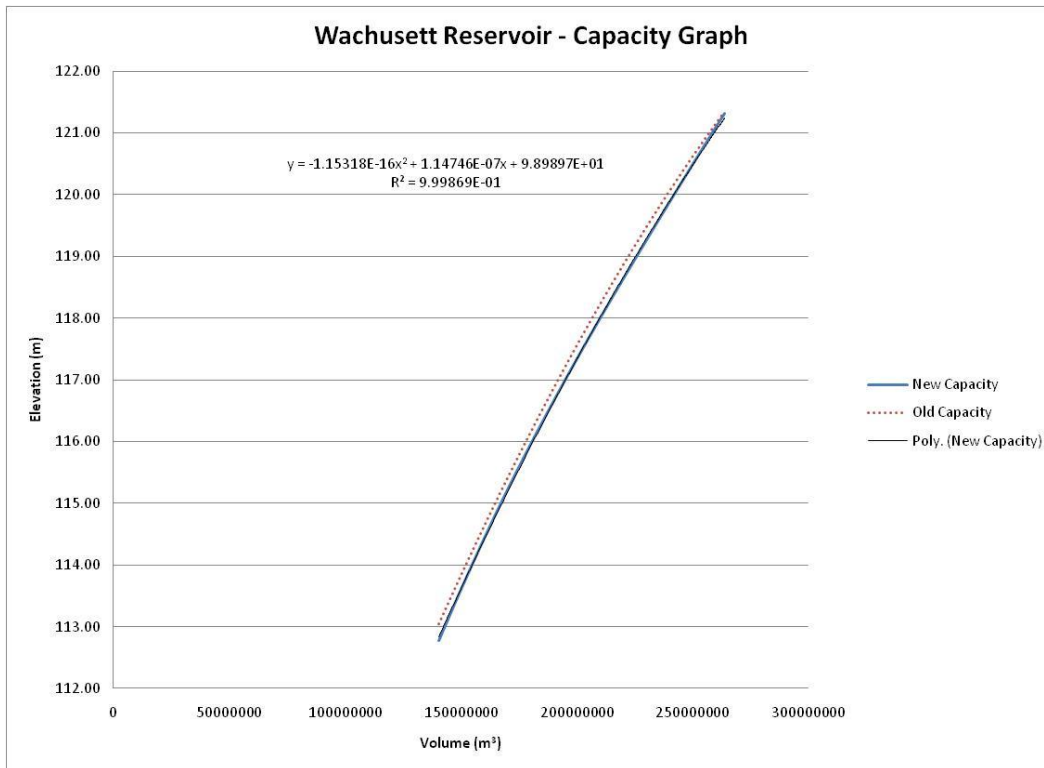


A. 9: Major Outflows into the Wachusett Reservoir for 2006



A. 10: Major Outflows into the Wachusett Reservoir for 2007

**APPENDIX B - WACHUSETT RESERVOIR CAPACITY AND ELEVATION
FROM MWRA**



B 1 – Wachusett Reservoir new capacity versus elevation graph